Anaerobic bacterial aggregates

Variety and variation

Beeftink, H.H.

Publication date
1987
Document Version
Final published version
License
Other

Link to publication

ANAEROBIC BACTERIAL AGGREGATES

VARIETY AND VARIATION

H.H. BEEFTINK

ANAEROBIC BACTERIAL AGGREGATES

VARIETY AND VARIATION
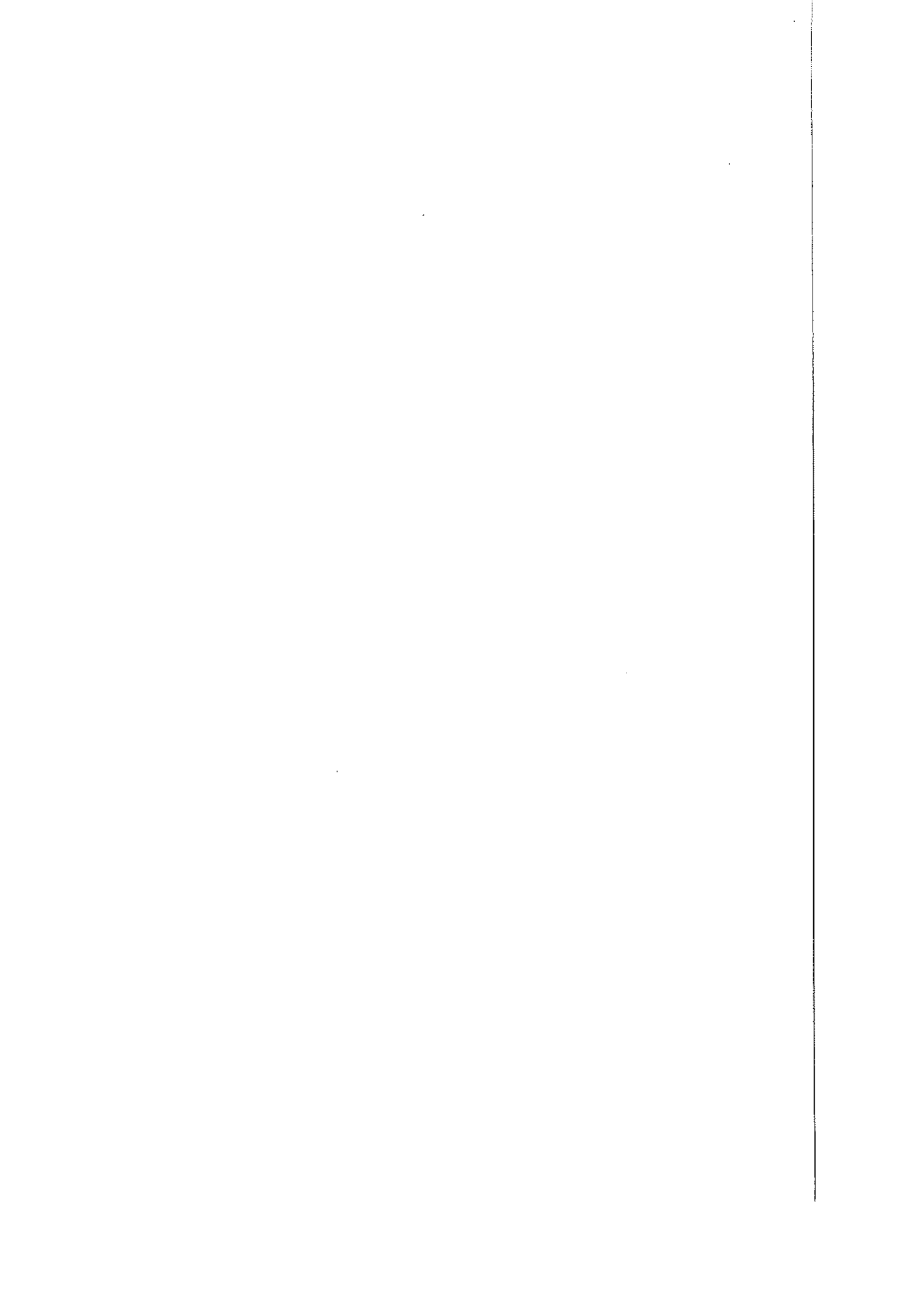
ANAEROBIC BACTERIAL AGGREGATES
VARIETY AND VARIATION

ACADEMISCH PROEFSCHRIFT

ter verkrijging van de graad van doctor
in de Wiskunde en Natuurwetenschappen
aan de Universiteit van Amsterdam
op gezag van de Rector Magnificus
Dr. S.K. Thoden van Velzen
hoogleraar in de Faculteit der Geneeskunde,
in het openbaar te verdedigen
in de Aula der Universiteit
(Oude Lutherse Kerk, Singel 411, hoek Spui),
op woensdag 11 maart 1987 te 13.30 uur.

door

HENDRIK HARMEN BEEFTINK

geboren te Hengelo (Ov.)

PROMOTOR   : PROF. DR. IR. C. BOELHOUWER
COPROMOTOR: DR. ING. J.C. VAN DEN HEUVEL

Aan mijn ouders,
aan Marianne.

CONTENTS

Bacterial aggregates, *i.e.* units in which micro–organisms are unable to move freely with respect to each other, recently have recieved interest from quite different disciplines. Such units may take different forms, *e.g.* bacterial films on a support material, or more discrete flocs or granules. Research on these aggregates is relevant to sueh different fields as for instance aquat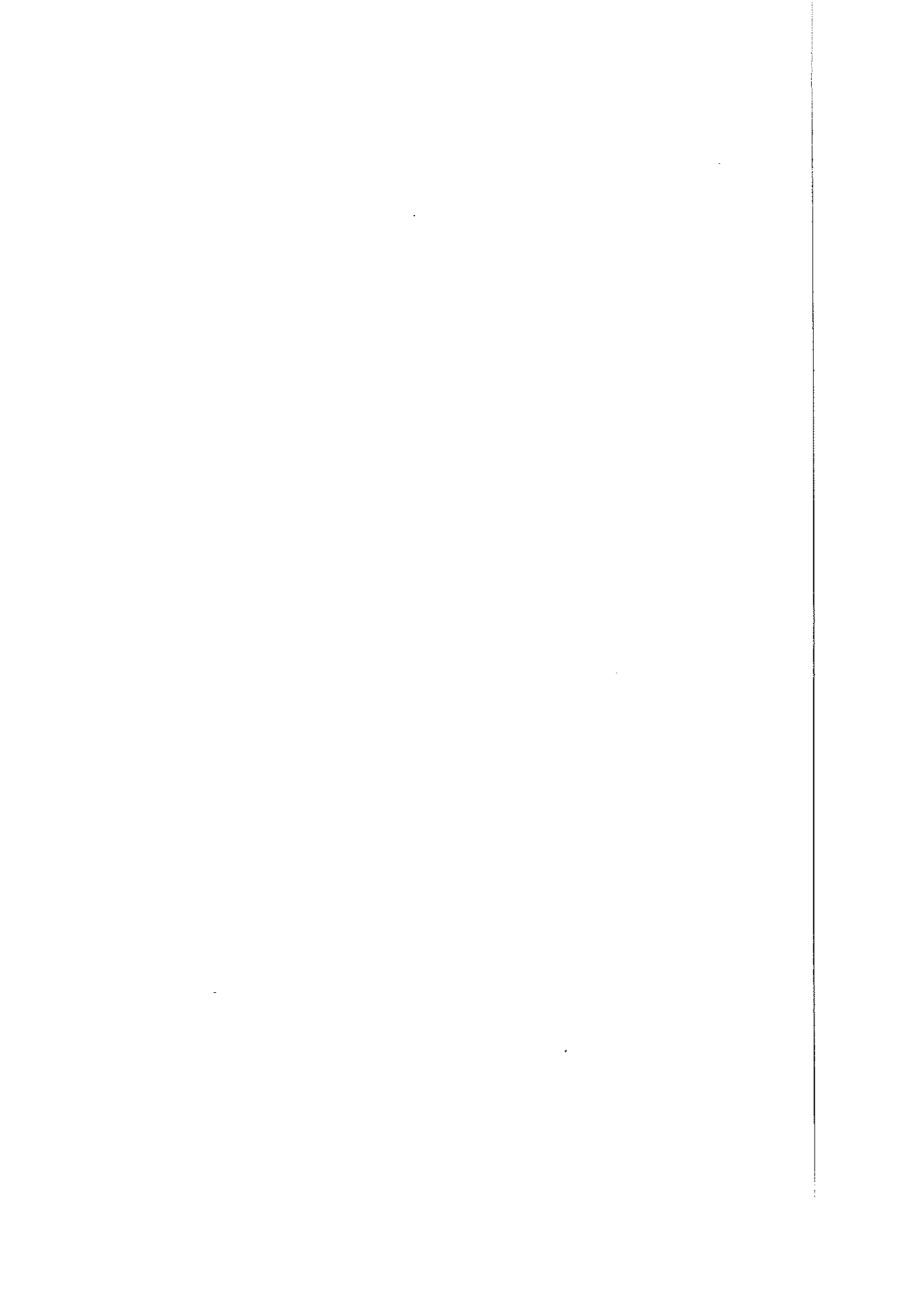ic ecology (Marshall, 1980; Wimpenny *et al.*, 1983), microbial fouling (Characklis & Cooksey, 1983), and medical bacteriology (Savage, 1980). This thesis is concerned with aggregates from a more technological angle, as they are frequently involved in improving the economic feasibility of large–scale bioconversions.

As a background to the research reported in the following chapters, the general impact of such aggregates on the performance of continuous–flow bioreactors is discussed. Furthermore, the importance of certain physical characteristics and of the dynamic behaviour of such aggregates for reactor design and operation is contrasted with the lack of knowledge in that area. Finally, the aim, scope and outline of this thesis are presented.

GENERAL BACKGROUND

Continuous–flow vs. batch operation.

As a rule, technical and economic utilization of the vast metabolic potential of micro–organisms involves batch–wise processing, while continuous–flow (CF) operation is limited to a few processes only. On the other hand, reactors for purely chemical conversions are frequently operated on a continuous–flow regimen.

Various rationales have been offered concerning the choice between these alternative modes of operation for bioreactors (*e.g.* Pirt, 1972; Wang *et al.*, 1979; Bailey, 1980; Cooney, 1983; MacDonald *et al.*, 1984;

Stewart & Russell, 1985). In general, however, simplicity on the one hand and tradition on the other seem to be rather decisive arguments in favour of batch—wise processing (with one major exception, as discussed below).

Simplicity refers in particular to problems associated with stability of the bacterial population: prolonged operation and the continuous addition of fresh medium render CF bioreactors highly susceptible to unwanted population changes (mutation and infection), whereas batch—wise operation entails an inherent stability since it allows for drastic corrections with every fresh batch (*i.e.* a new inoculum).

While batch reactors have a long—standing tradition, CF devices are relatively new for microbial conversions. Only decades ago, the chemostat or continuous culture (the microbiological equivalent of the continuous—flow stirred—tank reactor, CSTR) was introduced for laboratory purposes by Monod (1950) and by Novick & Szillard (1950). Consequently, the know—how concerning practical employment is still increasing.

Notwithstanding difficulties with population stability, CSTR reactors offer important advantages such as a time—invariant product composition. In addition, the volumetric productivity of biomass and growth—associated products is superior for CSTR, even if recharge times for batch reactors are neglected, and if batch reactions are taken to follow zero—order kinetics (Pirt, 1975; Wang *et al.*, 1979). Therefore, efforts are being made repeatedly to master problems and to adopt CF regimens for a wide range of biological conversions, such as the production of organic solvents (Häggström, 1981; Linden *et al.*, 1985), single—cell protein (Goldstein, 1985), beer (White & Portno, 1978; MacDonald *et al.*, 1984; Stewart & Russell, 1985), and antibiotics (Buckland *et al.*, 1985).

Guiding principles for the development of CF systems are available from long—time experiences with wastewater purification. Since the notion of infection has lost its meaning for the latter processes, biological wastewater treatment has always been amenable to CF operation. Due to the continuous supply of vast amounts of wastewater, batch processing is not feasible, as it would be too slow and would require an immense capacity for intermediate storage. Considering that for instance in the United Kingdom some 95 % of the total fermentor volume is dedicated to wastewater treatment (Dunnill, 1981), a vast experience on large—scale CF operation is available.

The ideal CSTR and its limitations.

In summarizing a number of profound differences between chemical and biological reactors, Moo—Young & Blanch (1983) draw attention to the kinetic limitations of bioconversions that result from their autocatalytic nature.

Microbial biomass is to be considered reactant and product in the

same reaction. As a reactant, it is rather peculiar in being absent from the reactor influent. Consequently, it has to be generated *in situ* (biomass as a product). The maximum rate at which this particular product can be generated (growth) sets the ultimate limit for reactor productivity, since it should not be exceeded by the rate at which it is removed (wash−out).

Microbial growth requires the availability of various chemical species (substrates), but in the simplest case only one — the growth−limiting substrate or simply *the* substrate — exerts kinetic influence, being available in low concentrations only, whereas all other substrates are in excess. Defining the specific growth rate μ as:

$$\mu = (1/x)\cdot(dx/dt) \tag{1}$$

with: μ: specific growth rate (h^{-1}); x: biomass concentration (g/l); t: time (h); subscript g: growth−attributable changes in x only,

balance equations for biomass and growth−limiting substrate on CSTR systems indicate that under stationary conditions (steady state):

$$\mu = D \tag{2}$$

$$x = Y\cdot(s_0 - s) \tag{3}$$

with: D: dilution rate, or reciprocal liquid residence time (h^{-1}); Y: stoichiometric yield coefficient, biomass growth per unit substrate consumed (g/mol); s_0: influent concentration growth−limiting substrate (mol/l); s: reactor concentration growth−limiting substrate (mol/l).

The Monod equation is a simple and commonly used expression for a saturation−type of dependency of the specific growth rate μ on the substrate concentration s:

$$\mu = \mu_{max}\cdot s \ / \ (K_s + s) \tag{4}$$

with: ; μ_{max}: maximum specific growth rate (h^{-1}); K_s: saturation constant, s at $\mu = \frac{1}{2}\mu_{max}$ (mol/l).

Substitution of this expression in Eq. 2 shows the steady−state concentration of growth−limiting substrate to be:

$$s = D\cdot K_s \ / \ (\mu_{max} - D) \tag{5}$$

with: K_s: saturation constant, s at $\mu = \frac{1}{2}\mu_{max}$ (mol/l); μ_{max}: maximum specific growth rate (h^{-1}).

In addition, a volumetric biomass output rate (productivity, p, g/l·h) may be defined:

$$p = D\cdot Y\cdot(s_0 - s) \tag{6}$$

Similar equations may be developed for the volumetric productivity of

growth—associated products other than biomass, using appropriate stoichiometric yield coefficients. Eqs. 2 — 6 may be generalized by making them dimensionless:

$$M = \Delta \qquad\qquad\qquad [7]$$

$$X = \Sigma_0 - \Sigma \qquad\qquad [8]$$

$$\Sigma = \Delta \ / \ (1-\Delta) \qquad\qquad [9]$$

$$\Pi = \Delta \cdot (\Sigma_0 - \Sigma) \qquad\qquad [10]$$

with: M: dimensionless specific growth rate, μ/μ_{max} (−); Δ : dimensionless dilution rate, D/μ_{max} (−); X: dimensionless biomass concentration, $x/Y \cdot K_s$ (−); Σ: dimensionless substrate concentration, s/K_s (−); Σ_0: dimensionless influent concentration, s_0/K_s (−); Π: dimensionless biomass output rate, $p/Y \cdot K_s \cdot \mu_{max}$ (−).

Fig. 1 gives an illustration of Eqs. 8 — 10. The biomass output rate is seen to increase almost linearly with the dilution rate at low Δ—values. If Δ increases further, however, Π passes though a maximum and drops off. Without giving the exact mathematical expression for this Π—maximum (Pirt, 1975; Wang *et al.*, 1979), it may be appreciated from Fig. 1[b] that its position and height are Σ_0—dependent. This is a

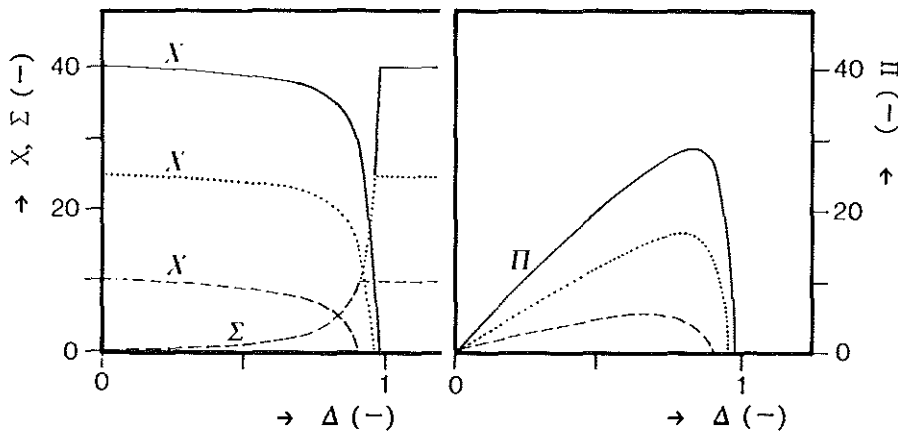**Fig. 1**: Steady—state CSTR behaviour without retention of biomass at three arbitrary influent substrate concentration (Σ_0 = 10, − − − ; Σ_0 = 25, ····· ; Σ_0 = 40, ——). **Fig. 1** : Dimensionless biomass and substrate concentrations (X and Σ, respectively) *vs.* dimensionless dilution rate (Δ). **Fig. 1[b]**: Dimensionless biomass output rate (Π) *vs.* Δ.

nuissance for low$-\Sigma_0$ influents in particular, as low productivities are implied. Furthermore, realization of maximum productivities for high$-\Sigma_0$ influents involves Δ-values close to unity. Although an analysis shows steady states to be inherently stable (Bazin, 1981), these elevated Δ-values would render a reactor operationally instable.

Ultimately, the kinetic characteristics of the micro-organism involved, especially μ_{max}, limit the maximum attainable Π-values (Eq.7). Since μ_{max} depends on temperature (among other factors), higher process temperatures may be applied in order to optimize productivity. As opposed to chemical processes, however, this option is only feasible within a narrow temperature range, due to loss of biomass viability at elevated temperatures. Consequently, other means to improve reactor productivity have been adopted. General experiences from wastewater treatment plants employing biomass retention (Eckenfelder *et al.*, 1985) have gained considerable interest.

Retention of biomass.

To increase the maximum reactor output rate, the limitation imposed by Eq. 7 has to be relaxed: the reactor should be operated at D-values exceeding μ_{max} while at the same time biomass wash-out is prevented, *i.e.* the mean biomass residence time in the reactor should exceed the mean liquid residence time. Conceptually, a separating device (*e.g.* a centrifuge or a settler) may be envisaged in series with the reactor, producing an effluent stream that is dilute with respect to biomass and returning a concentrated biomass suspension to the reactor.

Defining a hold-up ratio or retention R as:

$$R = x_r/x_e \qquad\qquad [11]$$

with: x_r: reactor biomass concentration (g/l); x_e: effluent biomass concentration (g/l),

and using the same conventions as above for representation in dimensionless form, balance equations on biomass and substrate for such CSTR systems with biomass retention show the former set of Eqs. 7 − 10 to be replaced by (see also Fig. 2):

$$M = \Delta/R \qquad\qquad [12]$$

$$\Sigma = \Delta \, / \, (R-\Delta) \qquad\qquad [13]$$

$$X_e = \Sigma_0 - \Sigma \qquad\qquad [14]$$

$$X_r = (\Sigma_0 - \Sigma)\cdot R \qquad\qquad [15]$$

$$\Pi = \Delta\cdot(\Sigma_0 - \Sigma) \qquad\qquad [16]$$

For $R = 1$ (absence of retention), these equations reduce to the normal CSTR case. If CF reactors with biomass retention are operated

at low Δ—values ($D < \mu_{max}$), the biomass output rate is similar as observed in CSTR. Eq. 12, however, indicates non—trivial steady states (*i.e.* $x_r \neq 0$) to be attainable at $D > \mu_{max}$, provided $R > 1$. Under the latter conditions, volumetric output rates exceed those in CSTR reactors without retention.

Apart from increasing productivity for $D > \mu_{max}$, some additional advantages of biomass retention may be inferred. If the process is aiming at low residual substrate concentrations s, rather than at high volumetric productivities, Eq. 13 predicts s—values to be inversely depending on R. So, even for $D < \mu_{max}$ retention of biomass may be beneficial. Furthermore, process temperatures may be decreased (decrease of rate constants) if the resulting loss in productivity can be compensated by retention of biomass. Finally, the feasability of treating low—Σ_0 influents may be improved.

Design and operation of CSTR systems based on Eqs. 12 — 16, however, is not straightforward since the system is incompletely determined by these equations. Predictions of reactor performance would
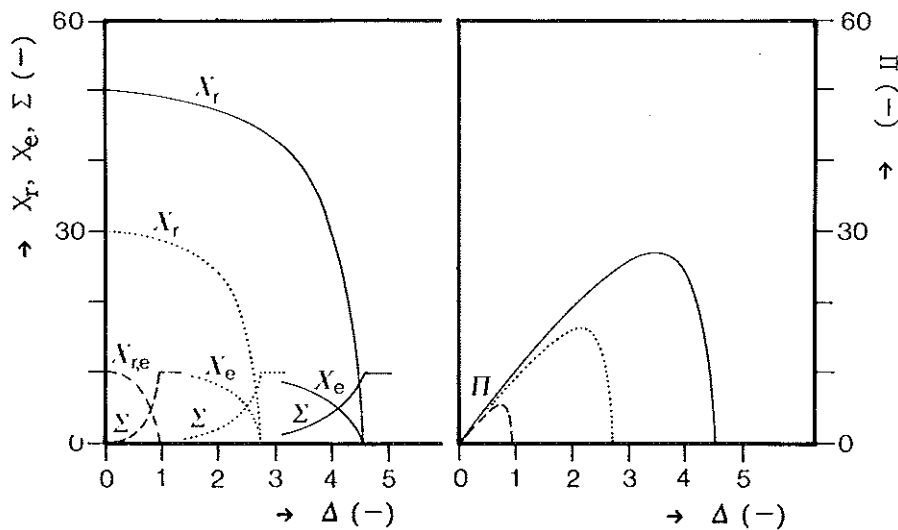
Fig. 2: Steady—state CSTR behaviour with retention of biomass at an arbitrary influent substrate concentration ($\Sigma_0 = 10$), and three levels of biomass retention ($R = 1$, — — —; $R = 3$, ···· ; $R = 5$, ———).

Fig. 2^a: Dimensionless substrate and reactor and effluent biomass concentrations (X_r, X_e, and Σ) *vs.* dimensionless dilution rate (Δ).

Fig. 2^b: Dimensionless biomass output rate (Π) *vs.* Δ .

require *a priori* knowledge of R, *i.e.* of the performance characteristics of the separating device producing dilute and concentrated biomass streams, and in particular of the physical characteristics of the biomass (cells) to be separated. Quantitative data on settling properties generally are not available, and are highly dependent on reactor performance. Therefore, trial−and−error experiments on a laboratory scale and careful scale−up are the only way to obtain data on reactor performance.

Employing a feedback−control mechanism, it is of course technically feasible to operate a reactor at any particular fixed R−value, *e.g.* by constantly monitoring x_r in combination with an adjustable biomass return from the separating device. Such a configuration has been described by Afschar *et al.* (1985). Without such a feedback control, however, reactor biomass concentrations would be rather unpredictable.

In addition, there is good reason to suppose R to be M−dependent. Some relevant characteristics of micro−organisms (*i.e.* cellular volume, mass and shape) are firmly established to depend on specific growth rate (*e.g.* Henrici, 1928; Herbert, 1961; Van Gemerden, 1968; Jagadish *et al.*, 1977; Tempest *et al.*, 1983; Nanninga & Woldringh, 1985; Sevilla & Odds, 1986), and thus on Δ. Consequently, the performance of a separating device, relying on these characteristics, would be M− and Δ−dependent.

It should be noted that bacterial requirements for maintenance energy have not been taken into consideration in the present discussion, which only served to illustrate some general principles. Final reactor descriptions, however, should not make this simplification, since low specific growth rates are involved.

Reactor systems employing biomass retention.

Up until now, it has been tacitly assumed that all micro−organisms were suspended as individual (small) cells in a well−mixed reactor. Since settling of individual cells is slow, expensive separating devices such as centrifuges are required to achieve substantial biomass retention. To circumvent such an unattractive configuration, in many bioreactors aiming at biomass retention micro−organisms are immobilized with respect to each other. Such "aggregates" either have high settling velocities, or are fixed to the reactor shell.

The words pellet, floc, aggregate, clump, granule (to name a few) are widely used to indicate such multicellular units of micro−organisms. This variegated linguistic collection at least suggests the existence of clearly differing classes of these units. The most conspicuous feature of these words, however, is their conceptual similarity, *i.e.* they all indicate that a number of micro−organisms is not able to move freely with respect to each other. Although acknowledging the various gradations in which such immobilized consortia occur, the recommendation of Atkinson (Atkinson & Daoud, 1976; Atkinson & Rahman, 1979) to regard all

terms as interchangeable shall be adopted. For reasons of consistency, the word aggregate is used throughout.

A wide variety of CF devices with bacterial aggregates is currently in use, and Fig. 3 gives a highly simplified classification. A stationary carrier material to support bacterial adhesion may be present, resulting in laterally extended microbial films (as in rotating biological contactors). On the other hand, small support particles are added to many fluid— —bed reactors in order to obtain discrete, more or less spherical, and rather heavy microbial "aggregates" that are suspended in the bulk liquid. Also, "flocs" or "granules" of micro—organisms may be formed spontaneously without mediation by any externally supplied carrier, as for instance in the activated—sludge and anaerobic digestion wastewater treatment processes. Finally, artificial immobilization by encapsulation or gel entrapment is often applied in the production of fine chemicals.
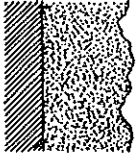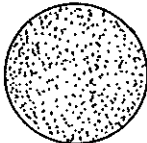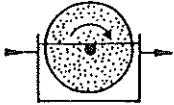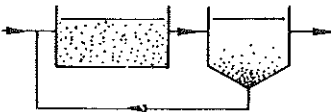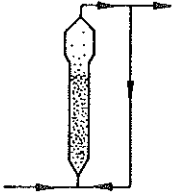
film, stationary support	aggregate, no carrier	aggregate, film on carrier	entrapped micro— —organisms
rotating disk contactor	activated sludge installation		fluidized bed reactor

Fig. 3 : Simplified classification of various forms of microbial aggregates and appropriate reactor types. Hatched: carrier or support material. Solid vertical line separates reactors that do not or do ʹrely on settling characteristics of biomass.

Characteristic dimensions for these immobilized consortia are such that spatial inhomogeneities and mass—transfer resistances are no longer negligible in mathematical reactor descriptions, which consequently become more complex. Although retention of biomass becomes increas—ingly efficient if aggregates are larger, diffusional barriers adjacent to and within large immobilized consortia concomitantly diminish the volumetric reactor output rates. Qualitatively, an optimal size is therefore to be expected for these immobilized units.

Excluding gel—entrapment from the present discussion, retention of biomass depends on the adhesion of micro—organisms to a support material or to each other. Subsequently, two ways to retain these adhering microbes in a reactor can be distinguished among the types of reactor mentioned above, according to the requirement for a sedimentation device (see also Fig. 3). In packed—bed reactors or in rotating biological contactors there is no absolute requirement to retain any liquid—suspended biomass, since the main part of biomass is attached to a stationary support connected to the reactor shell. Settlers thus may be absent, and selection of dilution rates to be applied should only take into consideration the transport of substrate towards and into the film, the intrinsic bacterial kinetics, and the hydromechanical forces exerted on the film.

When dealing with separately suspended aggregates, however, reactor design and operation should in addition provide the opportunity and the conditions for sedimentation, as retention finds its basis in the fact that aggregates have higher settling velocities than their constituent cells. For reasons of simplicity, discussion shall be confined to such CF reactors containing discrete individual aggregates with or without particulate carrier material.

Obviously, the dimensions and density of suspended aggregates have a direct bearing on the attainable levels of reactor biomass concentra—tions, whereas a reliable prediction of the latter quantity is of utmost importance to reactor design and performance (Shieh et al., 1981). Quite often, reactor models assume all aggregates to be of one singular size and density. Several processes and forces, however, would interact in determining the dimensions of aggregates (cellular growth and decay, attrition, sloughing, and break—up), and aggregates are obviously of a dynamic nature. Therefore, a range of aggregate sizes is to be expected; theoretical calculations on such size distributions have shown that they may affect reactor performance profoundly (Atkinson & Rahman, 1979).

At the same time, however, experimental data on the behaviour and the physical characteristics of aggregates are particularly sparse. This discrepancy between potential importance and available knowledge has been indicated repeatedly as a severe limitation for further optimization of bioreactor design (Atkinson & Daoud, 1976; Atkinson & Mavituna, 1983).

AIM AND SCOPE

In summary, it can be concluded that the phenomenon of biomass retention is of particular importance to the operation of continuous—flow bioreactors, while at the same time it is understood poorly. While effluent biomass concentrations are roughly equal to ideal CSTR biomass concentrations, predictions of reactor biomass concentrations are questionable.

The research presented in this thesis was started in appreciation of this lack of understanding, and meant to provide some insight in the mechanisms underlying development and behaviour of spontaneous microbial aggregates in a continuous—flow reactor. Fundamental physico— —chemical and physiological aspects of microbial adhesion are not dealt with in this thesis, although they are pertinent. These subjects are reviewed in some recent monographs (Berkeley *et al.*, 1980; Bitton & Marshall, 1980; Ellwood *et al.*, 1979; Savage & Fletcher, 1985).

As a model reaction, the anaerobic acidification of glucose by a mixed bacterial population was selected, since extensive knowledge on the physiology and kinetics of this process was available (Cohen, 1982; Zoetemeyer, 1982; Van den Heuvel, 1985; Breure, 1986). These complex reactions represent the practically important first step in the anaerobic mineralization of carbohydrates, as encountered in the two—phase digestion process. General conclusions from this research, however, should be applicable to other populations and conversions as well.

Experiments were carried out in an anaerobic gas—lift reactor (AGLR), which may be regarded as a continuous—flow three—phase circulating— —bed fermentor, containing sand as support material for bacterial adhesion. Reasons for this choice are discussed in Chapter II, which gives a description of reactor start—up and of the implications of aggregate formation on overall bacterial physiology. The influence of various amounts of carrier material for bacterial adhesion during reactor start—up is reported on in Chapter III, while electronmicroscopic observations on aggregate development are given in Chapter IV. Sub— sequently, Chapter V reports on physical characteristics of aggregates during reactor start—up and development of a steady—state. A mathe— matical summary of various data and observations on aggregate devel— opment and characteristics is given in Chapter VI, by presenting a model on the AGLR, describing reactor and effluent biomass concentrations, and distributions of aggregate characteristics.

Cumulative listings of symbols, dimensions, and abbreviations, and of the the literature cited, are provided after the final Chapter VI, and are followed by an English and Dutch summary of the thesis.

CHAPTER II	A NOVEL ANAEROBIC GAS−LIFT REACTOR WITH BIOMASS RETENTION: START−UP ROUTINE

SUMMARY

A start−up routine for a novel type of anaerobic gas−lift reactor, using sand as liquid−suspended support particles for bacterial adhesion, and involving a dilution−rate shift−up, is shown to result in rapid formation of mixed−culture aggregates from freely suspended cells. Aggregate formation coincided with a change in overall population metabolism from an acetate/butyrate fermentation to acetate/propionate production. This metabolic change is attributed to population selection by wash−out, favouring propionate−producing bacteria which apparently have superior adhesive properties. Sand is shown to be essential in establishing, but not in sustaining, elevated hold−up ratios. The importance of maintenance processes and cellular lysis in deeper parts of aggregates are manifest from a reduced effluent biomass concentration and a pronounced production of valeric acid.

INTRODUCTION

The attainable space loadings and volumetric productivities of continuous−flow bioreactors may be improved by biomass retention. Retention is feasible if micro−organisms can be made to grow as aggregates. As opposed to individual bacterial cells, such aggregates can easily be separated from the effluent stream by sedimentation, and subsequently can be recycled to the reactor proper (as for instance in the activated−sludge process).

Often, as in expanded− or fluidized−bed bioreactors, the reactor vessel itself serves as a sedimentation device, thus avoiding the mechanical damage inflicted upon bacterial aggregates by a recycling pump. Inert carrier particles are frequently added to these reactors to promote biofilm formation. Such configurations, however, require careful control of the upward liquid velocity in the reactor by means of an

external liquid recycle to regulate bed expansion. In addition, setting of the recycling rate is complex, since it has been demonstrated to be time−dependent, due to changing settling properties of the biological aggregates involved (Switzenbaum & Jewell, 1980; Heijnen, 1984).

Although industrial−scale installations may justify extensive control equipment to ensure stable fluidized−bed expansion, gas−lift reactors with biomass hold−up have attracted interest as an alternative for high−rate conversions (e.g. Bu'lock et al., 1984). In the latter type of reactor, a continuous gas flow from the bottom of the vessel induces internal circulation of the reactor contents through a riser and downcomer section, whence it may be characterized as a three−phase circulating−bed reactor. A separate settler on top of the reactor facilitates sedimentation of aggregates from the effluent stream back into the reactor. In case of aerobic applications (air−lift reactor), however, optimal utilization of higher volumetric productivities, as offered in theory by the retention of biomass, is often precluded by an insufficient oxygen−transfer capacity at shorter liquid residence times (Vanderborght & Gilliard, 1981; Heijnen, 1984).

Until now, the potential merits of gas−lift reactors for anaerobic conversions have recieved little attention. Yet, in such anaerobic gas−lift reactors with biomass retention (AGLR), attainable productivities are solely determined by the amount and settling characteristics of the biomass that can be retained, while mass transfer between the liquid and the gas phase (i.e. recycled culture off−gas) plays a less critical role. At the same time, the beneficial features offered by gas−lift systems in general can be fully exploited. Such features include a very efficient liquid mixing without the considerable shear involved with mechanical stirrers (Dussap & Gros, 1982). Excessive attrition or sloughing of aggregates by these forces is thus avoided. Also, local liquid velocities in the reactor proper are less critical than in fluidized−bed systems, as aggregates may be dispersed randomly through the well−mixed reactor liquid. Finally, gas−lift reactors are attractive due to the relatively easy scale−up (Onken & Weiland, 1983).

The present paper describes the start−up routine of a continuous−−flow AGLR utilizing sand as inert support media for attachment and aggregate formation by a mixed bacterial population. Under carbon−−limited conditions in a synthetic medium, glucose was acidified to short−chain fatty acids, carbon dioxide, and hydrogen, representing the acidogenic phase in the anaerobic digestion of carbohydrates. The kinetics, stoichiometry, and microbial physiology of acidogenesis are extensively documented (Cohen, 1983; Zoetemeyer, 1983; Van den Heuvel, 1985; Breure, 1986). Our study focussed on the feasibility of aggregate formation in the AGLR, and on the macroscopic consequences for microbial metabolism. The results of this study have been published separately (Beeftink & Van den Heuvel, 1986).
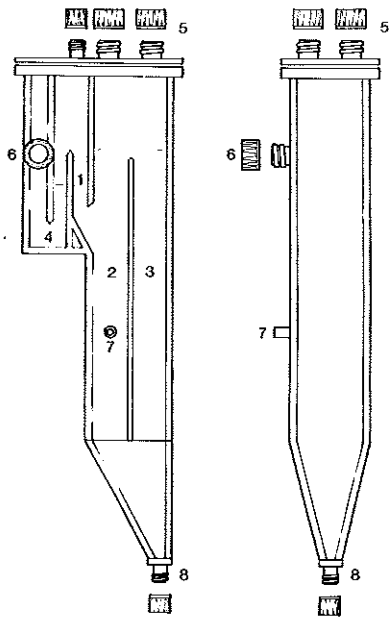
Fig. 1: Schematic view of anaerobic gas-lift reactor (AGLR, scale 1:7).
[1]: effluent section;
[2]: downcomer;
[3]: riser;
[4]: water seal;
[5]: influent, antifoam, hydroxide *etcetera*;
[6]: effluent port;
[7]: sample port;
[8]: gas inlet orifice.

MATERIALS & METHODS

Anaerobic gas-lift reactor (AGLR). The AGLR had a working volume of 1.9 l and is drawn to scale in Fig. 1; a general view of the culturing equipment is given in Fig. 2. The rectangular reactor had a liquid height of 45 cm, an aspect ratio of 6.5, and equal riser and downcomer cross-sectional areas (22 cm^2). Culture gas was recycled continuously from the reactor head space to the bottom of the fermentor (4 mm orifice), while a cooling jacket prevented vapour condensation in the compressor. In all experiments, the total gas hold-up amounted to *ca.* 40 ml, while the superficial gas velocity in the riser was 10 mm/s. Excess fermentation gas left the system via a washing bottle and a metering device. To allow retention of bacterial aggregates, liquid was made to leave the reactor in upward direction through a separate and quiescent effluent section (cross-sectional area 15 cm^2). Loss of culture gas and entrance of oxygen was precluded by a water seal, which was stirred to prevent clogging of the effluent. To compensate for minor but inevitable losses of culture gas in the compressor, a small stream of nitrogen gas was continuously supplied to the reactor vessel (5 ml/min).

Medium composition and culturing conditions. A simple well—defined salts medium was employed throughout, containing 55.5 mmol/l of glucose as the growth—limiting substrate (Cohen *et al.*, 1980; Zoetemeyer *et al.*, 1982). Medium was supplied to the reactor by metering pumps from two separate reservoir bottles, each containing a double—strength solution of organic and inorganic medium components, respectively (*loc.cit.*). The pH was maintained at 5.8 by means of automatic titration with 8 mol/l NaOH. Temperature was kept at 30 °C with a contact thermometer and a 0.25 kW incandescent light source (Fig. 2).

Inoculation and start—up procedure. The AGLR was inoculated with a fresh 300 ml sample from an activated—sludge treatment plant and filled up with medium. Upon addition of 20 g of silica sand (specific weight 2.65 g/ml, grain size 250—315 μm), the reactor contents were flushed thoroughly with nitrogen. When batch—wise operation resulted in

Fig. 2: Overall view of AGLR cultural equipment. [1]: AGLR; [2]: medium reservoirs; [3]: peristaltic pumps; [4]: burettes; [5]: cooling jacket; [6]: recycle gas; [7]: compressor; [8]: stirrer; [9]: pH—stat; [10]: antifoam addition; [11]: excess culture gas; [12]: wet gas meter; [13]: nitrogen gas cylinder; [14]: thermometer/heat lamp; ⋈: regulating valve; T : stopcock.
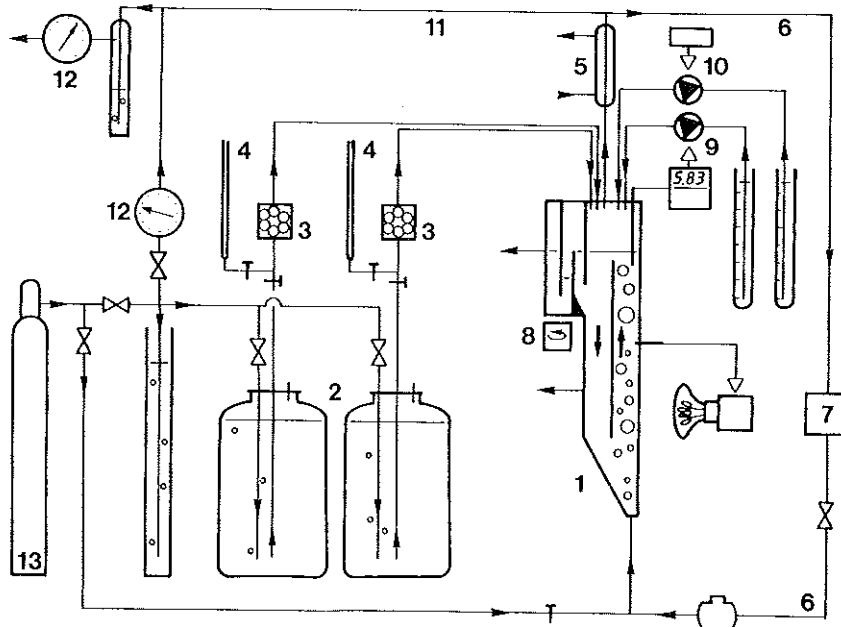
complete glucose conversion (*i.e.* overnight), the dilution rate (*D*) was set at 0.2 h^{-1}. Upon establishment of a steady state (as judged from a constant product composition for 10 liquid residence times), *D* was raised steeply to 0.6 h^{-1} (about 4 days after inoculation).

Biomass determination. Biomass samples (approximately 15 ml) were obtained by collecting effluent, or from the reactor through an 8 mm sampling port which allowed unobstructed flow of aggregate−containing sample. Sample volume was determined by weight (assumed specific weight 1 g/ml), and biomass concentrations as dry weight by centri− fugation (15 min at $2 \cdot 10^4 \cdot g$ and 5 °C) and subsequent lyophilization. Preliminary dry−weight values were corrected for any sand present by treatment of biomass pellets with hypochlorite (Characklis, 1973). Lyophilized pellets were resuspended in domestic NaOCl and incubated for 4 h at room temperature. Cellular debris was then removed by repeated washing with demineralized water. Remaining sand was deter− mined by weight after lyophilization. The hold−up ratio (*R*) was calcu− lated as the ratio of reactor and effluent biomass concentrations (x_r/x_e).

Calculation of specific growth rates. The mean specific growth rate (μ) of the total bacterial population in the AGLR during transient states was calculated on basis of a biomass balance:

$$(dx_r/dt) = \mu \cdot x_r - D \cdot x_e$$

which on rearranging gives:

$$\mu = (1/x_r) \cdot (dx_r/dt) + D/R$$

This calculation was used only when both (dx_r/dt) and x_e were found to be constant.

Glucose and lactate determinations. Glucose and lactate concentrations were measured in culture supernatants (5 min at $10^4 \cdot g$) with glucose oxidase and lactate dehydrogenase, respectively, utilizing an LM3 Analyser with an oxygen electrode (Analox Instruments, UK; Akazawa & Conn, 1958; Cheng & Christian, 1977).

Fatty acid determination. Short−chain fatty acid concentrations (C_2 − C_5) in culture supernatants (5 min at $10^4 \cdot g$) were determined gaschromatographically upon 1:1 dilution with 8 mol/l of formic acid containing 17 mmol/l iso−valeric acid as an internal standard (Chromosorb 101, 80−100 mesh, glass column 2×1000 mm, column temperature 160 °C, injector and detector temperature 180 °C, carrier gas 30 ml/min N_2, sample volume 1 μl; Ottenstein & Bartley, 1971).

Organic carbon mass balances. Concentrations of dissolved, organic, carbon−containing products and substrate were added after conversion to (mg C)/l as a unit. This sum was divided by the total organic carbon (TOC) reading from the same supernatant to obtain a liquid−phase

carbon recovery. TOC was measured using a Beckman 915A Total Organic Carbon Analyser (Cohen *et al.*, 1979).

RESULTS

The start–up procedure for the AGLR was aimed at establishing hold–up ratios (R) exceeding unity by means of bacterial aggregate formation. Fig. 3 shows a typical example of the time courses of the concentrations of glucose, volatile fatty acids, lactate, and biomass, as resulting from a shift–up in dilution rate (D) from 0.2 to 0.6 h^{-1} at dimensionless time $\tau = 0$ ($\tau = D \cdot t$; t: process time, h^{-1}).

The steady state at $D = 0.2$ h^{-1} preceding the shift–up was characterized by the absence of aggregates: biomass concentrations in the reactor (x_r) and in the reactor effluent (x_e) were found identical (2.35 g/l, Fig. 3^a), and thus $R = 1$. The growth–limiting substrate glucose was converted completely (Fig. 3^b), and acetate and butyrate were formed as main fermentation products (15 and 16 mmol/l, respectively), together with minor amounts of propionate (3 mmol/l; Fig. 3^c).

Upon the shift to $D = 0.6$ h^{-1}, substrate concentrations increased, and a severe wash–out of biomass and fermentation products was observed. As an exception, an increase in lactate production was observed (Fig. 3^b). Complete wash–out did not occur, however, and the maximum glucose concentration in the reactor was 47 mmol/l at $\tau = 8$ (influent concentration 55 mmol/l).

From about $\tau = 8$ onwards, glucose concentrations decreased again. Concomitantly, aggregate formation became visible to the eye, and biomass concentrations x_r and x_e increased again (Fig. 3^a). At $\tau = 20$ after shift–up, x_e was found to stabilize at 1.4 g/l. A continuing increase in x_r, however, resulted in a final value of $x_r = 7$ g/l and thus $R = 5.3$ at $\tau = 45$. At this stage, glucose was converted completely again.

The increase in x_r appeared to be linear from $\tau = 15$ to 40 (0.12 g/l·h). Since both (dx_r/dt) and x_e were found constant during this period, the mean specific growth rate of the bacterial population in the reactor was calculated to decrease gradually from 0.35 h^{-1} at $\tau = 15$ to 0.10 h^{-1} at $\tau = 40$.

When glucose conversion increased again at $\tau = 10$, fatty acid concentrations were seen to rise simultaneously (Fig. 3^c). In the final steady state at $D = 0.6$ h^{-1} (around $\tau = 50$), however, the composition of fermentation products differed markedly from the steady state at $D = 0.2$ h^{-1}. Propionate (23 mmol/l) was found as main product together with acetate (15 mmol/l), whereas butyrate was found in rather low amounts only (5 mmol/l). In addition, considerable amounts of valerate were detected (8 mmol/l), while lactate was absent again. As oppposed to the preceding steady state without aggregates, fatty acid

Fig. 3: Concentrations of biomass, substrate, and fermentation products *versus* dimensionless process time $(D \cdot t)$ after a shift—up in dilution rate (D) at $D \cdot t = 0$ (indicated by vertical dashed line). **Fig. 3^a:** Reactor and effluent dry—weight biomass concentrations (x_r and x_e, respectively). **Fig. 3^b:** Substrate and lactate concentrations (Glc and Lac, respectively). **Fig. 3^c:** Fatty acid concentrations (HAc: acetic acid; HPr: propionic acid; HBt: butyric acid; HVa: valeric acid).
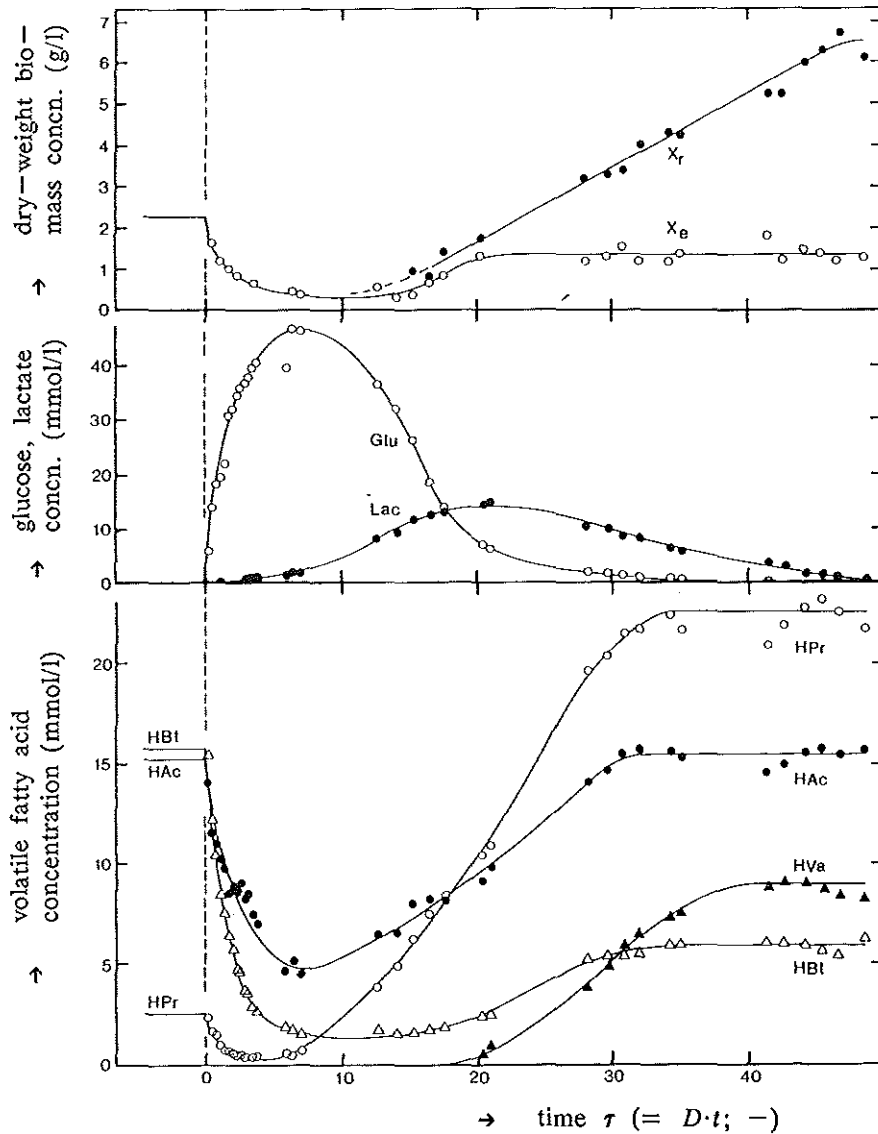
concentrations at $D = 0.6$ h^{-1} showed a tendency to fluctuate. The same holds for biomass concentrations.

Recovery of organic carbon was calculated with mass balances for the liquid phase only and varied between 90 and 95 %. No attempt was made to calculate overall carbon balances.

From the biomass determination employed, estimates were obtained of the total amount of sand remaining at any time in the reactor. It was found to decrease from an initial value of 17 g/l at $\tau = 0$ to less than 1 g/l at $\tau = 50$. On the other hand, however, a control experiment in which sand had been omitted *a priori* from the start−up routine failed to produce aggregates: a more severe wash−out was observed instead, followed by progressive wall growth at $\tau = 300 - 400$.

Mixing in all experiments was such that, notwithstanding the elevated concentration of titrant (8 mol/l), *pH* fluctuations did not exceed 0.15 units. Circulation time of the reactor contents was estimated to be $3 - 4$ s with the aid of an artificial 2 mm sphere with a density of 1000 kg/m^3.

Fig. 4. Biomass flotation upon interruption of gas flow in an aggregate−containing AGLR, producing major amounts of butyrate from glucose. **Figs. 4^a, 4^b, 4^c, and 4^d** : 25, 40, 60, and 150 s after interruption of gas flow, respectively.

Occasionally, start—up procedures resulted in the formation of butyrate/acetate—producing aggregates, as opposed to the propionate/ acetate—producing type described above (cf. Chapter III). In such cases, an incomplete glucose conversion and a more vigorous gas production was observed. Interrupting the recycle gas flow over a reactor containing such aggregates resulted in an initial settling of aggregates to the bottom of the reactor. Within a few minutes, however, a heavy gas production was observed, and the majority of the aggregates went to float at the liquid surface. The phenomenon is illustrated in Fig. 4.

DISCUSSION

The start—up procedure for the AGLR, involving carrier availability and a dilution—rate shift—up, proved to be very efficient and resulted in considerable hold—up within 6 days upon reactor inoculation. Sand was chosen as a carrier by virtue of its dimensions and specific weight (see also Andrews, 1986).

The increase in D imposes a strong selective pressure for bacterial adhesion to sand particles, and non—adhering bacteria are largely removed by wash—out. Similar principles for the start—up of anaerobic reactors were applied by Heijnen (1984), who advocated a shift—up in D beyond the maximum specific growth rate μ_{max} of the population under consideration. Zoetemeijer (1982) reported a μ_{max}—value of 0.33 h^{-1} for the population employed here; according to this latter value, a shift—up to $D = 0.6\ h^{-1}$ would comply to the recommendations of Heijnen. The findings of Zoetemeijer, however, were modified by Van den Heuvel (1985; Van den Heuvel & Beeftink, 1986), who established variation in attainable growth rates up to 0.6 h^{-1}, caused by the simultaneous inhibition of substrate and product. In any case, a D shift—up would select on the basis of hydraulic loading, as it requires an instantaneous growth—rate response from the bacterial population growing at $\mu = 0.2\ h^{-1}$. Also, it produces an instanteneous increase in growth—limiting substrate. Both phenomena may bear on the observed formation of aggregates. Generally, however, quite opposite recom— mendations are given for anaerobic bioreactor start—up, i.e. to avoid incomplete substrate conversion by careful and continuous adjustment of D (e.g. Salkinoja—Salonen et al., 1983).

This 6—day period for reactor start—up equals 70 minimum doubling times t_d reported for the population employed ($t_d =$ (ln 2)/μ_{max}). Literature provides a variety of data on establishment of hold—up in different types of reactors by various microbial populations and employing all kinds of start—up routines (e.g. Bull et al., 1983; Grin et al., 1983; Hulshoff Poll et al., 1983, 1984; Toldrá et al., 1986). In principle, the various times required to establish hold—up should be compared only after conversion to a dimensionless unit as above (i.e.

t/t_d). When done so, start—up times appear to range from 75 to 150 times (t/t_d), although the actual time spans vary from one day to several months. An exact comparison, however, is precluded by difficulties in precisely determining the beginning and end of the period of interest.

Establishment of hold—up ratios exceeding unity required the availability of sand, as evident from control experiments without sand. This requirement, however, appeared to be time—dependent: in regular experiments, elevated hold—up ratios and ample amounts of aggregates could be maintained notwithstanding the virtual absence of sand in the final steady state at $D = 0.6 \ h^{-1}$. Similar phenomena were observed in an electronmicroscopic study of aggregate formation (Beeftink & Staugaard, 1983, 1986; *this thesis*, Chapter IV). An explanation is found by postulating sand to provide a rather heavy adhesion support for biofilm formation during the initial phase of reactor start—up only. At this stage, aggregates formed by clumping of individual cells would be too small and too light to sediment from the effluent stream. Once biofilms grown on sand grains have acquired a certain critical thickness, however, substrate depletion at the biofilm basis may induce locally lysis and disintegration of cells, since maintenance requirements are no longer met. Such a weakening would seriously aggrevate detachment of biofilm fragments from the sand surface (sloughing) by external or internal forces (*e.g.* liquid shear, or gas bubbles arising from metabolic activity). A similar sloughing mechanism has been postulated before (Howell & Atkinson, 1976[a,b]). Such fragments could be large enough to be retained by the settling device, as opposed to aggregates originating from clumping of individual cells. Gradually, sand disappears from the reactor by *e.g.* sampling, and a steady state with aggregates but without sand results.

The importance of maintenance processes in case of biomass retention may be appreciated also by comparing data on effluent biomass concentrations at $D = 0.2$ and $0.6 \ h^{-1}$. The relatively low x_e—value at $D = 0.6 \ h^{-1}$ likely reflects substantial maintenance requirements due to the concomitantly elevated x_r—value. The specific maintenance coefficient may be estimated from these x_r and x_e data by means of a biomass balance on the reactor (Roels, 1983) to be approximately 0.05 g (glucose)/h·g (dry matter). Although this estimate should be considered tentative due to the limited number of data, the value is within the range reported for various organisms (Roels, 1983). It has been shown that higher R—values may be expected to decrease x_e still further (Heijnen, 1984).

Concomitantly with the main increase in x_r, *i.e.* from $\tau = 15$ to 40, the overall specific growth rate was found to decrease from 0.35 to 0.10 h^{-1}. Likely, this decrease is a direct consequence of the formation of aggregates and reflects the increasing limitations imposed on glucose transport into aggregates.

A marked difference in composition of fermentation products was

observed between the steady states at $D = 0.2$ h^{-1} (freely suspended cells) and $D = 0.6$ h^{-1} (aggregates). First of all, large amounts of valeric acid were formed upon formation of aggregates, pointing to the importance of lysis processes. Valerate is quite commonly formed in the fermentation of complex macromolecules (Doelle, 1975). This latter type of substrate would be available as debris from lysis in deeper parts of thick biofilms or aggregates, where glucose availability falls short of maintenance requirements. Interestingly, valerate has also been found an important fermentation product when the present population was grown in continuous culture with gelatin as a substrate (Breure & Van Andel, 1984). Therefore, substrate depletion and lysis may have contributed to the present production of valeric acid. On the other hand, valerate production by fermentation of simple substrates (C_2 and C_3) has also been reported before (Bornstein & Barker, 1948). In our case, glucose was the original substrate, but propionate and ethanol could have served as intermediates in such metabolism. However, the capability to ferment C_2 with C_3 to valerate seems to be limited to a very particular type of microorganism.

Furthermore, a transition was observed from an acetate/butyrate type of fermentation at $D = 0.2$ h^{-1} to an acetate/propionate fermentation at $D = 0.6$ h^{-1}. Micro—organisms which produce acetate and butyrate as well as propionate from glucose appear to be rather incommon. Thus, although metabolic adaptation cannot be excluded completely, this transition is thought to reflect a shifting composition of the microbial population. Such a shift is quite conceivable, since increasing D from 0.2 to 0.6 h^{-1} imposes a severe selective pressure for either high specific growth rates or good adhesive properties. Since the metabolic transition was not observed in the control experiment without sand (absence of adhesion), selection for a high specific growth rate alone cannot explain this phenomenon. It is concluded therefore, that propionate—forming organisms have better adhesive properties than their butyrate—forming competitors. The latter organisms may be envisaged to be entrapped during biofilm formation by propionate—producing bacteria, thus explaining the residual production of some butyric acid. Such entrapment of non—adhesive bacteria has been reported before (Costerton et al., 1978; c.f. this thesis, chapter IV).

Putatively identical start—up procedures were used in all experiments, but occasionally aggregates were formed that produced butyrate/acetate from glucose instead of propionate/acetate. The phenomenon is poorly understood at the moment, and likely has to be attributed to inoculum variations (cf. this thesis, chapter III).

Although the final state at $\tau = 60$ is referred to as "steady", product concentrations were seen to fluctuate somewhat. Interestingly, various authors indicate a fluctuating performance to be characteristic for reactors with retention of micro—organisms (Hawkes, 1957; Heukelian & Crosby, 1956; Howell & Atkinson, 1976[a,b]; Sanders, 1966). Sometimes,

such fluctuations are explained with a periodicity of the sloughing process. Further research on the development of an eventual steady state will be presented elsewhere (*this thesis*, Chapter V).

From the absence of appreciable *pH* fluctuations during titration, it is concluded that the liquid phase in the AGLR should be considered well−mixed. This is in agreement with the very short circulation time of the reactor contents, which even at $D = 0.6$ h^{-1} does not exceed $(1/D)\cdot10^{-3}$. The literature provides ample data indicating air− or gas−lift reactors to be comparable to the classical completely−stirred tank reactor with respect to mixing efficiency (e.g. Kubota *et al.*, 1978; Merchuk *et al.*, 1980; Verlaan, 1985). The construction details of the AGLR employed in our study (equal riser and downcomer areas), and the operating conditions employed (superficial gas velocity in the riser of 6 mm/s) are within ranges reported as optimal for mixing in airlift fermenters (Blenke, 1979; Rousseau & Bu'lock, 1980; Hsu & Duduković, 1980; Moresi, 1981; Onken & Weiland, 1983). As a result of mixing, aggregates were seen to be dispersed randomly throughout the reactor, without the stratification of aggregates of different size, density, or composition as may be observed in fluidized−bed reactors (Bull *et al.*, 1984; Fan *et al.*, 1984; Matsuura & Fan, 1984; Cooper & Clough, 1985; Muroyama & Fan, 1985; Patwardhan & Tien, 1985).

Apparently, the reactor configuration and operating conditions employed in this study facilitated efficient transport of fermentation products from within aggregates to the bulk liquid. This is of particular importance if gaseous fermentation products are involved, as is strongly the case with the butyrate−producing aggregates that were sometimes obtained upon reactor start−up. Such aggregates were efficiently retained during normal reactor operation, but rapidly began to flotate upon interruption of reactor mixing. The phenomenon is attributed to a hampered transport of e.g. carbon dioxide, resulting in a decrease in aggregate density due to internal gas bubble formation.

The fact that all aggregates in the AGLR are subjected to identical environmental conditions, and are dispersed throughout the reactor, renders the present AGLR configuration particularly suited for the analysis of aggregate development (*cf. this thesis*, Chapters IV and V). Such analysis would be important for other reactor types as well (upflow anaerobic sludge−blanket, fluidized−bed, and tower reactors). These latter types, however, are less appropriate for research due to liquid inhomogeneities or aggregate stratification.

ACKNOWLEDGEMENTS

ESTABLISHMENT OF BIOMASS HOLD−UP
IN A GAS−LIFT REACTOR : INFLUENCE
OF CARRIER AVAILABILITY

SUMMARY

A dilution−rate shift−up was employed to induce bacterial hold−up in a continuous−flow gas−lift reactor. A minimum availability of carrier material (sand, ca. 2−5 g/l) was found a prerequisite for aggregate formation. When the amount of sand exceeded 5 g/l, either propionate/acetate− or butyrate/acetate−producing aggregates were formed, which was attributed to inoculum variations and could not be related to sand availability. A complex relation between the amount of sand on one hand and the onset and subsequent rate of aggregate formation on the other was observed. Increasing the amount of available sand beyond the minimum value decreased the rate at which propionate/acetate−producing aggregates were formed, whereas the onset of formation of these aggregates remained virtually unaffected. A reverse effect was found for butyrate/acetate−producing aggregates, which grew at a constant rate whereas the onset of their formation was progressively retarded by increasing amounts of sand.

INTRODUCTION

Retention of biomass aggregates is a widespread technique aiming at improvement of the volumetric loading capacity of continuous−flow bioreactors. Often, an inert carrier is added to the reactor contents as a support material for bacterial adhesion, thus promoting formation of relatively heavy bacterial aggregates (Andrews, 1986; Andrews & Przezdziecki, 1986), which subsequently may be retained in the continuous−flow system by sedimentation.

Recently, a continuous−flow well−mixed anaerobic gas−lift reactor (AGLR) was described in which formation of mixed−culture aggregates from freely suspended cells was induced by means of a dilution−rate

shift—up (Beeftink & Van den Heuvel, 1986; *this thesis*, Chapter II). In these experiments, the AGLR contained sand as a carrier for bacterial adhesion. Preliminary data indicated that aggregates were not formed if sand was absent during the early stages of a start—up procedure. Electronmicroscopic data also indicated the importance of sand as adhesion support (Beeftink & Staugaard, 1986; *this thesis*, ChapterIV).

Formation of aggregates after a dilution—rate shift—up has been shown to coincide with a linear increase in reactor biomass concentration with time. This increase is preceded by a period of severe biomass wash—out and incomplete substrate conversion (*this thesis*, Chapter II). In view of the requirement for a carrier, it is conceivable that the extent of the wash—out period and/or the rate of aggregate formation are related to the amount of sand being available as adhesion support. Therefore, a series of start—up experiments was carried out with varying initial amounts of sand.

The results presented in this chapter have been submitted for publication elsewhere (Beeftink *et al.*, 1986).

MATERIALS & METHODS

Reactor, medium, growth conditions, and analytical determinations have been described previously (*this thesis*, Chapter II).

Start—up procedure and inoculation. The AGLR was inoculated with fresh or lyophilized samples from an activated—sludge plant treating municipal wastewater. Reactor inoculation and start—up routine have been described previously (*this thesis*, Chapter II), and involved a dilution—rate (D, h^{-1}) shift—up from 0.2 to 0.6 h^{-1}. Varying concentrations of sand at the start of each experiment were used, however (2.5, 5, 7.5, 12.5, and 25 g/l). Since the quantity of sand in the reactor decreased with time due to sampling for analytical purposes, all eventual data were related to the concentration present at the moment of D shift—up (z_0).

Rate of aggregate formation. In each experiment, reactor biomass concentrations $(x_r, g/l$ dry weight) started to increase significantly and linearly after a period of wash—out following the dilution—rate shift—up; ultimately, x_r—values leveled off (*this thesis*, Chapter II). After conversion to dimensionless time $(\tau = D{\cdot}t; t$: time, h), the slope of the linear part of the reactor—biomass curve, as obtained by least—squares analysis, was defined as the rate of aggregate formation $(dx_r/d\tau, g/l)$.

Onset of aggregate formation. The onset of aggregate formation was characterized by an abscissa value τ_x, obtained upon extrapolation towards $x_r = 0$ g/l of the linear part of the x_r *vs.* τ relationship (see paragraph above). Similarly, the time courses of the sum of short—

Fig. 1   Fig. 2
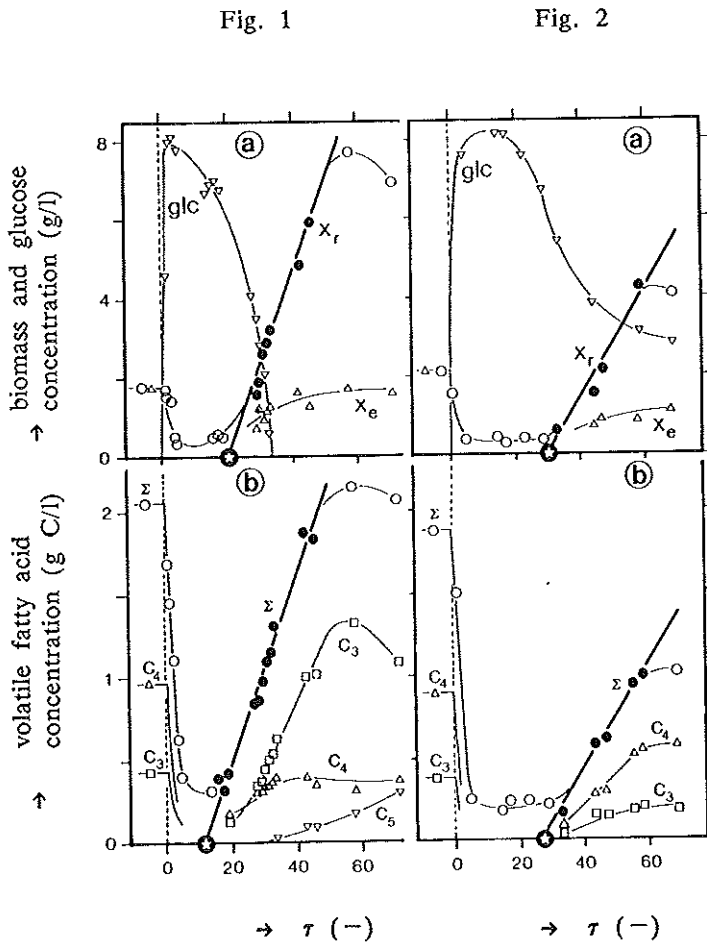
Fig. 1^a : Formation of HPr−aggregates: time courses of concentrations of reactor biomass (x_r, $\circ$ and $\bullet$; solid symbols are used for calculation of linear relation), effluent biomass (x_e, $\triangle$), and glucose (glc, ∇). Asterisk indicates $\tau_{3,x}$, and slope $(dx_r/d\tau)_3$. **Fig. 1^b** : *idem*, time courses of short−chain fatty acids; propionate (C_3, $\square$), butyrate (C_4, $\triangle$), valerate (C_5, ∇), and total fatty acid (Σ, $\circ$ and $\bullet$; solid symbols used for calculation). Asterisk: $\tau_{3,a}$. **Fig. 2^a** : Formation of HBt−aggregates. Symbols as in Fig. 1^a; asterisk and slope indicate $\tau_{4,x}$ and $(dx_r/d\tau)_4$, respectively. **Fig. 2^b** : *idem*, time courses of short−chain fatty acids. Symbols as in Fig. 1^b; asterisk indicates $\tau_{4,a}$. Shift−up in dilution rate from $D = 0.2$ h^{-1} to $D = 0.6$ h^{-1} at $\tau = 0$ in all cases.

—chain fatty—acid concentrations were used to obtain an alternative characterization τ_a of the onset of aggregate formation.

RESULTS

The results of two typical start—up experiments are shown in Figs. 1 and 2. Starting points for both experiments were steady states at low dilution rate ($D = 0.2$ h^{-1}), characterized by the absence of biomass retention ($x_r = x_e$; x_e: effluent biomass concentration, g/l dry weight). In the experiment represented by Fig. 1, the AGLR contained an initial sand concentration of 25 g/l, which at $\tau = 0$ had decreased to $z_0 = 19$ g/l. As a result, aggregates were formed that, in addition to butyric and acetic acids, fermented glucose to significant amounts of propionic acid (HPr). In the second experiment (Fig. 2), the AGLR contained an initial sand concentration of 12.5 g/l, which had decreased to $z_0 = 11$ g/l at $\tau = 0$. Although experimental conditions were putatively unchanged, a metabolically quite different type of aggregate was formed in this second experiment, producing butyric acid (HBt) in excess to propionic acid. Also, an incomplete substrate conversion was observed
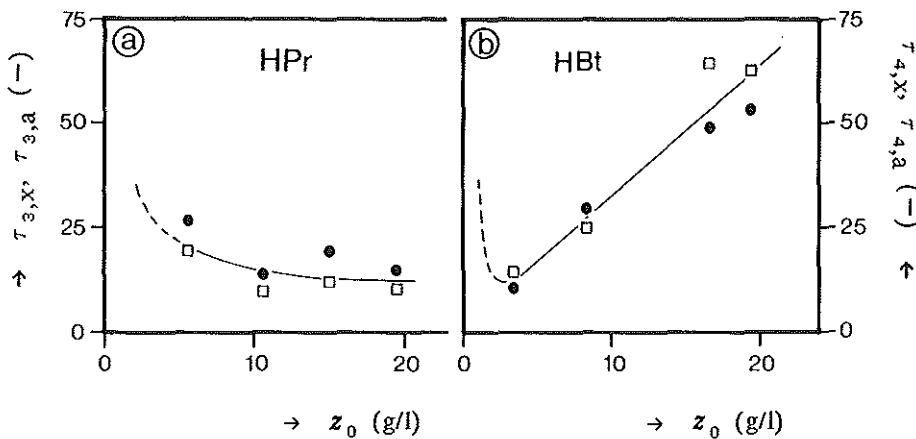
Fig. 3 : Influence of the concentration of carrier material at dilution—rate shift—up (z_0) on time span preceding the onset of aggregate formation. Dimensionless time spans were estimated from biomass data as well as from total fatty—acid data (τ_x and τ_a, respectively). Dashed line: extrapolation (see text). **Fig. 3a** : Propionate—forming aggregates (● : $\tau_{3,x}$; □ : $\tau_{3,a}$). **Fig. 3b** : Butyrate—forming aggregates (● : $\tau_{4,x}$; □ : $\tau_{4,a}$).
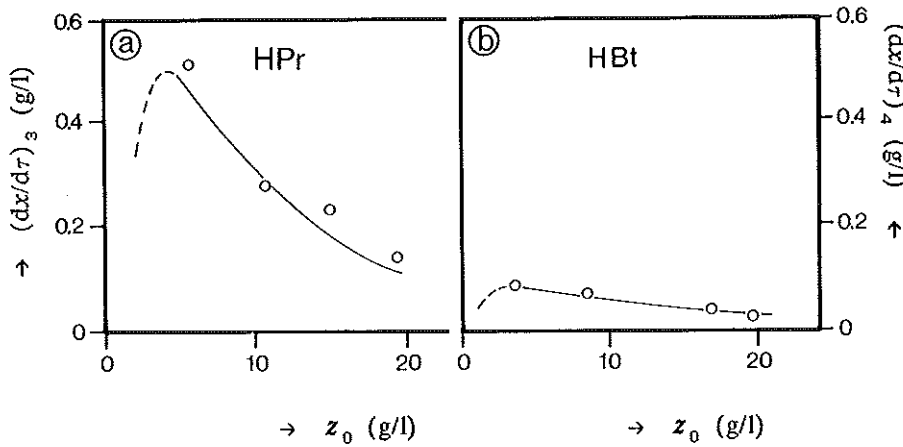
Fig. 4 : Rate of formation of aggregates $(dx_r/d\tau)$ after a dilution—rate shift—up as depending on the concentration of available carrier material at D shift—up (z_0). Dashed line: extrapolation (see text). **Fig. 4a** : Propionate—forming aggregates: $(dx_r/d\tau)_3$. **Fig. 4b** : Butyrate—forming aggregates: $(dx_r/d\tau)_4$.

for prolonged periods of time, while x_r—values remained moderate. In either case, no difference was observed with respect to acetate production (not shown). But whereas propionate/acetate production coincided with production of valerate (*cf. this thesis*, Chapter II), the latter acid was absent in case of butyrate/acetate production. Both types of aggregates will subsequently be referred to as HPr—aggregates and HBt—aggregates, respectively.

In Fig. 1a, the rate of HPr—aggregate formation $(dx_r/d\tau)_3$ equals 0.23 g/l, and is indicated as the slope of the straight line fitted to x_r—data. The time elapsing before the onset of formation of HPr—aggregates was estimated from this linear biomass relation and equalled $\tau_{3,x} = 21$ (Fig. 1a). From short—chain fatty—acid concentrations in Fig. 1b, an alternative for this latter value was obtained as $\tau_{3,a} = 12$.

Similar calculations were performed with the data on HBt—aggregates (Fig. 2). The onset of formation of HBt—aggregates occurred at $\tau_{4,x} = 30$ (Fig. 2a) or $\tau_{4,a} = 25$ (Fig. 2b), whereas the rate of formation was estimated as $(dx_r/d\tau)_4 = 0.13$ g/l (Fig. 2a).

Data on τ_x, τ_a, and on $(dx_r/d\tau)$ from Figs. 1 and 2 as well as from other experiments with different z_0—values are summarized in Figs. 3 and 4 for HPr— and HBt—aggregates, respectively. First of all, either

HPr—aggregates or HBt—aggregates were formed at all z_0—values tested (except the lowest), thus excluding any role for z_0 in determining the type of aggregate. While τ_3—values were virtually independent of z_0 (Fig. 3^a), a positive correlation between τ_4 and z_0 was observed, $i.e.$ formation of HBt—aggregates was progressively retarded with increasing concentrations of sand (Fig. 3^b). Start—up experiments with an initial sand concentration $z_0 = 2$ g/l, failed to produce either HPr—aggregates or HBt—aggregates (results not shown). Accordingly, lines in Figs. 3^a and 3^b were not extrapolated towards the origin, but exhibit an upward curvature at low z_0, indicating a minimum sand concentration to be required for any aggregate formation.

Fig. 4^a shows a negative correlation between z_0 and $(dx_r/d\tau)_3$, $i.e.$ the rate at which HPr—aggregates are formed was lower at high sand concentrations. Such an effect was not observed for HBt—aggregates; the dependency of the rate of their formation $(dx_r/d\tau)_4$ on the sand concentration z_0 was, if anything, far less pronounced than with HPr—aggregates (Fig. 4^b).

DISCUSSION

Low levels of carrier availability are shown to have a beneficial effect on bacterial aggregate formation. Below 3 g/l of sand at $\tau = 0$, neither HPr—aggregates nor HBt—aggregates were formed. This is in agreement with preliminary observations (*this thesis*, Chapter II). Therefore, it is concluded that sand is essential for aggregate formation during the initial phase of reactor start—up. Due to its dimensions and specific weight, sand has a relatively long residence time in the AGLR, thus providing an excellent substratum for bacterial attachment and subsequent biofilm formation (Andrews, 1986). As apparent from absence of hold—up in the steady state at low dilution rate ($D = 0.2$ h^{-1}, $R = 1$), and from the initial wash—out of biomass upon the shift—up to $D = 0.6$ h^{-1}, individual bacterial cells are not retained by the settling device. Depending on the fluid turbulencies in the effluent section, retention of particulate material is not only determined by its settling velocity, but has stochastic characteristics as well. However, if settling velocities (v_∞) are high with respect to the mean upward liquid velocity in the effluent section, retention becomes increasingly efficient. The liquid velocity may be calculated to average 0.2 mm/s at $D = 0.6$ h^{-1}, $i.e.$ largely exceeding v_∞ for individual bacterial cells. With sand as adhesion support, however, v_∞ values exceeding 0.2 mm/s are easily attainable for sand/biomass aggregates: v_∞ values for bare sand grains may be calculated to average 32 mm/s.

Literature provides some conflicting data on requirement for carrier material during start—up of various reactors. Hulshoff Pol *et al.* (1984) postulate that a carrier would be superfluous in any bioreactor. Wiegant
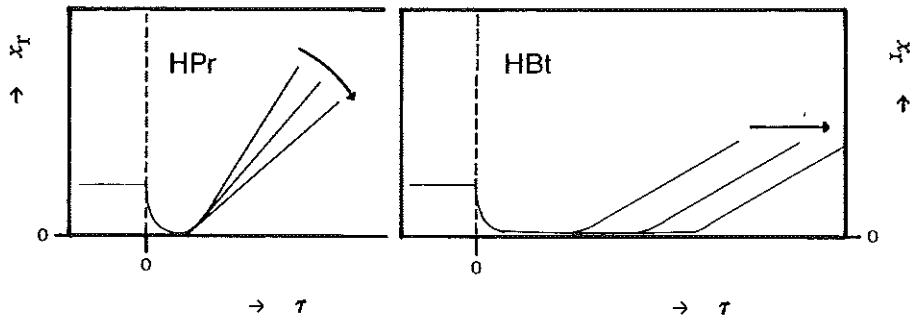
Fig. 5 : Summary of the effects of varying availability of carrier material on time courses of reactor biomass concentrations x_r after a dilution rate shift−up at $\tau = 0$, indicated by vertical dashed lines. Arrows indicate increasing concentrations of sand. Axes are arbitrary but identical for a and b. **Fig. 5a** : HPr−aggregates. **Fig. 5b** : HBt−aggregates.

& De Man (1986) demonstrated that formation of methanogenic aggre− gates is not depending on the presence of support material (which, however, might have been present in their seed material). Still, the latter authors suggested at the same time carrier availability to influence the onset and rate of aggregate formation.

Although a minimum level of carrier availability was required in our experiments, a further increase in sand concentration beyond this level had negative effects. Such negative effects can be explained as reflecting increasingly frequent collisions of sand grains, resulting in damage to biofilms originating on them. Biofilm damage due to carrier collisions has been demonstrated before (Weise & Rheinheimer, 1978; Molin & Nilsson, 1985). Manifestation of these effects took different forms, however, depending on the type of aggregate formed (i.e. propionate− and butyrate−producing types, respectively). Fig. 5 gives a summary of these effects for both types of aggregates.

In case of HPr−aggregates, the time elapsing before the onset of aggregate formation showed, if any, a slightly negative correlation with the concentration of sand z_0. The rate of formation of these aggregates, however, was more strongly influenced by z_0, as it decreased with increasing amounts of sand (Fig. 5a).

A reversal of these effects was observed for HBt−aggregates, which were formed at a constant rate, but progressively later when z_0 was increased (Fig. 5b).

At present, it is not understood why HPr−aggregates behave

differently from HBt−aggregates with respect to variations in z_0. Structural differences between these two types have been demonstrated microscopically (*this thesis*, Chapter IV), and might be of interest. HPr−aggregates were shown to be rounded with a deteriorated interior, whereas HBt−aggregates have a more open and presumably more flexible structure. Conceivably, such differences would render aggregates more or less susceptible to forces from liquid turbulencies or from collisions.

The mere formation of HBt−aggregates was initially looked upon as an occasional and rather annoying experimental aberration, as HPr−aggregates are the more common type (*cf. this thesis*, Chapter II). At the moment, variations in the seeding material are thought to cause this variation in type of aggregate formed. Still, this unwanted variation has elucidated interesting variations in aggregate behaviour, which merits further research. A mechanistic analysis of events during aggregate development would require data on the number and physical characteristics of individual aggregates as depending on z_0. At the moment, such information is not available.

ACKNOWLEDGEMENTS

SUMMARY

Electronmicroscopic examination revealed incipient colonization of sand grains by bacteria from the bulk liquid to occur in surface irregularities, conceivably reflecting local quiescence. Subsequent confluent biofilm formation on sand grains proved to be unstable, however. Substrate depletion is assumed to weaken deeper parts· of the biofilm due to cellular lysis, whereafter production of gas bubbles and liquid shearing forces cause sloughing. The resulting fragments, although sand—free, are nevertheless large enough to be retained in the reactor and gradually gain in size by bacterial growth and by clumping together with other fragments. Numerical cell densities within aggregates range from 10^{12} ml^{-1} at the periphery to very low values in the centre. Cells are enmeshed in a polymer matrix containing polysaccharides; nevertheless, carbon sufficiency is not a prerequisite to sustain high hold—up ratios.

INTRODUCTION

Unlike many other bioreactors, wastewater treatment plants are commonly operated on a continuous—flow basis. Such process conditions require retention of active micro—organisms to obtain elevated biomass concentrations, which improve reactor loading capacity and stability (Atkinson, 1981; Hamer, 1982; Van den Heuvel & Zoetemeyer, 1982). This holds in particular for anaerobic treatment processes, which are characterized by undesirably low biological rate constants.

Retention may be achieved by the adhesion of micro—organisms on a stationary support, as in packed—bed reactors. Fluidized—bed bioreactors on the other hand rely on the settling of aggregates, thus circumventing the channeling problems frequently encountered with packed—bed configurations.

Clearly, the mechanisms by which bacterial aggregates are formed

are of particular relevance, not only to the field of wastewater treatment, but to continuous−flow devices employing biomass retention in general as well. Electronmicroscopy may provide important information pertaining to these mechanisms. Reports are available on the microstructure of bacterial aggregates from aerobic or partly aerobic plants (Mack *et al.*, 1975; Tago & Aida, 1977; Wheatly, 1981; Alleman *et al.*, 1982; Eighmy *et al.*, 1983; Kinner *et al.*, 1983), but data on completely anaerobic systems are scarce (Robinson *et al.*, 1984). In either case, medium composition and hydraulic regimen are often ill−defined and constantly varying, and the reactor contents may be poorly mixed in order to promote settling and retention.

In the present paper light− and electronmicroscopic techniques were used to study the structure of mixed−culture aggregates formed under well−defined conditions of substrate feed (carbon limitation) and hydraulic regimen. As a laboratory model process, we investigated the acidification of glucose in a well−defined mineral medium, representing the first stage in the mineralization of carbohydrates in anaerobic digestion.

Aggregates were formed in a novel continuous−flow anaerobic gas−lift reactor (AGLR) from freely suspended cells with liquid−suspended sand as adhesion support. Electronmicroscopic examination of aggregates was carried out at several stages during reactor start−up (*cf. this thesis,* Chapter II) and the subsequent steady state. The AGLR was designed to enable retention in an otherwise well−mixed reactor, thus improving mass transport in the liquid phase and allowing of high−rate acidification and of optimal control of process conditions.

The contents of this chapter have been published elsewhere (Beeftink & Staugaard, 1983, 1986)

MATERIALS AND METHODS

AGLR, medium, culturing conditions, inoculation, start−up routine and chemical analyses have been described earlier (*this thesis,* Chapter II).

Transmission electronmicroscopy (TEM). Aggregate−containing samples (20 ml) from the AGLR were decanted and 20 ml 0.15 mol/l NaCl was gently added. Washing with saline was repeated twice and followed by pre−fixation for 60 min in 2 % glutaraldehyde in phosphate buffer (0.1 mol/l, *pH* 7.0). Subsequently, the sample was washed three times in a veronal/acetate buffer (VA; Ryter *et al.*, 1958), and fixed for 16 h in VA buffer containing 10 g/l osmium tetroxide and 3 g/l ruthenium red. Dehydration in an ethanol series made up with 1 g/l ruthenium red in VA buffer was followed by embedding in araldite CY212. Thin sections were cut with an ultramicrotome, mounted on clean 400−mesh grids or on formvar−covered 100−mesh grids, and examined in a Philips EM300

transmission microscope at 40 or 60 kV.

Scanning electronmicroscopy (SEM). Samples were washed in saline as described for TEM, dehydrated in an ethanol series made up with 0.15 mol/l NaCl, and critical—point dried in liquid carbon dioxide. Dry samples were mounted on SEM stubs with silver paint, sputter—coated with gold/ palladium, and examined in a Cambridge Stereoscan MkII at 20 or 30 kV, or in an ISI DS130 at 3 to 40 kV.

Alcian—blue staining. Smears of aggregates were made on a specimen slide, heat fixed, stained with alcian blue, and examined microscopically (Gurr, 1965).

Lightmicroscopy (LM). Samples were fixed and embedded as described for TEM. Semi—thin sections were embedded in Entellan® (Merck, Darmstadt, FRG) on a specimen slide, covered with a covering slip, and examined in a Zeiss Photomicroscope III under dark—field illumination.

Numerical and volumetric cell concentrations. For cell—density measurements, appropriate TEM micrographs (linear magnification 10^4) were covered with a square lattice (8.65 intersection points per cm^2). The fractional area A_a of bacterial cells (i.e. total area occupied by cells per unit area of the micrograph) was measured as the fraction of intersection points coinciding with bacterial cells. According to the principle of Delesse (Weibel, 1979), A_a was used as an unbiased estimate for the fractional volume V_v (i.e. the total volume of cells per unit volume of aggregate; Weibel, 1979). Calculation of numerical concentrations (N_v, number of cells per unit volume of aggregate) could not be done straightforwardly due to large variations in cell shapes and volumes. Therefore, N_v values were estimated as V_v/V_c, V_c being individual cell volumes as estimated from SEM micrographs.

Table 1 : Comparison of concentrations of fermentation products (mmol/l) and biomass retention R $(-)$ before and after formation of aggregates (*i.e.* at $D = 0.2$ h^{-1} and $D = 0.6$ h^{-1}, respectively).

D	acetate	propionate	butyrate	valerate	R
0.2	18	4	23	0	1
0.6	17	29	9	9	6
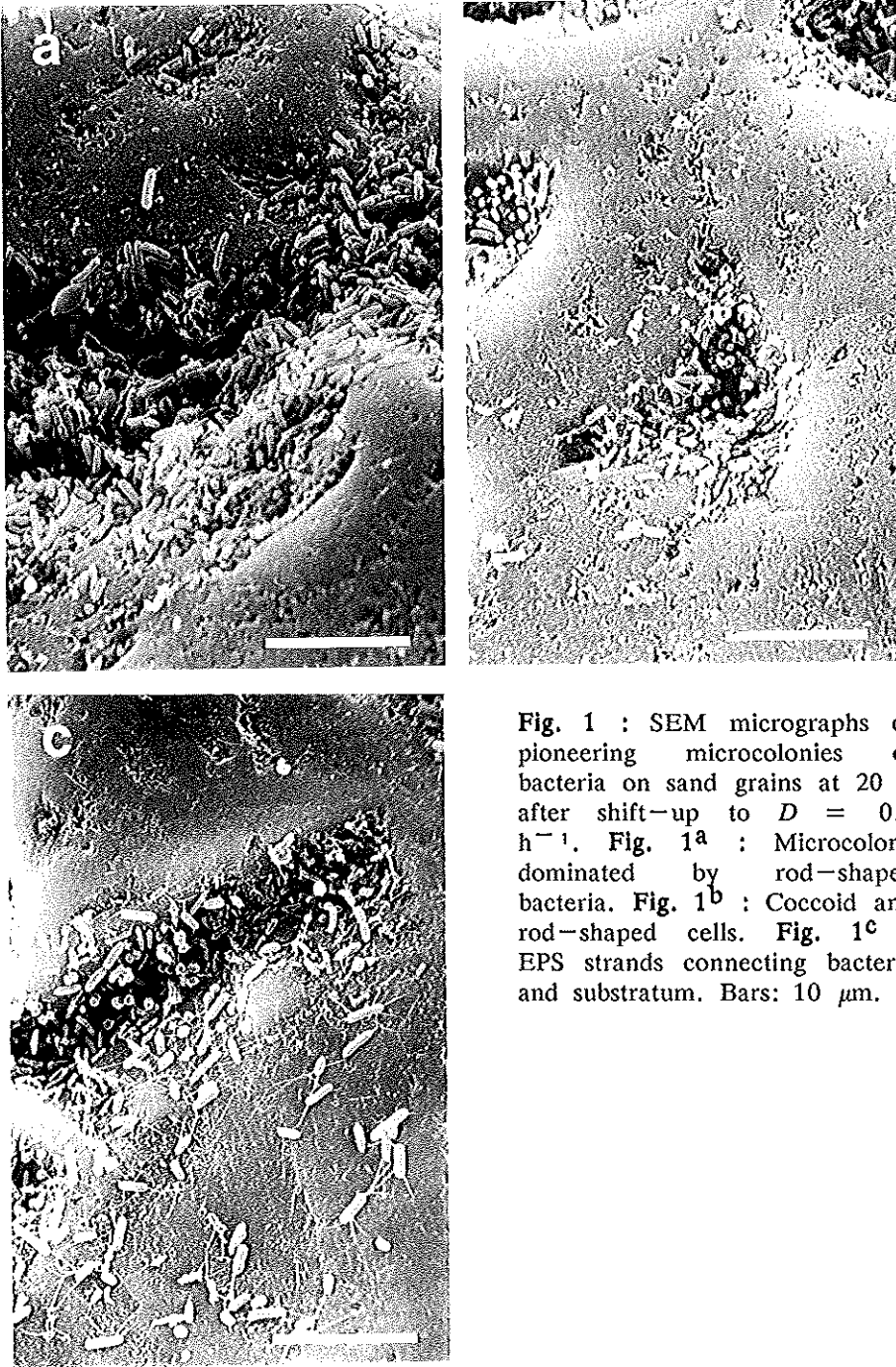
Fig. 1 : SEM micrographs of pioneering microcolonies of bacteria on sand grains at 20 τ after shift−up to D = 0.6 h^{-1}. Fig. 1^a : Microcolony dominated by rod−shaped bacteria. Fig. 1^b : Coccoid and rod−shaped cells. Fig. 1^c : EPS strands connecting bacteria and substratum. Bars: 10 μm.

RESULTS

Electronmicroscopic data on aggregate development were obtained at various stages during reactor start—up and during the subsequent steady state. Table 1 gives steady—state concentrations of biomass and short—chain fatty acids before and after the formation of aggregates (D = 0.2 h^{-1} and D = 0.6 h^{-1}, respectively), showing a shift from butyrate/acetate to propionate/acetate fermentation. In addition, hold—up establishment coincided with the production of valerate. These data are in agreement with the general pattern described before (*this thesis*, Chapter II).

    A visual indication on the role of sand during early stages of the start—up procedure was obtained from SEM micrographs. Figs. 1 and 2 represent very early forms of aggregates, sampled from the reactor at 20 τ after the shift—up in dilution rate, *i.e.* at a stage when the glucose concentration was 4 g/l (τ = $D \cdot t$; τ = 0 is defined as the momemt of D shift—up). The sand is seen to be preferently colonized in crevices or depressions (Fig. 1). Microcolonies generally were heterogeneous, but sometimes were predominated by a single morphological type. More detailed micrographs indicate rod—shaped bacteria to be linked to each other and to their substratum by a fibrous material (Fig. 2^a), whereas coccoid cells showed, if any, a different and less abundant type of extracellular material (Fig. 2^b). In addition, the sand surface itself was

Fig. 2 : SEM details of pioneering bacteria on sand surface at 20 τ after shift—up. Fig. 2^a : Strand—like EPS between rod—shaped cells and sand surface. Fig. 2^b : Cocci, with less extensive EPS. Bars: 1 μm.
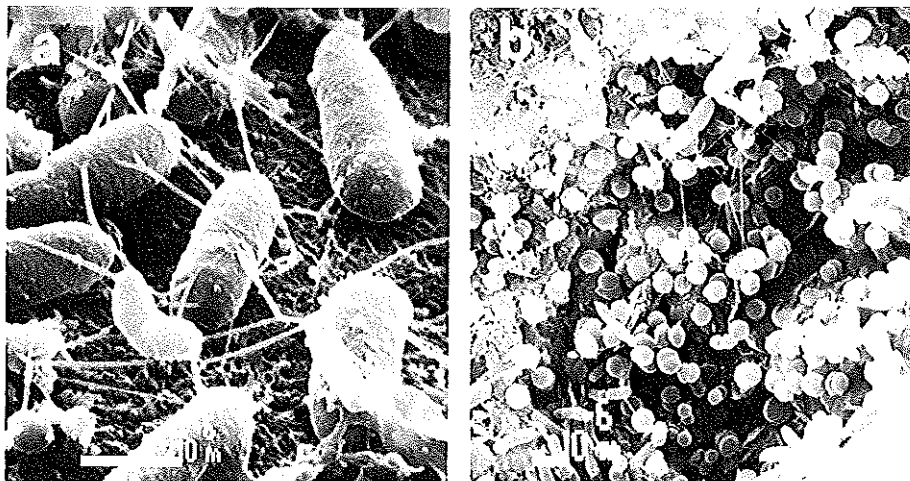
Fig. 3 : SEM view of biofilm—covered sand grain; sloughing exposed part of the sand surface. Bar: 10 μm.

Fig. 4 : Overall SEM appearance of steady—state aggregate at 80 τ. Fissures and irregularities (arrows) between rather smooth sub—aggregates. Bar: 500 μm.
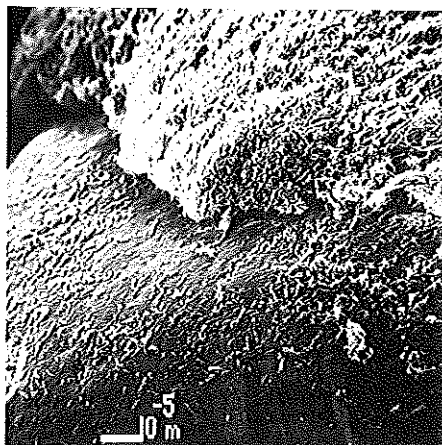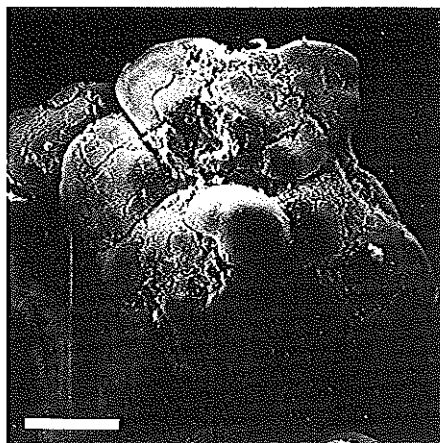
Fig. 3   Fig. 4

covered with an amorphous substance.

Fig. 3 represents a further stage of aggregate development (40 τ after shift—up, when glucose conversion was complete again). Generally, a confluent biofilm was observed, but quite often parts had sloughed off the sand surface. In such cases, biofilm thickness was estimated to range from 20 — 50 μm.

Fig. 4 shows the general SEM appearence of the eventual form of aggregate, sampled from the AGLR 80 τ after shift—up, i.e. when the new steady state at $D = 0.6$ h^{-1} had become established. Typically, such aggregates had a diameter of 1.0 — 1.5 mm. Although some parts were very smooth, the overall aggregate surface appeared to be divided in sub—regions by fissions and irregularities.

TEM sections were prepared also from steady state aggregates. Unexpectedly, no difficulties were encountered in sectioning, obviously indicating the absence of sand grains in the centre of these aggregates. Such ruthenium—stained TEM sections are shown in Fig. 5. At high magnification (Fig. 5^a), a considerable amount of extracellular ruthenium—positive polymeric substance (EPS) is seen to be intimately connected with Gram—negative rod—shaped bacteria. However, a morphologically distinct rod—shaped cell was often seen to lack directly

Fig. 5 : Ruthenium red—stained TEM section of a steady—state aggre—gate at 80 τ. **Fig. 5^a** : Gram—negative rod—shaped bacteria, intimately connected with surrounding EPS (bar: 1 μm). **Fig. 5^b** : Bacterium in a clear zone without EPS; same aggregate (bar: 1 μm). **Fig. 5^c** : TEM overview at low magnification. Coccoid cells are seen to lie a in a clear zone (arrow), and may dominate larger areas (left side). Bar: 5 μm.
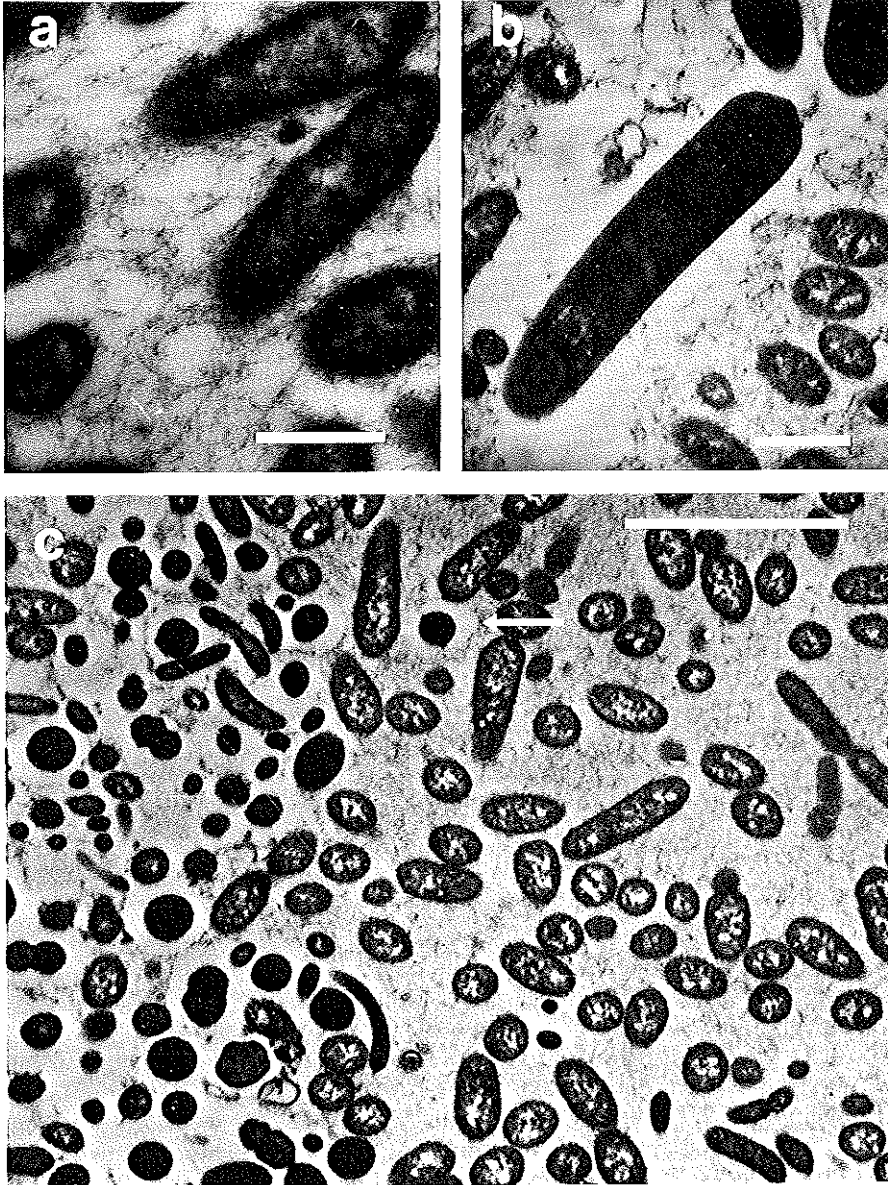
Fig. 6^a : Low magnification LM view of an entire steady—state aggregate under dark—field illumination (80 r). A central area of low bacterial density and various sub—aggregates are seen. Bar: 250 μm. **Fig. 6^b** : High—magnification detail of upper boxed area in panel a. The fissure between two subaggregates is seen to be occupied by a micro— scopically distict population. Bar: 50 μm. **Fig. 6^c** : High—magnification LM micrograph of the outer boundary of an aggregate (lower boxed area in panel a). Separate population is seen at the periphery. Bar: 50 μm.
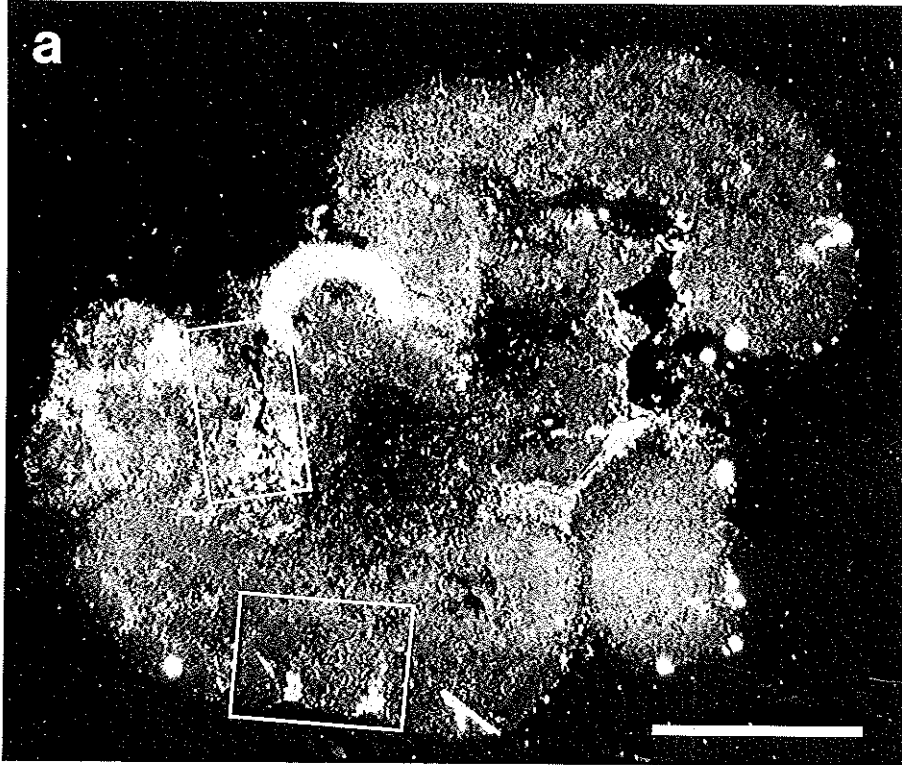
adhering EPS and to lie in a clear zone (Fig. 5^b). The same held for Gram—positive coccoid cells, which, at lower magnification, were observed to form microcolonies within areas predominated by EPS—forming rod—shaped cells (Fig. 5^c).

Apart from its reaction towards ruthenium, a further indication on the chemical nature of the EPS was obtained from anthrone determinations. Steady—state aggregates contained 15 — 25 % (w/w) sugar (expressed as glucose on a dry weight basis), whereas this figure was three times as low for freely suspended cells, taken from the AGLR
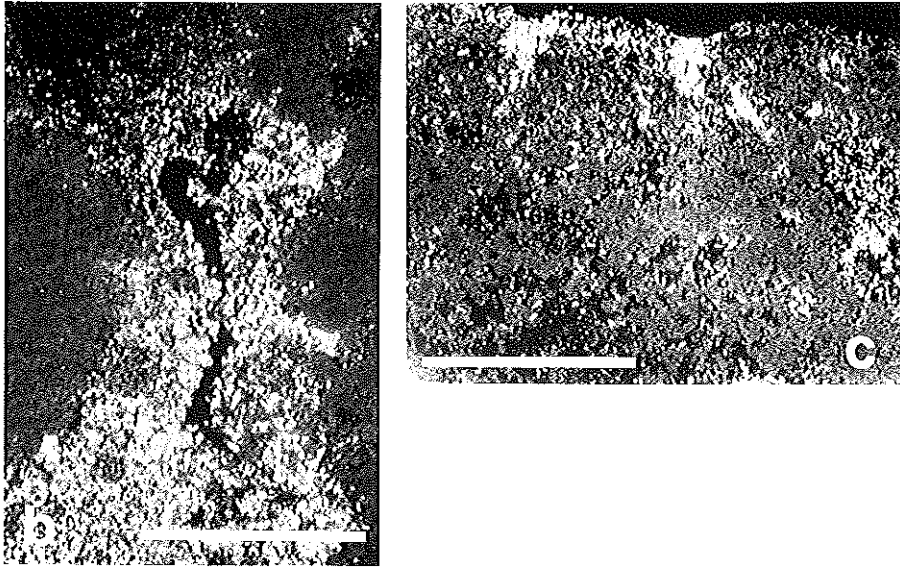
at low dilution rate ($D = 0.2$ h^{-1}). In addition, staining smears of steady−state aggregates clearly indicated the presence of alcian−blue positive extracellular material (not shown).

From low−magnification TEM micrographs (e.g. Fig. 5^c), the fractional bacterial volume within aggregates (V_v) was calculated to range from 0.21 − 0.27 for steady−state aggregates. Based on individual cell volumes (V_c) of 0.2 − 0.5 μm^3, numerical cell concentrations N_v may be estimated as 0.4x10^{12} − 1.4x10^{12} ml^{-1}.

As with TEM, sand grains were not encountered in sectioning for LM. A general LM overview of a steady−state aggregate is given in Fig. 6^a. Towards the centre, a deteriorated appearance with very low cellular densities is observed. Furthermore, aggregates consisted of several sub−aggregates. At the aggregate/liquid interface (Fig. 6^b), and at separations between sub−aggregates (Fig. 6^c), population differences could be observed microscopically. Often, microcolonies appeared to penetrate from the surface into deeper regions (Fig. 6^c).

As has been shown previously, start−up procedures may result in the occasional formation of aggregates that mainly produce butyric and acetic acid instead of propionic, acetic, and valeric acid (*this thesis*, Chapter III). Fig. 7 gives an overall lightmicroscopic view of such a butyrate−producing aggregate, demonstrating marked differences with propionate−forming aggregates (*cf*. Fig. 6^a). A more diffuse and loose
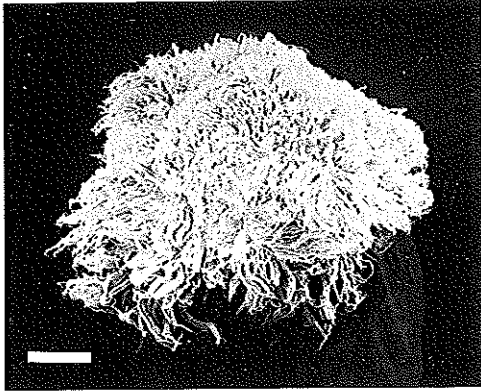
Fig. 7 : General SEM view of a butyric—acid producing aggregate, with a loose and hairy appearance. Bar: 500 mm.

morphology is observed, with liquid channels penetrating into the interior of the aggregate.

DISCUSSION

With the aid of SEM techniques, the onset of biofilm formation was observed as microcolonies, preferently located in depressions or crevices in the surface of sand grains. A similar phenomenon has been observed before with marine sediments and was ascribed to mechanical damaging by adjacent sand grains (Weise & Rheinheimer, 1978). In the present case, however, surface irregularities of sand grains probably create regions of low liquid turbulency and thus of low shearing forces. Such forces are reported to remove attached bacteria from inert surfaces (Powell & Slater, 1982; Trulear & Characklis, 1982).

Notwithstanding these shearing forces, a confluent biofilm developed from these microcolonies 40 τ after start—up. For several reasons, however, it is concluded that such biofilm—covered sand grains only represent an intermediate type of aggregate, and that eventual steady—state aggregates are essentially free of sand and of a quite dynamic nature. First of all, SEM micrographs of the intermediate type of aggregate at 40 τ showed severe sloughing of biofilm, exposing the sand surface. Furthermore, sand grains were not detected in sectioning steady—state aggregates at 80 τ for TEM and LM. It is postulated therefore that the settling velocity of the biofilm fragments, detached by sloughing, is high enough to enable efficient retention even though they do not contain any sand. Such fragments would gain in size again by

bacterial growth. Notwithstanding its high settling velocity, sand gradually disappears from the reactor, since, unlike biomass, it is not re-generated *in situ*. Effluent samples did contain small amounts of sand, but the major losses of sand are attributed to sampling of the reactor contents. From the biomass determination employed, the remaining sand in the reactor at 60 τ after shift-up was estimated to be less than 10 % of the initial amount. In summary, detachment of rather large biofilm fragments from sand grains on one hand, and sampling losses and wash-out of sand on the other, result in a transition from sand-containing aggregates to aggregates without sand.

A further complication has to be taken into account. If aggregate-containing samples from the reactor were left to stand for 15 min, aggregates were found to stick together. Therefore, the *in situ* clumping of small aggregates into larger units is conceivable. In this respect, it is of interest that LM and SEM micrographs of steady-state aggregates reveal them to consist of several smaller subunits.

LM micrographs (Fig. 6) showed cell concentrations to be high at the periphery and low in the centre of aggregates. Conceivably, these low concentrations reflect a locally insufficient glucose supply caused by diffusional limitation. As a result, maintenance requirements are not met and cell lysis occurs. Consequently, the mechanical strength of aggregates is affected, and the combination of this internal weakening by substrate deficiency and external shearing forces arising from liquid turbulency may result in fragmentation. In addition, fragmentation may be aggravated by the production of gaseous metabolites within the aggregates. An identical mechanism is thought to underly the abovementioned detachment of biofilm fragments from sand grains. Such mechanical effects by gas bubbles arising within biofilms have been postulated before (Kierstan & Bucke, 1977; Atkinson *et al.*, 1979; Harremoës *et al.*, 1980; Krouwel & Kossen, 1980; Nilsson *et al.*, 1980). Bochem *et al.* (1982) have reported microscopic evidence for gas bubbles arising inside methanogenic aggregates.

The importance of cell lysis can also be inferred from the abundant production of valeric acid, coinciding with aggregate formation. With glucose as a substrate, valeric acid generally is not a major fermentation product. Large amounts of valeric acid, on the other hand, are often found in the fermentation of complex macromolecules. The latter type of substrate would be amply available as a result of cell lysis.

Light microscopic observations on butyrate-producing aggregates showed them to have a very open structure. Conceivably, this is the result from the vigorous production of gaseous metabolites. Such an open structure would facilitate substrate transport into the interior of these aggregates. The absence of valerate production indeed suggests that cellular lysis is not occurring on a large scale.

Data on cellular densities, which are relevant to future model calculations on aggregate performance, were obtained from TEM

micrographs. Morphometric measurements revealed V_v values to range from 0.21 to 0.27, whereas N_v values between 0.4×10^{12} and 1.4×10^{12} ml^{-1} were measured. Likely, these V_v and N_v estimates are not mean values for the whole aggregate, since selection of TEM micrographs tends to be biased against the centre of aggregates with its low cellular densities. Furthermore, inaccuracy may arise from shrinking of samples in the dehydration procedure. However, the present data are in good agreement with the data of Strand et al. (1985), who reported viable counts of 10^{11} to 10^{12} ml^{-1} for partly aerobic biofilms. A large discrepancy, on the other hand, exists with data of Trulear & Characklis (1982, cf. Characklis & Cooksey, 1983), who reported viable counts as low as 10^4 ml^{-1}. Surprisingly, the latter figure is several orders of magnitude lower than common densities in cultures of freely suspended bacteria.

TEM and SEM micrographs indicated most cells to be intimately enmeshed in an extensive matrix of EPS. However, not all population members were equally active in EPS formation, since some rod−shaped and coccoid cells in particular were seen to be lying in an EPS−free zone. Such non−adhering cells may have been entrapped from the bulk liquid during biofilm formation, a phenomenon which has been reported before (Costerton et al., 1978). Since formation of aggregates in the AGLR implies selection for adhesive properties, the observed metabolic shift from butyrate to propionate production upon aggregate formation could, at least partly, be due to a shift in population composition. Entrapment of non−adhering, butyrate−producing bacteria in films of propionate−forming organisms could explain the continuing production of moderate amounts of butyrate. At present, however, no evidence is available that biofilm entrapped cells do indeed produce butyric acid.

EPS appearance in electronmicroscopic preparations was strongly dependent on the procedure employed. Whereas TEM micrographs showed very thin and almost amorphous fibrils, the EPS in SEM micrographs was seen as thick strands. These differences are generally believed to reflect different extents of dehydration artifacts of the EPS, which is quite diffuse in vivo.

The positive reaction of EPS towards ruthenium red, as well as towards alcian blue, and the rather high sugar content of whole aggregates from anthrone analysis, all indicate sugars to be an important component of EPS. This is in agreement with previously published findings on various bacterial aggregates (Deinema & Zevenhuizen, 1971; Fletcher & Floodgate, 1973). In view of the high sugar content of EPS, various authors have postulated carbon sufficiency to be a prerequisite for extensive EPS formation and bacterial adhesion (Matson & Characklis, 1976; Williams & Wimpenny, 1978; Zevenhuizen, 1981). In the present case, however, considerable hold−up ratios could be sustained in the final steady state notwithstanding glucose limitation.

In summary, the working hypothesis developed above implies final

Fig. 8 : Outline of a working hypothesis on development of anaerobic mixed—culture aggregates. 1: bare sand grain; 2: progressive biofilm formation; 3: detachment/sloughing of biofilm fragments; 4: clumping; 5: growth of sand—free aggregates; 6: loss of sand; 7: recolonization; 8: fragmentation of large aggregates; 9: wash—out of aggregates.
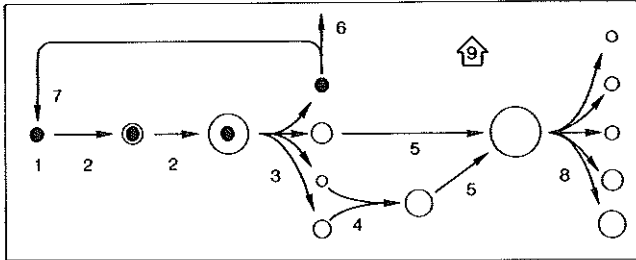
steady—state aggregates to be of a very dynamic nature. Individually, they do not reach a true steady—state condition, but gain in size continuously by bacterial growth and a tendency to stick to each other. On the other hand, their maximum diameter is limited, due to desintegration of large aggregates. As an important consequence, the relative position of an individual bacterium within an aggregate is continuously changing, and so are its environmental conditions. Fig. 8 gives a schematic representation of these processes. A continuous distribution of aggregate diameters over a wide range is thus predicted. Quantitative data on diameter distributions will be reported separately (*this thesis*, Chapters V and VI).

The dynamic behavior of bacterial aggregates as described here quite likely is applicable to other reactor configurations in which biomass is retained. However, the relative contributions of individual processes (shearing forces, cell lysis, gas production, *etc.*), may depend on the specific experimental conditions used (reactor, substrate, bacterial species, *etc.*).

ACKNOWLEDGEMENTS

CHAPTER V	SPECIFIC DENSITY, DIAMETER, AND SETTLING VELOCITY OF INDIVIDUAL BACTERIAL AGGREGATES

SUMMARY

An anaerobic gas—lift reactor in which bacterial aggregates were formed and retained was operated at a high dilution rate for prolonged periods of time to study its operational stability. A true steady state was not established readily, once aggregates were formed: a gradual shift was observed from a low specific growth rate and a high biomass retention to a more rapid growth at reduced biomass hold—up. To explain this phenomenon, physical characteristics of the aggregates were studied. A novel method is described that allows the simultaneous determination of diameter and settling velocity of a large number of individual aggregates. With isopycnic density—gradient centrifugation, also the specific density of aggregates could be measured directly. It was shown to decrease with the aggregate diameter. The decrease in density is attributed to substrate insufficiency in large aggregates and the subsequent autolysis. The lesser densities are inferred to explain the relatively low settling velocities that were observed for large aggregates. Such aggregates, being inefficiently retained and susceptible to shear stress, disappear with time from the reactor. The remaining aggregates are small, and this consequently facilitates the higher specific growth rates observed.

INTRODUCTION

Practical operation of various types of continuous—flow bioreactors (*e.g.* upflow and fluid—bed reactors) heavily relies on the presence of suspended bacterial aggregates, which are formed either with or without the aid of inert carrier particles. Such a mode of bacterial growth facilitates high—rate reactor performance, since the good settling properties of these aggregates may prevent to some extent biomass

wash—out from the reactor.

Previously (*this thesis*, Chapter II), doubts have been expressed as to whether a true steady state would become established in one particular type of a continuous—flow bioreactor (AGLR), once bacterial aggregates had been formed. In a more general sense also, it has been acknowledged (Atkinson & Daoud, 1976; Atkinson & Mavituna, 1983) that data on physical characteristics of aggregates are wanting or simply absent. This lack is a major bottleneck in the rational operation of continuous—flow bioreactors.

Therefore, the present contribution reports on the overall characteristics of an anaerobic gas—lift reactor during prolonged operation. For this purpose, an extended run exceeding 400 liquid residence times was performed, which started with the formation of aggregates from freely suspended cells (*cf. this thesis*, Chapter II). In view of the importance of the settling properties of aggregates, their number, diameter, specific density, and settling velocity were investigated at various stages of reactor operation.

Two techniques were used to measure aggregate characteristics. On the one hand, data are presented on the relationship between the diameter and the settling velocity of a large number of individual aggregates. Data were obtained from the projection of photographic negatives on which sedimenting aggregates were recorded.

On the other hand, simultaneous measurements on the specific density and the diameter of individual bacterial aggregates are presented. Data were obtained from isopycnic density—gradient centrifugation with Percoll, a colloidal suspension of coated 20—nm silica particles. The technique represents a novel application of Percoll gradients, which hitherto have been employed only to measure densities of cells or subcellular particles. Literature provides only indirect data on specific density of aggregates, as, invariably, these densities were calculated from settling velocities (Magara *et al.*, 1976; Tambo & Watanabe, 1979; Shieh *et al.*, 1981; Brohan & McLaughlin, 1984; Timmermans & Van Haute, 1984).

MATERIALS AND METHODS

Reactor, medium, growth conditions, and analytical determinations. Aggregates to be analyzed were sampled from an anaerobic gas—lift reactor (AGLR), in which glucose was fermented to short—chain fatty acids by a natural mixed population (Beeftink & Staugaard, 1983, 1986; Beeftink & Van den Heuvel, 1986; *this thesis*, Chapter II). Details on growth and operating conditions, on medium composition (glucose limitation), on reactor start—up, and on analytical determinations are given elsewhere (*this thesis*, Chapter II). The reactor contents were

considered to be well—mixed; sampled aggregates, therefore, were taken to represent the whole aggregate population in the reactor.

Specific growth rate calculations. With data on reactor and effluent dry—weight biomass concentrations (x_r and x_e, respectively; g/l) and on dilution rate (D, h^{-1}), values for a population—averaged specific growth rate (μ, h^{-1}) during transient conditions may be obtained from a biomass balance (*this thesis*, Chapter II). As an approximation, however, μ—values between subsequent biomass data points were calculated as:

$$\mu = 2 \cdot (x_{r2} - x_{r1})/(x_{r1} + x_{r2}) \cdot (t_2 - t_1) + D \cdot (x_{e1} + x_{e2})/(x_{r1} + x_{r2})$$

with subscripts 1 and 2 indicating two subsequent samples at times t_1 and t_2 (h).

Sampling procedure. A wide sample port (8 mm ⌀) allowed unobstructed sampling from the AGLR. Settling—velocity/diameter measurements were combined with counting numbers of aggregates. To facilitate comparison of numbers in subsequent samples, the sample volume (*ca.* 10 ml) was determined gravimetrically (assuming a specific weight of 1000 kg/m³). Errors in sample volume were considered negligible, since specific weight of biomass in general only slightly exceeds 1000 kg/m³ (*e.g.* Woldringh *et al.*, 1981), whereas aggregates did not occupy more than 20% of the total sample volume.

Settling experiments: simultaneous measurement of velocity and diameter of individual aggregates. Aggregate—containing samples (*ca.* 10 ml) were
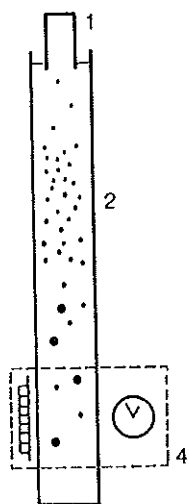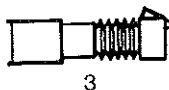

Fig. 1 : Schematic set—up for diameter/settling—velocity measurements (not drawn to scale). 1: sample vial; 2: perspex chamber with settling swarm of aggregates; 3: 35—mm camera; 4: field of view of camera with chronometer and scale.

collected in small wide—mouthed vials, which were then covered with a flat lid. Subsequently, the vial was held top—down at the top of a water column (perspex container; 0.07×0.07×2 m), with the rim just below the meniscus (Fig. 1). Swiftly but gently, the lid was removed laterally from the vial, a chronometer was started, and all particular material was allowed to sediment undisturbed from the vial. A 35—mm camera with a bellows and a 400—mm lens was placed at a distance of 2 m from the perspex column, and viewed a 0.07×0.10—m section (including the chronometer) of the column at 1.5 m from the top (Fig. 1). Aggregates that passed the field of view of the camera were recorded in a series of 24×36 mm negatives (linear magnification 0.35; illumination with two electronic flashes). Care was taken to record all settling aggregates once, but some duplication on subsequent negatives was inevitable. Furthermore, aggregates were increasingly smaller on subsequent negatives, and ultimately were hardly discernible.

Settling velocities v_∞ (m/s) were calculated for each negative (and thus for the aggregates on it) from elapsed time and from the distance to the water surface. Each negative represented a velocity class; the mean of this class was used as v_∞—estimate for the aggregates in it. Inherently, class width decreased with every subsequent negative.

Negatives were projected on a transparent tablet digitizer screen (Summagraphics, Fairfield, USA; final linear magnification *ca.* 3.5), connected to a HP 9825A calculator. With a computer—connected marker, the largest and smallest diameter (length *l*, and width *w*, respectively) of each aggregate were marked on the screen and recorded. In general, these were the horizontal and vertical diameters, respectively, as would be expected for such somewhat irregular bodies at intermediate Reynolds—values (Becker, 1959; Clift *et al.*, 1978). The aggregate diameter *d* (m) was defined as $d = (l+w)/2$. The total number of aggregates analysed per sample was between 200 and 1400. All diameters measured were attributed to diameter classes, while numbers in each class were normalized with respect to sample volume. According to Shieh *et al.* (1981), such size distributions were characterized by their Sauter mean diameter d_s (mm), which was calculated as:

$$d_s = \Sigma_i n^i \cdot (d^i)^3 / \Sigma_i n^i \cdot (d^i)^2$$

with: *i*: indication of diameter class; n^i: number of aggregates in that class (l^{-1}); d^i: mean diameter of a class (mm).

Theoretical settling velocities of aggregates. Assuming aggregates to be spherical with a specific density ρ_a, theoretical settling velocities were calculated according to:

$$v_\infty = [4 \cdot (\rho_a - \rho) \cdot g \cdot d^3 / 3 \cdot \rho \cdot C_D]^{\frac{1}{2}}$$

with: v_∞: terminal settling velocity (mm/s); ρ: density of water (g/ml); *g*: acceleration due to gravity (mm/s^2); C_D: drag coefficient ($-$).

Fig. 2 : AGLR characteristics after a dilution—rate shift—up at $\tau = 0$ from $D = 0.2$ to 0.6 h^{-1}. Numbers indicate aggregate samples at $\tau = 32$, 44, 60, and 100. **Fig. 2^a** : Concentrations of volatile fatty acids; C_2: acetic acid; C_3: propionic acid; C_4: butyric acid; C_5: valeric acid; **Fig. 2^b** : Glucose concentration (Glc); reactor and effluent biomass concentrations (x_r and x_e, respectively); **Fig. 2^c** : Specific growth rate (μ).
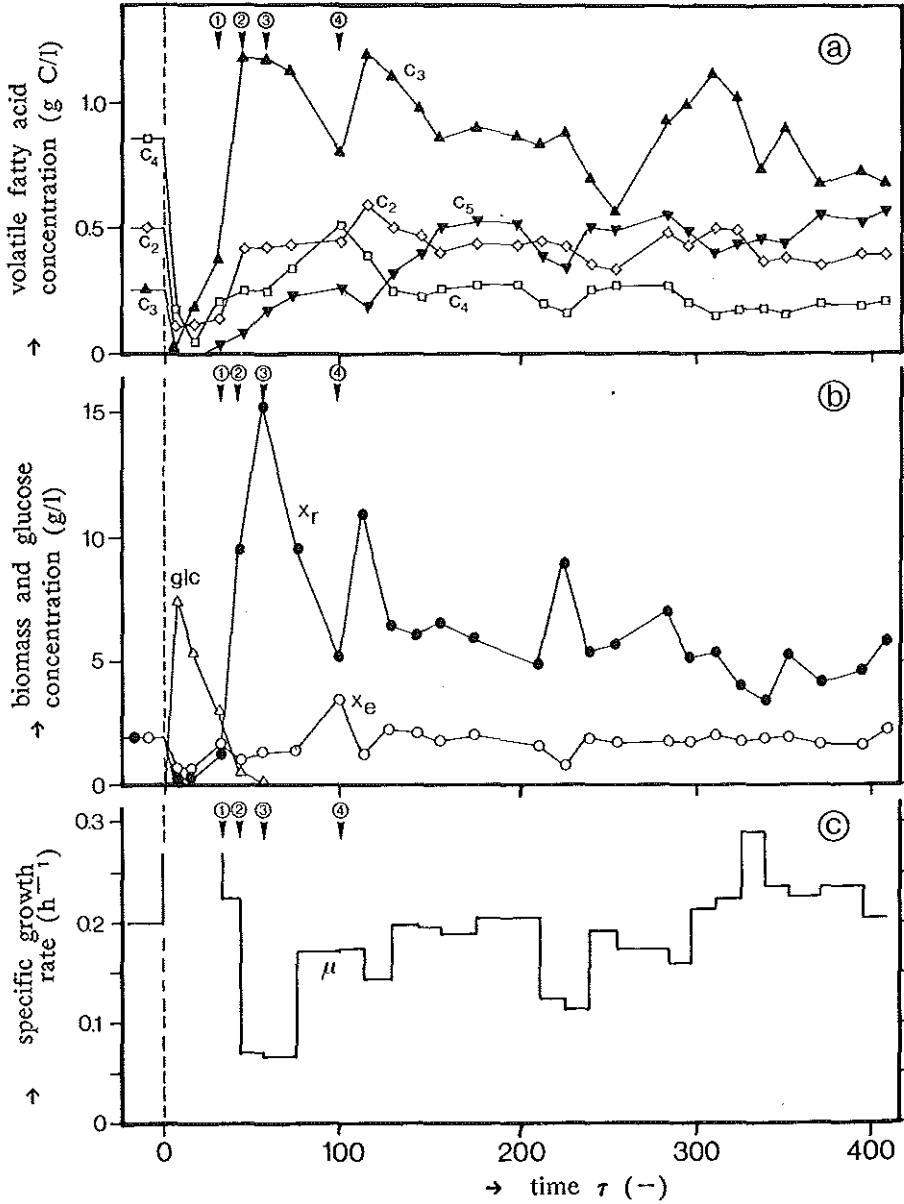
to Lapple & Shepperd (1940), the expression $18.5/(Re)^{0.6}$ was used as an estimate for the drag coefficient C_D (Re: Reynolds number for a sphere, $-$). In addition, a diameter$-$dependent ρ_a was substituted from experimental observations (*cf.* Fig. 4).

Percoll gradients: simultaneous measurement of density and diameter of individual aggregates. Specific densities of bacterial aggregates were measured by centrifugation in isopycnic density$-$gradients of Percoll (Pharmacia, Uppsala). Gradients were prepared from suspensions of Percoll in 0.15 mol/l saline. According to the manufacturers instructions (Anonymus, 1980), the required amount of Percoll was calculated so as to give optimal resolution at $1040 - 1060$ kg/m^3. To allow internal calibration, a mixture of density marker beads was added (DMB, Pharmacia, Uppsala; Anonymus, 1980), with respective densities of 1033, 1048, 1062, 1076, 1087, and 1101 kg/m^3. Pre$-$centrifugation of this mixture in a 40 ml polycarbonate centrifuge tube (25 min at $25000 \times g$, Beckmann JA$-$20 rotor) yielded a sigmoidal density gradient. A 0.25 ml sample from the reactor (with $35 - 55$ aggregates) was placed directly on top of the gradient and centrifuged for another 5 min ($700 \times g$), whereafter aggregates had equilibrated at their buoyancy position.

Subsequently, gradients were photographed (35$-$mm camera, 135$-$mm lens; linear magnification *ca.* 0.5). To minimize refraction, the centrifuge tube was placed in a transparent square container with water. After projection of the negatives (final linear magnification *ca.* 10), length and width of each aggregate were measured, and a diameter was established as defined above. According to its vertical position in the tube, each aggregate was attributed to a density class. Appropriate density classes were chosen from the positions of the respective DMB$-$bands.

RESULTS

Fig. 2 shows the time courses of the concentrations of biomass, glucose, and of various metabolic products after after the dilution$-$rate shift$-$up that induced aggregate formation from freely suspended cells. Subsequently, steady$-$state operation was prolonged at $D = 0.6$ h^{-1} until $\tau = 400$ ($\tau = D \cdot t$, $-$; D: dilution rate, h^{-1}; t: time, h). After a transient maximum in glucose concentration, a peak value in reactor biomass concentration x_r of 15 g/l (dry weight) was observed to coincide with complete substrate conversion at $\tau = 60$ (Fig. 2[b]). The production of large amounts of propionate from glucose fermentation (Fig. 2[a]) is characteristic for so$-$called HPr$-$aggregates (propionate$-$forming aggregates; *cf. this thesis*, Chapters II and III).

After the initial maximum, $x_r$$-$values were seen to fluctuate; over prolonged periods of time, however, x_r decreased. Accordingly, biomass

Fig. 3   Fig. 4
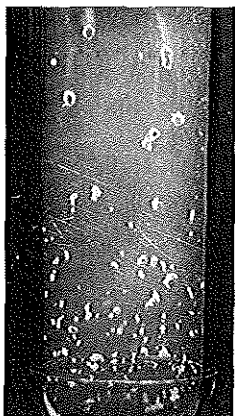
Fig. 3 : Percoll density gradient, containing large aggregates at the top (low specific weight) and small aggregates near the bottom (high specific weight).
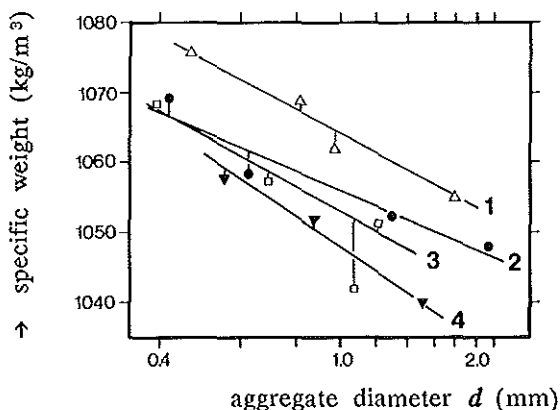
Fig. 4 : Relation between specific density ρ_a and diameter d of bacterial aggregates at various stages after reactor start−up (sample numbers 1 to 4 correspond to τ = 32, 44, 60, and 100, respectively; cf. Fig. 2).

retention (R = x_r/x_e, −; x_e: effluent dry−weight biomass concentration, g/l) decreased from R = 11 to R = 3 (τ = 60 and τ = 400).

Fluctuations were observed also in the concentrations of volatile fatty acids, but the general pattern did not change once retention had been established (propionate in excess of acetate and butyrate). The only exception was found with valerate, which was formed at increasingly higher rates with progress of time (Fig. 2a).

From the biomass data in Fig. 2b, specific growth rates were calculated (Fig. 2c). Due to very low concentrations, biomass data between τ = 0 and τ = 20 were not considered for calculation. From 20 to 60 τ, μ decreased to reach a minimum. In agreement with the subsequent decline in R, μ−values were increasing between τ = 60 and τ = 400. After the minimum at τ = 60 (μ = 0.06 h^{-1}), a rapid increase was observed. Thereafter, the increase was more gradual (with occasional fluctuations), and ultimately, μ = 0.25 h^{-1} was attained between τ = 300 and 400.

At different instants during reactor operation, samples were withdrawn from the AGLR for density/diameter analysis on aggregates with the aid of Percoll gradients. Fig. 3 presents a typical result. Apparently, smaller aggregates had found their buoyancy position in the

lower parts of the density gradient, $i.e.$ had a high specific density ρ_a; larger aggregates were seen at higher positions in gradients; accordingly, they had lesser specific densities. Aggregate diameters (d, mm) were measured and Fig. 4 gives data on the relation between d and ρ_a for four of these samples (sampling times indicated in Fig. 2). In each case, an apparently linear negative relation between ρ_a and log (d) was found. However, whereas aggregates from the earliest sample (no. 1, $\tau = 32$) were relatively heavy at all diameters, a general decrease in density with time was observed with later samples.

At the same four instants as above (cf. Fig. 2), aggregate——containing reactor samples were subjected to a settling—velocity/ diameter (v_∞/d) analysis on individual aggregates; the results are given in Figs. 5^a to 5^d. The earliest sample (no. 1, $\tau = 32$; Fig. 5^a) represents the onset of aggregate formation; at this stage, glucose conversion was still incomplete (cf. Fig. 2^b). In comparison to subsequent samples, low numbers of aggregates were observed; their diameters ranged from 0.25 to 2 mm. As would be expected, the larger aggregates had higher settling velocities.

The next sample (no. 2, $\tau = 44$; Fig. 5^b) showed an increase in the maximum diameter of aggregates in the sample (up to 3.5 mm). As sample volumes were roughly equal, a preliminary comparison of aggregate counts can be made, and shows a considerable increase in number also.

Subsequently (sample 3, $\tau = 60$; Fig. 5^c) a stage was analysed at which glucose conversion was complete and biomass hold—up R was at its maximum. Comparison with the previous sample does not reveal significant changes in numbers or maximum diameters. Strikingly, however, a general decrease in settling velocity was observed. For large aggregates, this decrease was particularly prominent. Apparently, settling velocity was almost diameter—independent for $d > 2$ mm.

The final sample (no. 4, $\tau = 100$; Fig. 5^d) represents the stage at which the reactor biomass concentration and hold—up had decreased again after their initial maxima, and the specific growth rate had increased. The most significant difference with the preceding sample is the complete absence of aggregates with diameters exceeding 2.5 mm.

The trend in aggregate diameters in samples 1 — 4 may be judged more quantitatively from Figs. 6^a — 6^d. Size distributions for all four samples are shown, which were normalized with respect to sample volume. Characterization of all four distributions by their Sauter mean diameter d_s reveals a sharp increase between $\tau = 32$ and $\tau = 44$, and a decrease again from $\tau = 60$ to $\tau = 100$.

Several samples were analysed after $\tau = 100$, but although some fluctuation in biomass and fatty—acid concentrations was persistent, the general picture for v_∞/d relations as represented in Fig. 5^d remained unchanged (data not shown).

Occasionally, very small aggregates with high settling velocities were

Fig. 5 : Relation between settling velocity v_∞ and diameter d for individual aggregates at four stages after shift—up. **Fig. 5^a** : Sample 1, $\tau = 32$. **Fig. 5^b** : Sample 2, $\tau = 44$. **Fig. 5^c** : Sample 3, $\tau = 60$. **Fig. 5^d** : Sample 4, $\tau = 100$. Drawn lines: theoretical velocities (see text). **Fig. 6** : Histograms of diameters at four stages during aggregate development (*cf.* captions Fig. 5); arrows: Sauter mean diameters d_S.

Fig. 5   Fig. 6
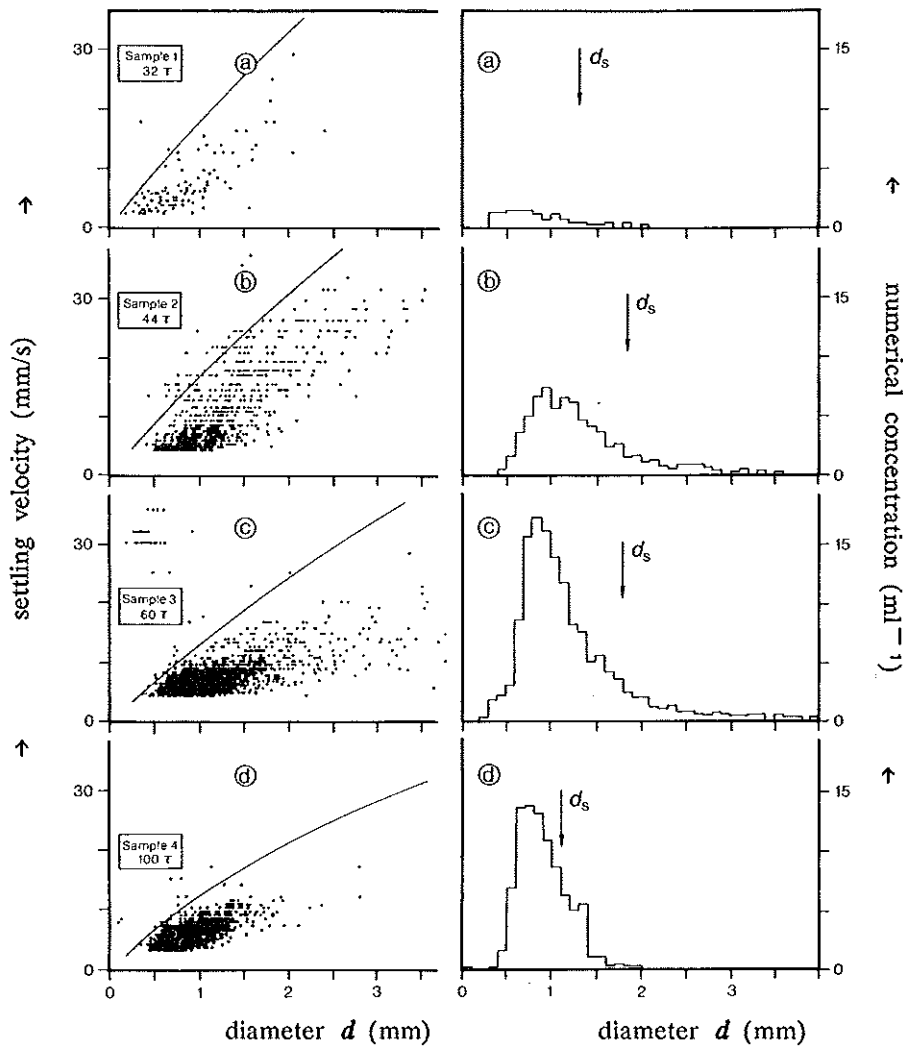
observed (d = 0.4 mm, v_∞ = 30 mm/s). Such aggregates were en-
countered in particular shortly after start-up. From the combination of
their size and settling velocity, it is concluded that these aggregates
contain sand (bare sand grains were found to have a settling velocity of
35 - 40 mm/s).

Theoretical settling velocities were calculated from d and ρ_a, and
are represented in Figs. 5a - 5d. A comparison with experimental data
shows a qualitative agreement. A constant, diameter-independent density
would have resulted in a slightly upward curvature for v_∞/d relations, but
the present expression predicts the decreasing slopes that were observed
experimentally. However, predicted values for v_∞ were consistently too
high.

DISCUSSION

From the data obtained on prolonged AGLR operation, it is apparent
that a true steady state did not become established readily upon
formation of aggregates. Reactor biomass concentration x_r and biomass
hold-up R gradually decline after initial peak values. Ultimately,
however, this decline seems to level off at 100 τ after the D shift-up,
thus allowing continued reactor operation at elevated D-values. In fact,
the experimental run shown in Fig. 2 was continued until τ = 600,
maintaining complete substrate conversion all the time.

From data on biomass concentrations x_r and x_e on the one hand,
and from the physical characteristics of the aggregates on the other, a
general scenario may be constructed for the events between the onset of
aggregate formation (τ = 20) and the stabilization of reactor
performance around τ = 100. Specific growth rates as calculated from
biomass data showed a sharp decline upon aggregate formation, while at
the same time glucose conversion was almost complete (Table 1; *cf.*
Fig. 2). Such a decrease in μ was observed before (*this thesis*, Chapter
II) and may be attributed to increasing transport limitations for substrate.
Surprisingly, however, an increase again in μ-values is observed at a
stage when the growth-limiting substrate glucose was already fully
depleted. An explanation for this phenomenon is obtained from the size
distributions of aggregates. Table 1 shows the increase in μ to coincide
with a decrease in aggregate diameter as represented by their Sauter
mean diameter d_s.

When glucose concentrations in the bulk liquid are assumed to
remain constant and negligibly low from τ = 60 onwards, the general
decrease in aggregate diameter d_s would relieve limitations in glucose
transport. As a consequence, the general substrate concentrations within
aggregates would be higher, thus facilitating more rapid growth. The data
obtained on dimensions of aggregates do indeed call for this conclusion.

From data on specific density and settling velocity of aggregates, an

Table 1 : Comparison of specific growth rate μ (h^{-1}), Sauter mean diameter d_S (mm), and glucose concentration glc (g/l) at subsequent times τ ($-$) during reactor start$-$up; nd : not detectable.

τ	μ	d_S	glc
32	0.22	1.31	2.9
44	0.07	1.83	0.3
60	0.06	1.78	nd
100	0.18	1.11	nd

explanation for the decrease in diameter can be inferred, in particular concerning the disappearance of large aggregates ($d > 2.5$ mm) between $\tau = 60$ and $\tau = 100$. Direct measurements of specific density showed a negative relationship with aggregate diameter. Although this inverse relation was found at all stages, it was the most prominent when bulk$-$ $-$liquid glucose concentrations became vanishingly low. As a result, large aggregates lose in settling velocity to such an extent, that v_∞ becomes almost diameter$-$independent for $d > 2$ mm. Likely, the efficiency with which such aggregates are retained deteriorated due to worsened settling characteristics, which cannot be estimated from their diameter alone.

The specific aggregate density ρ_a was shown experimentally to de$-$ crease with time and with aggregate diameter. Simultaneously, an in$-$ creasing production of valeric acid was observed. These data are in good agreement with the previously stated hypothesis on lysis within large aggregates due to substrate insufficiency (*this thesis*, Chapter II). Micro$-$ scopic evidence for "hollowing" of large aggregates by lysis has been presented before (*this thesis*, Chapter IV); and was reported for mold pellets also (Clark, 1962). Conceivably, these "hollow" structures were more susceptible to shear stress from the reactor liquid. In addition to the abovementioned wash$-$out therefore, disappearance of large aggre$-$ gates from the reactor may have resulted from their desintegration also.

Changes in microbial population composition could contribute to time spans required to establish stable conditions. Characteristic times would depend on *differences* in specific growth rates of the various population components. Due to biomass hold$-$up, specific growth rates are low; consequently, relaxation times greatly exceeding the mean liquid residence time might be involved. However, population changes were not immediately obvious from the mean metabolic products. The only major change in fermentation products was found with valerate. A highly limited number of bacteria has been reported to produce valerate from

simple substrates (*Clostridium kluyveri*, from ethanol and propionate; Bornstein & Barker, 1948). Therefore, fermentation of debris from cellular lysis likely contributed to valerate formation (*cf*. Chapter II). The latter phenomenon does not involve population changes.

In summary, the stabilization of reactor performance depended on changes in aggregate properties. Depletion of the growth−limiting substrate after a transient glucose peak triggers a rearrangement of aggregate characteristics; the time span required for its completion presumably will reflect the relaxation times of the processes involved (in particular autolysis). Subsequent reactor operation was highly stable in terms of substrate conversion, although the establishment of formal steady−state conditions remains uncertain, as some fluctuations in metabolic products were persistent. Even so, the general metabolic pattern remained unchanged.

The present report employs Percoll density gradients to measure the specific mass of bacterial aggregates in a direct experimental way. The diameter−dependend specific density established this way was used to calculate settling velocities as a function of aggregate diameter. These calculated velocities were consistently higher than experimental data on settling velocity, *i.e.* specific densities as measured with Percoll were seemingly too high. This discrepancy may be explained on the basis of shape factors. Bacterial aggregates are not perfect spheres, and may contain pockets of liquid at their perifery. During gradient centrifugation, such pockets may become penetrated with Percoll particles by convective transport due to local density differences; therefore, they would not belong to the aggregate proper. In a settling experiment, however, such differences are absent, and the same pockets may belong to the aggre− gate. Any determination or calculation of specific density of an aggregate assumes an aggregate/bulk−liquid boundary. Necessarily, this boundary, if physically real at all, reflects the experimental determination employed.

The precise location of this boundary, however, does not affect the conclusions on the diameter dependency of specific density. Any transport of Percoll into the interior of an aggregate would be by molecular diffusion. A conservative estimate of the Percoll diffusivity within an aggregate amounts to 10^{-11} m^2/s, yielding a characteristic diffusion time that exceeds the centrifugation time with several orders of magnitude. The experimental demonstration of density differences within one sample of aggregates indeed shows the latter process to be unimportant.

ACKNOWLEDGEMENTS

AGGREGATES OF VARIOUS AND VARYING

SIZE AND DENSITY : A MODEL FOR

A CONTINUOUS−FLOW REACTOR

SUMMARY

Models for completely−mixed continuous−flow systems that retain bacterial aggregates up until now only considered reactors containing a single type of aggregate. A novel model is presented, accounting for dynamic behaviour of a variety of aggregates in such a reactor during steady−state operation. The model aims at predicting reactor performance (in particular biomass concentrations) as resulting from individual aggregate characteristics that are size−dependent. The main features incorporated are the continuous growth of aggregates, their size−dependent specific density due to cellular lysis, and the disintegration of large aggregates. Wash−out of individual aggregates, or, reversely, their retention, is formulated as a function of their settling velocity. The overall biomass hold−up therefore is a complex function, resulting from the interaction of various processes. It was shown to be variable and to decrease with dilution rate (D). The reactor biomass concentration depended in a complicated way on D and on the mechanism of fragmentation. The influent substrate concentration (s_0) positively affected the reactor and effluent biomass concentrations, while biomass retention remained unchanged. Distribution of aggregate dimensions was s_0−independent, but was strongly influenced by D. Increasing D provoked a general increase in aggregate diameters. In nearly all cases, a bimodal distribution of substrate conversion over diameter categories was observed; especially at elevated D−values the contribution of intermediate aggregate sizes to total conversion was negligible.

INTRODUCTION

Modeling of biological continuous−flow reactors that contain discrete

bacterial aggregates in a more or less fluidized state is considered highly important (Atkinson & Daoud, 1976; Atkinson & Mavituna, 1983). Reliable prediction of reactor biomass concentrations is of particular relevance, since these concentrations have a direct bearing on reactor loading capacity.

An extensive review on fixed—film models in general has been given by Grady (1982). It shows that equations are available that more or less satisfactorily describe the interaction of substrate consumption and transport within a single aggregate of a stationary nature. To facilitate the use of such equations, especially in case of reactors with discrete bacterial aggregates, a rather drastic and often quite unrealistic assumption has to be made: all aggregates are taken to be identical, and of a constant size that is not influenced by bacterial growth. Shieh et al. (1981) and Shieh & Chen (1984) for instance have used this approach in modeling a fluidized—bed reactor. From upward superficial liquid velocity they calculate bed voidage by means of the correlation by Richardson & Zaki (1954). With a known number of biological particles, biofilm thickness and total biomass are then calculated.

The assumption of such an uniform particle size indeed can be substantiated. Atkinson et al. (1979, 1984) have developed so—called biomass support particles (BSP, spherical knittings of stainless—steel wire with 80% porosity). These BSP yield bacterial aggregates with predetermined dimensions, as bacterial growth takes place only within the BSP; any additional growth is removed mechanically from the outside of the BSP, e.g. by mutual collisions.

Another approach is often encountered for systems with alginate—
—immobilized cells. To circumvent the problem of biomass production due to substrate consumption, biomass purportedly is not produced at all, and consumption and growth are completely uncoupled. Cells would maintain low or zero growth rates and high conversion rates indefinitely. Such an assumption, however, is "not well supported by a large base of scientific information" (Emery & Mitchell, 1986), even though a partial uncoupling of energy metabolism and biosynthesis under energy—sufficient conditions is now well—established (Neijssel & Tempest, 1976; Tempest & Neijssel, 1984). Indeed, alginate beads with immobilized microorganisms have been observed to swell and even fragment as a result of bacterial growth (Shiotani & Yamane, 1981; Lee et al., 1982; Emery & Mitchell, 1986; Kossen, 1986).

In some cases, finally, consumption is indeed allowed to result in growth, but the additional biomass is taken to be released from the surface of the aggregate. Such a scheme then invokes a rather mild process as attrition to remove individual cells from the aggregate surface into the bulk liquid. Since cells have poor settling characteristics, they can not be retained efficiently and are rapidly removed from the reactor. The aggregate itself does not change.

Although studies have been performed on sloughing, i.e. the

removal of larger fragments from the surface of an aggregate (Howell & Atkinson, 1976[a], 1976[b]), it is generally disregarded in reactor models. As sloughing is rather drastic in comparison with attrition, it may produce aggregate fragments of such dimensions, that they are retained with a certain effectiveness. As a result, an aggregate population would exhibit a range of diameters instead of being of one single size.

Experimental data clearly have demonstrated a non−uniformity in aggregate sizes for a number of micro−organism/reactor combinations (*e.g. this thesis*, Chapter V; Leschber & Haacke, 1975; Davis & Hunt, 1986; Wiegant & De Man, 1986; Hulshoff Pol *et al.*, 1986). Since such distributions are not considered in models, reactor performance remains to be established empirically. To our knowledge, the paper by Atkinson & Rahman (1979) is the only exception and evaluates the impact of size distributions on the behaviour of a completely−mixed fermentor. However, these authors use distributions as input parameters for their calculations and cannot predict distributions.

The present contribution attempts to model a continuous−flow reactor (anaerobic gas−lift reactor, AGLR) containing bacterial aggregates with varying and various sizes. The reactor is taken to consist of a well−mixed compartment containing the aggregates in series with a simple settler. The model incorporates several experimental observations on these aggregates. Fig. 1 gives a schematic representation of the processes that are thought to influence number, size, and density of aggregates in an AGLR. Based on previous data (*this thesis*, Chapters II, IV, and V; Beeftink & Staugaard, 1986), steady−state aggregates are assumed to consist of cells (and glycocalyx) only, without any inert carrier material. In addition, the size of an individual aggregate is allowed to increase, the increase being related to substrate consumption. In particular for large aggregates, which may be incompletely penetrated

Fig. 1 : Schematic representation of processes governing distribution of aggregates; gr: growth due to substrate consumption; wo: wash−out; fr: fragmentation; dashed line: system boundary.
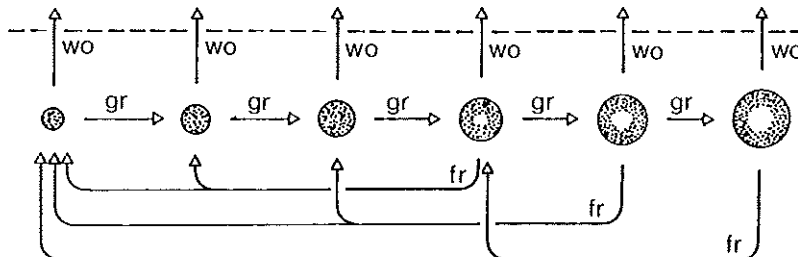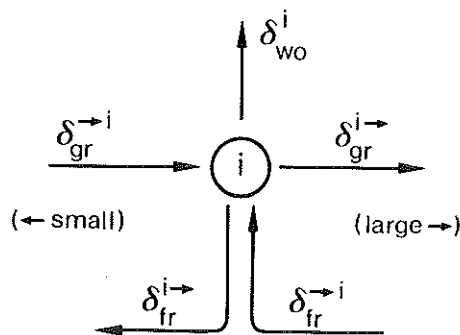
Fig. 2 : Specific rates influ—encing numerical concentrations of aggregates in a category i. $\delta_{gr}^{\rightarrow i}$ and $\delta_{gr}^{i\rightarrow}$: specific rates of change by growth (*cf*. eqs. 13 and 16); δ_{wo}: specific rate of change due to wash—out (*cf*. eq. 29); $\delta_{fr}^{\rightarrow i}$ and $\delta_{fr}^{i\rightarrow}$: specific rates of change due to frag—mentation (*cf*. eqs. 30 and 33.

by substrate, a decrease in specific density of their inner parts by cellular lysis is accounted for; experimental evidence for such a process has been presented before (*this thesis*, Chapters II, IV, and V). Wash—out of aggregates from the reactor is described as a function of their settling velocity, which, in its turn, is calculated from size and density (assuming sphericity). Finally, large aggregates may disintegrate into small fragments; disintegration is expressed as a function of aggregate overall density, and of the production of internal gas bubbles due to fermentation. The model, accounting for a dynamic aggregate behaviour, predicts distributions of size and specific density, which have been observed previously (*this thesis*, Chapter V).

The interrelation of the processes which influence the distribution of aggregate sizes is summarized in Fig. 1, which also gives a preliminary introduction to symbolism. It is almost identical to a previous summary (*this thesis*, Chapter IV, Fig. 8). The present formulation, however, does not take into consideration the possibility of the sticking together of small aggregates.

THEORETICAL

Technically speaking, the heart of the model is the assumption that all aggregates belong to one out of a number of discrete size categories or classes. In doing so, balance equations can be formulated for the number of aggregates in each category, provided that equations are available that describe the processes influencing numerical concentrations. As outlined above, numbers decrease or increase by growth of aggregates; similarly, fragmentation may decrease or increase numerical concentrations in a particular category; finally, wash—out always decreases numbers. The five different contributions of these three processes are summarized in Fig. 2.

Below, the corresponding equations will be formulated. Equations describing the individual processes are not always available from the literature. If so, tentative equations are adopted. Finally, a balance equation for any diameter category is presented, which allows calculation of a complete distribution.

Basic assumptions. The reactor is assumed to be in steady state, and to consist of a well−mixed compartment containing the aggregates (referred to as 'reactor'), in series with a settler of negligible volume. Such a set−up corresponds to the anaerobic gas−lift reactor described in this thesis (AGLR). The reactor working volume consists of bulk liquid (volume V_b; m³), gas, and aggregates. Assuming a constant gas hold−up, a constant volume V (m³) of bulk liquid *cum* aggregates is defined. The bulk liquid in the AGLR is considered well−mixed; any transport limitations on the liquid side of aggregates are disregarded. Although previous experimental data were obtained with a heterogeneous population, there are no local variations in population composition, *i.e.* the population is considered homogeneous with respect to kinetic constants. All aggregates in the AGLR are assumed to be spherical, and to consist of cells and extracellular polymeric material only (collectively referred to as biomass); carrier material, although essential during reactor start−up, is absent from steady−state aggregates.

Aggregate size distribution. Aggregate diameters d (m) are thought to belong to a total number of z size categories with class width Δ_d (m). Each diameter class is represented by a single diameter d^i (m; equal to the median of that class):

$$d^1 \ldots \qquad \ldots d^{i-1} \ldots d^i \ldots d^{i+1} \ldots \qquad \ldots d^z \tag{1}$$

$$d^i = (i - \tfrac{1}{2}) \cdot \Delta_d \tag{2}$$

with: d^i: diameter of the ith type of aggregate (m); i: integer, $1 \leqslant i \leqslant z$
(−); z: integer (−), $\geqslant 1$, indicates theoretically largest type of aggregate; Δ_d: constant diameter difference between two subsequent sizes of aggregate (m).
If a sufficiently low Δ_d−value is chosen, a continuous distribution function may be approached. The value for z is arbitrary, but large, *i.e.* indicates an aggregate of rather unrealistic size (see below: "*Overall reactor characteristics*").

Substrate conversion per aggregate. The use of an effectiveness factor η (−; $0 < \eta < 1$) facilitates calculation of the amount of substrate converted by one aggregate of category i per unit time (λ^i; mol/h) as a function of the bulk−liquid substrate concentration s_b. The effectiveness factor is the ratio between the actual rate of substrate consumption and the virtual rate that would be attained in the absence of transport

limitations (*i.e.* when substrate concentrations within the aggregate would equal s_b throughout). The intrinsic kinetics of substrate consumption within an aggregate are governed by local substrate concentrations s (mol/m^3) according to the Monod equation (saturation kinetics; Button, 1985):

$$(ds/dt)_{cons} = (\mu_{max} \cdot x_0 / Y) \cdot s / (K_s + s) \tag{3}$$

with: μ_{max}: maximum specific growth rate (h^{-1}); x_0: local dry−weight biomass concentration within an aggregate, constant (kg/m^3); Y: yield coefficient, amount of dry−weight biomass formed by growth per unit amount of substrate consumed (kg/mol); s: local concentration of rate−limiting substrate (mol/m^3); K_s: kinetic constant (mol/m^3).

If a dimensionless Monod−number Mo ($-$; $0 \leqslant$ Mo < 1), representing the degree of saturation of intrinsic kinetics, is defined with reference to the bulk−liquid substrate concentration as:

$$Mo_b = s_b / (K_s + s_b) \tag{4}$$

with: s_b: bulk−liquid substrate concentration defined with reference to the bulk liquid volume V_b (mol/m^3),

and defining the specific rate λ^i of substrate consumption by an individual aggregate of class i as:

$$\lambda^i = (1/n^i) \cdot (ds_b/dt)_{cons}^i \tag{5}$$

with: λ^i: amount of substrate consumed by one aggregate of type i per unit time (mol/h); n^i: numerical concentration of aggregates of type i, defined with respect to total reactor volume V (m^{-3}),

an expression for the conversion by one aggregate of class i is obtained:

$$\lambda^i = \eta^i \cdot V_a^i \cdot (\mu_{max} \cdot x_0 / Y) \cdot Mo_b \tag{6}$$

with: η^i: effectiveness factor for an aggregate of type i ($-$); V_a^i: volume of an aggregate, $(\pi/6) \cdot (d^i)^3$ (m^3).

The above equation assumes the biomass concentration within all aggre− gates to be equal and constant. Below, this assumption will be modified (Eqs. 21 and 23), without consequences, however, for the validity of Eq. 6.

As indicated by the superscripted i, η^i−values depend on the diameter d^i of the particular type of aggregate under consideration. Values for η^i may be calculated with the aid of the Thiele modulus φ ($-$), a dimensionless expression for the relative rates of reaction and diffusion within an aggregate. As does η^i, φ depends on aggregate diameter. Defining a dimension−less diameter β ($-$) as a first−order Thiele modulus:

$$\beta = (d^i/6) \cdot (\mu_{max} \cdot x_0 / D_e \cdot Y \cdot K_s)^{\frac{1}{2}} \tag{7}$$

with: D_e: effective diffusivity of substrate in an aggregate (m^2/h),

a modified Thiele modulus for a sphere with Monod kinetics φ is calculated as a linear function of the dimensionless aggregate diameter β (Bischoff, 1965; Moo—Young & Kobayashi, 1972):

$$\varphi = \beta \cdot Mo_b \cdot \{2 \cdot [(s_b/K_s) - \ln (1+s_b/K_s)] \}^{-\frac{1}{2}} \qquad [8]$$

For $\varphi \leqslant 1$ (conversion limited by intrinsic kinetics), values of η^i approach unity and are calculated as (Atkinson & Mavituna, 1983):

$$\eta^i = 1 - (1/\beta) \cdot \tanh(\beta) \cdot [(\varphi/\tanh \varphi) - 1] \qquad [9]$$

while for $\varphi > 1$ conversion is limited by substrate transport, and η^i—values are accordingly low (Atkinson & Mavituna, 1983):

$$\eta^i = (1/\varphi) - (1/\beta) \cdot \tanh(\beta) \cdot [(1/\tanh \varphi) - 1] \qquad [10]$$

The above expressions disregard any concentration profiles on the liquid side of an aggregate. Evaluation of Eq. 10 shows that for $\varphi > 3$, η^i values virtually equal $1/\varphi$. For large aggregates, therefore, $\eta^i \propto 1/d^i$.

Growth of aggregates. Growth of an aggregate is represented by moving it up one category. The rate at which this happens is dependent on the amount of biomass by which two subsequent aggregates differ, and the rate at which this biomass is synthesized. From diameters d^i and d^{i+1}, the required amount of biomass for the transition from i to $i+1$ may be calculated as:

$$\Delta_x^i = x_0 \cdot (V_a^{i+1} - V_a^i) \qquad [11]$$

Given a value $Y \cdot \lambda^i$ for the specific rate of biomass synthesis according to Eq. 6, $Y \cdot \lambda^i / \Delta_x^i$ is taken as an estimate for the specific rate at which one aggregate of diameter d^i increases its diameter to d^{i+1} ($\delta_{gr}^{i \to}$). Accordingly, the numerical concentration n^i of aggregates in class i decreases due to transition (growth) from i to $i+1$:

$$\delta_{gr}^{i \to} = (1/n^i) \cdot (dn^i/dt)_{gr}^{i \to} \qquad [12]$$

with: $\delta_{gr}^{i \to}$: specific rate of change in n^i due to growth of category i (h^{-1}; $\delta_{gr}^{i \to} \leqslant 0$); i→: shorthand indicating growth of i resulting in $i+1$.

Combination of Eqs. 6, 11, and 12 yields:

$$\delta_{gr}^{i \to} = -\eta^i \cdot \mu_{max} \cdot Mo_b / \{ (d^{i+1}/d^i)^3 - 1 \} \qquad [13]$$

Similarly, a rate may be calculated at which n^i increases due to growth of smaller aggregates (transition from $i-1$ to i):

$$\delta_{gr}^{\to i} = (1/n^i) \cdot (dn^i/dt)_{gr}^{\to i} \qquad [14]$$

with: $\delta_{gr}^{\to i}$: specific rate of change in n^i due to growth of $i-1$ (h^{-1}; $\delta_{gr}^{\to i} \geqslant 0$); →i: shorthand for the transition from $i-1$ to i.

For obvious reasons:

$$(dn^i/dt)_{gr}^{\rightarrow i} = -(dn^{i-1}/dt)_{gr}^{i-1\rightarrow} \qquad [15]$$

and thus:

$$\delta_{gr}^{\rightarrow i} = -(n^{i-1}/n^i) \cdot \delta_{gr}^{i-1\rightarrow} \qquad [16]$$

As a special case, it is postulated that the largest type of aggregate does not produce still larger ones (which do not exist), and similarly, that the smallest type of aggregate is not formed from even smaller ones (which do not exist either). Thus:

$$\delta_{gr}^{\rightarrow 1} = \delta_{gr}^{\cancel{\mathit{K}}\rightarrow} = 0 \qquad [17]$$

Penetration depth of substrate. Cellular lysis within bacterial aggregates is conceivable if local substrate concentrations become too low to satisfy maintenance requirements. Mathematical analysis of gradients in immobilized bacterial systems shows substrate concentrations to be finite at all depths, and to approach zero values only asymptotically (with a theoretical exception for zero−order kinetics). As a simplification, however, vanishingly low concentrations at greater depths may be equated to zero. Accordingly, a penetration depth may be defined as the radial position within the aggregate at which substrate concentrations fall below an arbitrary, low, value (s_e, mol/m^3). However, an analytical expression for local substrate concentrations in immobilized systems with complex Monod kinetics is not available. Nevertheless, gradients may be calculated. An iterative 4th−order Runge−Kutta procedure was used to this end. From the constants for transport and kinetics and the bulk−liquid substrate concentration, a penetration depth p_f (m) was calculated for a flat microbial film as the depth at which the local substrate concentration equalled s_e. Subsequently, penetration in spherical aggregates was characterized by a penetration diameter and calculated as:

$$d_p^i = d^i \cdot \{ 1 - [(p_f/d^i) + (p_f/d^i)^3] \} \qquad [18]$$

with: d_p^i: diameter of the substrate−depleted core of an aggregate, *i.e.* position at which $s = s_e$ (m; $d_p^i \geqslant 0$).

This equation accounts for enhanced penetration of substrate in spherical aggregates as compared to flat films, and was obtained empirically by comparing Runge−Kutta gradients for both geometries. Theoretically, Eq. 18 could have been avoided, as Runge−Kutta gradients might have been calculated for each separate aggregate. Such an approach, however, would involve a time−consuming calculation of z gradients instead of one. The extent of substrate penetration obtained this way was used to specify cellular lysis in large aggregates on the one hand, and aggregate fragmentation on the other.

Specific density of aggregates. To allow for a diameter−dependent specific density of aggregates, cellular decay by lysis is inferred. The penetration depth calculated from Eq. 18 demarcates an outer shell and

an inner core of the aggregate. Substrate conversions calculated according to Eq. 6 are assumed to occur in the outer shell only, while substrate concentrations within the inner core are equated to zero. If such an inner core exists at all ($d_p^i > 0$), i.e. for large aggregates, a constant specific rate of cellular decay μ_e (h^{-1}) is defined as:

$$\mu_e = (1/x_c) \cdot (dx_c/dt)_{decay} \qquad [19]$$

with: μ_e: constant, specific rate of decay (h^{-1}; $\mu_e < 0$); x_c: local dry-weight biomass concentration (kg/m^3) within the inner substrate--depleted core of an aggregate.

While biomass concentrations in the outer shell remain constant and i-independent (x_0), they decrease in the core of an aggregate if $d_p^i > 0$. Such decreased biomass concentrations for class i (x_c^i, kg/m^3) are calculated from the time the aggregate belongs this class on one hand,

$$t^i = -1 \ / \ \delta_{gr}^{i\rightarrow} \qquad [20]$$

with: t^i: time required for an aggregate to increase its diameter from d^i to d^{i+1},

and from the dry-weight biomass concentration in its core (x_c^{i-1}, kg/m^3) with which the aggregate originated as a member of class i. Thus, by integrating Eq. 19, and from Eq. 20:

$$x_c^i = x_c^{i-1} \cdot \exp(\mu_e \cdot t^i) \qquad [21]$$

If Δ_d-values (eq.2) are chosen sufficiently small, aggregates of the first category (i = 1) will be fully penetrated at the prevailing s_b-value (i.e. substrate concentrations throughout these aggregates are finite, and $d_p^1 = 0$). Therefore these aggregates have a mean biomass concentration (x^1, kg/m^3) equal to the standard biomass concentration x_0:

$$x^1 = x_0 \qquad [22]$$

Overall dry-weight biomass concentrations x^i (kg/m^3) within subsequently larger aggregates may be lower due to cellular decay and are calculated:

$$x^i = (d_p^i/d^i)^3 \cdot x_c^i \cdot \exp(\mu_e \cdot t^i) + [1 - (d_p^i/d^i)^3] \cdot x_0 \qquad [23]$$

with: x^i: mean dry-weight biomass concentration within an aggregate of class i (kg/m^3).

Overall biomass concentrations calculated according to Eq. 23 are used to calculate the overall specific density of a particular type of aggregate, assuming a specific weight for bacterial dry matter:

$$\rho_a^i = (1 - x^i/\rho_x) \cdot \rho_0 + x^i \qquad [24]$$

with: ρ_a^i: overall specific density of an aggregate of type i (kg/m^3); ρ_x: specific density of bacterial dry matter (kg/m^3); ρ_0: specific density of bulk liquid (kg/m^3).

Wash—out of aggregates. The rate at which aggregates are removed from the reactor is described as a stochastic process, depending on hydrodynamic conditions in the settler compartment and the settling velocity v_∞^i (m/h) of aggregates in a stagnant liquid. The latter quantity depends on diameter d^i and overall specific density ρ_a^i, according to an expression used previously (*this thesis*, Chapter V). Rearranging this expression yields:

$$v_\infty^i = Q \cdot (d^i)^{1.94} \cdot (\rho_a^i - \rho_0)^{0.71} \qquad [25]$$

with: Q: lumped constant of, among others, bulk—liquid viscosity and density ($m^{2.09}/kg^{0.71} \cdot s$).

The other parameter taken to influence wash—out of aggregates is the upward liquid velocity v_l (m/h) in the effluent section, which is calculated as:

$$v_l = D \cdot V / A \qquad [26]$$

with: D: dilution rate (h^{-1}), ratio of influent flow and total reactor volume V; A: cross—sectional area (m^2) of the effluent section normal to the direction of effluent liquid flow.

The rate at which the numerical concentration of aggregates of class i decreases due to wash—out (δ_{wo}^i, h^{-1}; $\delta_{wo}^i \leqslant 0$) is defined as:

$$\delta_{wo}^i = (1/n^i) \cdot (dn^i/dt)_{wo} \qquad [27]$$

With a tentative calculation of a retention value R^i ($-$) for each separate category of aggregates as:

$$R^i = \sqrt{(v_l + v_\infty^i) / v_l} \qquad [28]$$

the following expression is obtained:

$$\delta_{wo}^i = -D / R^i \qquad [29]$$

These expressions satisfy the abovementioned boundary condition and describe wash—out of a stochastic nature: all aggregates may be removed from the reactor, but, depending on settling velocity, the efficiency of retention varies.

Disintegration of aggregates. A specific rate of decrease of numerical concentrations in category i due to fragmentation ($\delta_{fr}^{i\rightarrow}$, h^{-1}; $\delta_{fr}^{i\rightarrow} \leqslant 0$) is defined as:

$$\delta_{fr}^{i\rightarrow} = (1/n^i) \cdot (dn^i/dt)_{fr}^{i\rightarrow} \qquad [30]$$

with: superscripted i→: indicating fragmentation of type i, and resulting in smaller aggregates (to be defined below).

Quantitative expressions to describe this rate are not available from the literature. However, it has been suggested repeatedly that the production of gaseous metabolites may lead to disintegration of aggregates (Krouwel & Kossen, 1980, 1981; Emery & Mitchell, 1986). Therefore, fragmenta—

tion is taken to be proportional to the export flux of metabolic products, and, consequently, to the import flux of substrate (*i.e.* proportional to $\lambda^i/(d^i)^2$. Furthermore, disintegration would depend on shear forces exerted by the liquid, which are taken to be proportional to a charac—teristic aggregate surface $(d^i)^2$. Finally, the progress of decay processes as represented by the decrease in overall biomass concentration with respect to the standard biomass concentration $(x_0 - x^i)/x_0$ is taken as a general measure for aggregate strength, and therefore influences disinte—gration. Combining these three factors, the following expression is obtained:

$$\delta_{fr}^{i\rightarrow} = f \cdot \lambda^i \cdot (x_0 - x^i) \: / \: x_0 \qquad\qquad [31]$$

with: f: proportionality constant (mol^{-1})
Such a formulation implies that aggregates do not fragment unless substrate penetration is incomplete, *i.e.* unless $d_p^i > 0$ and thus $x^i < x_0$.

Disintegration of aggregates in category m is assumed to result in the production of a variety of smaller ones, with conservation of the total volume that is liberated by fragmentation. A fraction a of the volume of a disintegrating aggregate is split in two halves $a/2$ and attributed to a category of corresponding aggregate volume, while the remaining part $1-a$ is taken to reappear as members of the first category ($i = 1$). As a ($-$) determines the ratio between large and small fragments produced, it shall tentatively be referred to as the sloughing/attrition ratio. A specific rate may now be defined with which numerical concentrations in any category increase due to fragmentation of larger aggregates. Thus, for $i > 1$:

$$\delta_{fr}^{\rightarrow i} = -(1/n^i) \cdot \Sigma_{m=i+1}^{z} \: n^m \cdot \delta_{fr}^{m\rightarrow} \cdot a \cdot V_a^m \: / \: V_a^i \qquad\qquad [32]$$

with: superscripted i→: indicating fragmentation of one or more large aggregates, resulting in the production of i.
where m is the smallest integer satisfying the condition:

$$(a/2) \cdot V_a^m = V_a^i \qquad\qquad [33]$$

Due to this latter condition, the cumulative term in Eq. 32 shall contain only one or two members. For $i = 1$ on the other hand:

$$\delta_{fr}^{\rightarrow 1} = (1/n^1) \cdot \Sigma_{m=2}^{z} \: n^m \cdot \delta_{fr}^{m\rightarrow} \cdot (1-a) \cdot V_a^m \: / \: V_a^1 \qquad\qquad [34]$$

with: $\delta_{fr}^{\rightarrow i}$: specific rate of increase of numerical concentration for type i due to fragmentation of larger aggregates (h^{-1}; $\delta_{fr}^{\rightarrow i} \geqslant 0$); $\delta_{fr}^{\rightarrow 1}$: idem, for $i = 1$ (h^{-1}; $\delta_{fr}^{\rightarrow 1} \geqslant 0$); m: integer ($-$; $i < m <$ n).

Balance for a single class of aggregates. The equations obtained thus far allow a complete description of the change in numerical concentration of aggregates in any particular category. The increase and

decrease due to growth result from Eqs. 13 and 16, while increase and decrease by fragmentation are given by Eqs. 30 and 33. Eq. 29 provides a description of decrease due to wash−out. The assumption of steady−state conditions dictates that there is no net change in the number of aggregates in any class i. Thus:

$$\delta_{gr}^{\rightarrow i} + \delta_{gr}^{i\rightarrow} + \delta_{wo}^{i} + \delta_{fr}^{i\rightarrow} + \delta_{fr}^{\rightarrow i} = 0 \qquad [35]$$

where the first and last terms of the left−hand side are positive, and the remaining terms are negative. Substitution from Eq. 16 then yields:

$$n^{i-1}/n^{i} = (\delta_{gr}^{i\rightarrow} + \delta_{wo}^{i} + \delta_{fr}^{i\rightarrow} + \delta_{fr}^{\rightarrow i})/(\delta_{gr}^{i-1\rightarrow}) \qquad [36]$$

If the operational conditions are known (D, s_0), Eq. 36 allows calculation of a complete distribution in a top−down fashion. To this end, a tentative value for the bulk−liquid substrate concentration s_b is assumed. If the numerical concentration for the largest category is known (n^z), Eq. 30 can be evaluated for the fragmentation of these aggregates, while Eqs. 32 and 33 dictate whether the latter process yields any aggregates of category $z-1$. Next, n^{z-1} is calculated according to Eq. 36. This routine is repeated for subsequently smaller aggregates, until all n^i−values (*i.e.* a complete distribution) are obtained. In the process, subsequent contributions are gathered for the cumulative term in Eq. 33. Finally, the validity of a complete distribution is judged with the aid of Eq. 33. By means of iteration of s_b, a final distribution was obtained that satisfies Eq. 33. It should be noted that validity of a distribution is depending on relative and not on absolute n^i−values.

Steady−state bulk−liquid substrate balance. If density differences between reactor influent and effluent are neglected, a balance on substrate supply, consumption, and discharge over the bulk liquid in the reactor yields:

$$D \cdot (s_0 - s_b) + s_b \cdot \Sigma_{(1,z)} \, n^i \cdot \delta_{wo}^{i} \cdot V_a^i = \Sigma_{i=1}^z \, n^i \cdot \lambda^i \qquad [37]$$

The second term on the left−hand originates from the fact that the reactor influent is liquid only, while the effluent consists of liquid *cum* aggregates.

With the aid of an arbitrary numerical concentration n^z, a distribution was obtained (*"Balance for a single class of aggregates"*), which now may be tested against Eq. 37. Subsequently, all n^i−values are multiplied with a common factor (*i.e.* the level of the distribution is adapted), until the distribution satisfies Eq. 37. The latter routine does not affect the validity of the distribution.

Overall reactor characteristics. On the basis of the final distribution, the volume−averaged reactor and effluent dry−weight biomass concentrations x_r and x_e (kg/m^3) were calculated as:

Table 1 : Standard set of parameter values used in model calculations.

μ_{max}	: 0.4 h^{-1}	D_e	: $5 \cdot 10^{-8}$ m^2/s
K_s	: 0.05 mol/m^3	V	: $2 \cdot 10^{-3}$ m^3
Y	: 0.025 kg/mol	f	: 10^4 mol^{-1}
μ_e	: 0.04 h^{-1}	Q	: 2.095 m$^{2 \cdot 09}$/kg$^{0.71} \cdot$s
s_e	: 0.015 mol/m^3	a	: 0.9
Δ_d	: 10^{-4} m	s_0	: 50 mol/m^3
z	: 100	x_0	: 150 kg/m^3
n^z	: 10^{-50} m^{-3} (initial)	ρ_0	: 1000 kg/m^3

$$x_r = \Sigma_{i=1}^z \ n^i \cdot V_a^i \cdot x^i \qquad\qquad [38]$$

$$x_e = (1/D) \cdot \Sigma_{i=1}^z \ n^i \cdot \delta_{wo}^i \cdot V_a^i \cdot x^i \qquad\qquad [39]$$

To judge the general effect of lysis, virtual reactor and effluent biomass concentration $x_{r,0}$ and $x_{e,0}$ (kg/m^3) were calculated assuming biomass concentrations in all aggregates to equal x_0, i.e. by substituting x_0 for x^i in Eqs. 38 and 39. Values for $x_{r,0}$ and $x_{e,0}$ therefore are proportional to the volume of aggregates per unit reactor or effluent volume. By expressing biovolume on a biomass basis, a direct comparison with x_r—data is facilitated.
An overall efficiency $\bar{\eta}$ (−) was obtained from:

$$\bar{\eta} = \{ \ \Sigma_{i=1}^z \ n^i \cdot \lambda^i \ \} \ / \ \{ \ \Sigma_{i=1}^z \ n^i \cdot V_a^i \cdot (\mu_{max} \cdot x_0/Y) \cdot Mo_b \ \} \qquad [40]$$

The use of x_0 in the denominator of this expression implies that $\bar{\eta}-$ −values reflect the combined effect of transport limitation and the resulting cellular lysis.

Choice of parameter values. A standard set of parameter values was used for calculations, which involved variation in D, s_0, and a only. Only if explicitly mentioned, values differed from the ones in Table 1. Data on kinetic parameters, on medium, and on reactor construction were obtained from several sources (Zoetemeijer, 1982; Cohen, 1982; Van den Heuvel, 1985; *this thesis*, Chapter II). Following the reasoning of Atkinson & Rahman (1979), substrate diffusivity in aggregates was taken to equal diffusivity in aqueous solution. The specific lysis rate μ_e was in agreement with data of Novitsky (1986) on decay of a natural population. The standard biomass concentration within aggregates x_0 was about twice the concentrations found in some extremely dense suspended cultures.
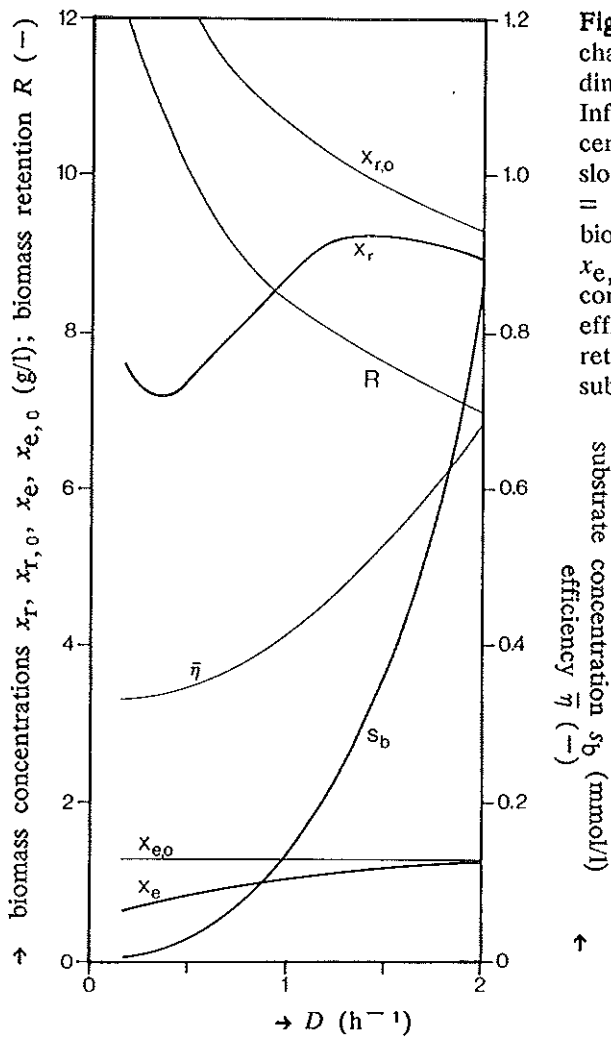
Fig. 3 : Overall reactor characteristics as depen—ding on dilution rate D. Influent substrate con—centration $s_0 = 50$ mmol/l, sloughing attrition ratio a = 0.9. x_r, $x_{r,0}$: reactor biomass concentration; x_e, $x_{e,0}$: effluent biomass concentration; $\bar{\eta}$: overall efficiency; R: biomass retention; s_b: bulk—liquid substrate concentration.

RESULTS

With the standard set of parameters, an influent substrate concentration s_0 of 50 mol/m^3, and a sloughing/attrition ratio a of 0.9, a general picture was obtained of overall reactor characteristics as depending on the dilution rate D (Fig. 3). For the reactor biomass concentration x_r in particular, this picture was quite complex: a minimum x_r-value of 14 7 g/l was observed at $D = 0.3$ h^{-1} and a maximum of 18.5 g/l at $D = $

$1.3 \ h^{-1}$. As a contrast, the volume occupied by aggregates in the reactor (represented by $x_{r,0}$) was seen to decrease continuously (or, reversely, the voidage was seen to increase). At elevated dilution rates, x_r and $x_{r,0}$ were nearly identical, indicating that the major part of the aggregates were not subject to lysis and therefore had an overall biomass concentration equal to x_0. Enhanced penetration of substrate at elevated D—values may also be inferred from bulk—liquid substrate concentrations s_b, which increased continuously with D.

Effluent biomass concentrations, when expressed on a biovolume basis $(x_{e,0})$, equalled the value that would be expected for a regular CSTR at the present influent concentration, i.e. $Y \cdot (s_0 - s_b)$. At elevated dilution rates, x_e and $x_{e,0}$—values (on dry—weight and biovolume basis, respectively) were almost identical. At $D = 0.15 \ h^{-1}$, however, x_e was substantially lower than $x_{e,0}$. Again, this decrease reflects substrate insufficiency in a major part of the aggregates.

From the reactor and effluent dry—weight biomass concentrations, bacterial retention R was evaluated. Over the entire range of D—values tested, R was seen to decrease gradually, from $R = 12$ at $D = 0.15$ h^{-1} to $R = 1.25$ at $D = 2.0 \ h^{-1}$. An identical result was obtained when biovolume data were used instead of dry—weight values (not shown).

As does the bulk—liquid substrate concentration s_b, the overall efficiency $\bar{\eta}$ increases with the dilution rate. At a dilution rate of $D = 2.0 \ h^{-1}$, $\bar{\eta}$—values rapidly approached unity, indicating a large fraction of the aggregates to be completely penetrated with substrate at a concentration s_b.

The reactor biomass concentration x_r is a volume—averaged lumped variable, reflecting, among others, the particular aggregate size distribution. Fig. 4 gives distributions of aggregate sizes at four different D—values. While biomass concentrations were calculated by an integrating procedure up until the largest category $(z = 100; cf.$ Eq. 38), distributions are shown up until the category with a cumulative biomass concentration of 99.999 %. Using this criterion, distributions are seen to widen when the dilution rate is increased. For $D = 0.15 \ h^{-1}$, a narrow distribution was observed, with a maximum aggregate diameter of 3.15 mm. At $D = 1.90 \ h^{-1}$, the maximum aggregate diameter was 5.35 mm. The general shape of all four distributions is seen to be sigmoid, but, depending again on the dilution rate, the individual functions exhibited interesting ideosyncrasies. At $D = 0.15 \ h^{-1}$, numerical concentrations n^i were seen to decrease continuously with d^i. At elevated D—values $(1.9 \ h^{-1})$, however, distribution functions with a very pronounced sigmoid character were observed. As a result, distributions were bimodal, with high frequencies for small and large aggregates, whereas intermediate sizes were quite sparse.

Some specific characteristics of individual aggregates, pertaining to the size distributions and biomass concentrations shown above, are

Fig. 4 : Numerical concentrations n^i of various aggregate sizes at, respectively, $D = 0.15, 0.70, 1.30,$ and 1.90 h^{-1}.
Fig. 5 : Specific mass ρ_a^i of aggregates as depending on diameter d^i at $D = 0.15, 0.70, 1.30,$ and 1.90 h^{-1}, respectively.


Fig. 4
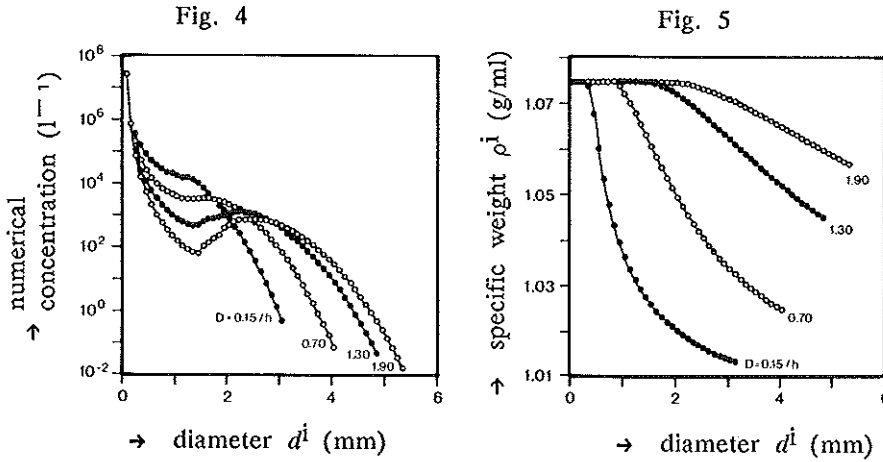
Fig. 5

depicted in Figs. 5 and 6. The overall specific density of aggregates ρ_a^i reflects their mean biomass concentration x^i and is shown to depend on the diameter at all four dilution rates (Fig. 5). In all cases, a more or less extended range of small aggregates was found to have identical ρ_a^i−values, corresponding to the standard biomass concentration x_0. Larger aggregates, however, showed increasingly lower specific densities, reflecting lysis due to substrate insufficiency. The decrease in specific density was most prominent at moderate D−values (and thus at low bulk−liquid substrate concentrations). At $D = 1.9$ h^{-1}, on the other hand, ρ_a^i was almost diameter independent over the entire range of diameters.

Settling velocities v_∞^i for individual aggregates (Fig.6) depended on the combined effect of diameter and specific density (cf. Fig. 5). In agreement with the diameter−independency of specific density at $D = 1.9$ h^{-1} (Fig. 5), an almost linear relation between v_∞^i and d^i was calculated for this dilution rate. At lower D−values, the pronounced diameter dependency of ρ_a^i entered the picture, resulting in a convex v_∞^i/d^i relation.

The settling velocities shown in Fig. 6 have a direct bearing on the retention R^i of individual aggregates (Fig. 7). The latter parameter, however, also strongly depends on dilution rate, and Fig. 7 shows that the influence of the upward liquid velocity in the settler is quite

Fig. 6 : Settling velocity v_∞^i of aggregates as a function of their diameter d^i. $D = 0.15, 0.70, 1.30,$ and 1.90 h^{-1}, respectively.
Fig. 7 : Retention R of different categories of aggregates; $D = 0.15, 0.70, 1.30,$ and 1.90 h^{-1}, respectively.

Fig. 6

Fig. 7
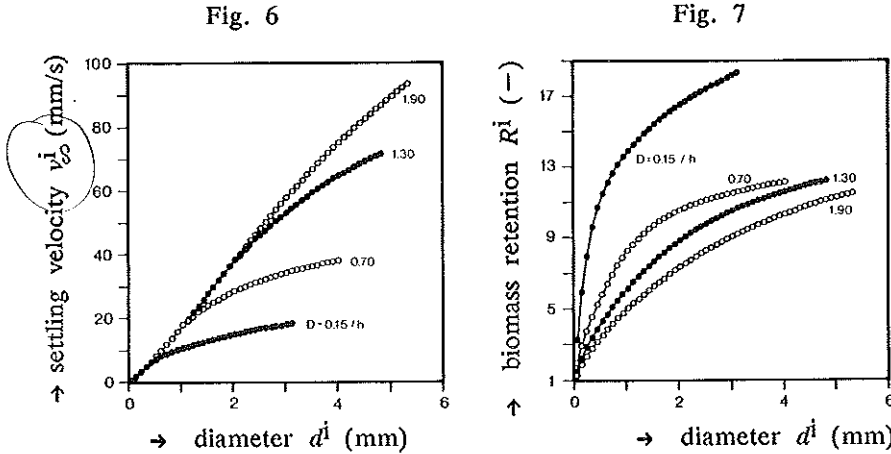
prominent. Although an increase in D resulted in higher settling velocities v_∞^i (cf. Fig. 6), lower R^i—values were observed throughout. Consequently, the overall retention R is lower.

The contribution of separate categories of aggregates to total substrate conversion is depicted in Fig. 8. Except for the lowest dilution rate ($D = 0.15$ h^{-1}), a bimodal distribution of activity was observed. A substantial fraction of the total substrate conversion was performed by large aggregates, notwithstanding low numerical concentrations n^i (cf. Fig. 4).

The above results pertain to an influent concentration of substrate of 50 mol/m^3. Further s_0—values were tested, ranging from 25 to 200 mol/m^3. Variation in s_0 was found to have no effect at all on the bulk—liquid substrate concentration, the particular shape of the distribution function (i.e. the relative values of n^i), and specific characteristics such as settling velocity and specific density (results not shown). Only absolute n^i—values (i.e. the level of the distribution function) and, consequently, reactor biomass concentrations x_r were a direct function of s_0. This result may be summarized as $x_r = R \cdot Y \cdot (s_0 - s_b)$, with R and s_b being s_0—independent.

Up until now, only one type of fragmentation has been considered, whereby a fragmenting aggregate produced for 10 % of its volume aggregates of the smallest category while the remainder was split in two ($a = 0.9$). Fig. 9 presents the effect of a decrease in a, i.e. a decrease
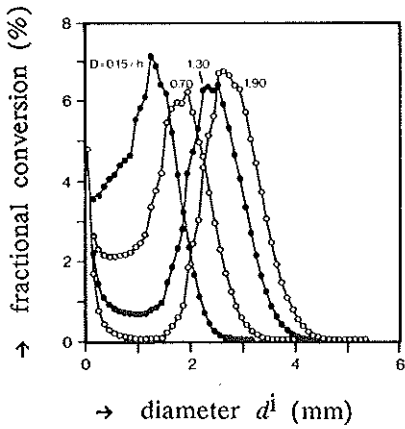
Fig. 8 : Rate of substrate conversion in the various categories of aggregates; influence of dilution rate. $D = 0.15$, 0.70, 1.30, and 1.90 h^{-1}, respectively.
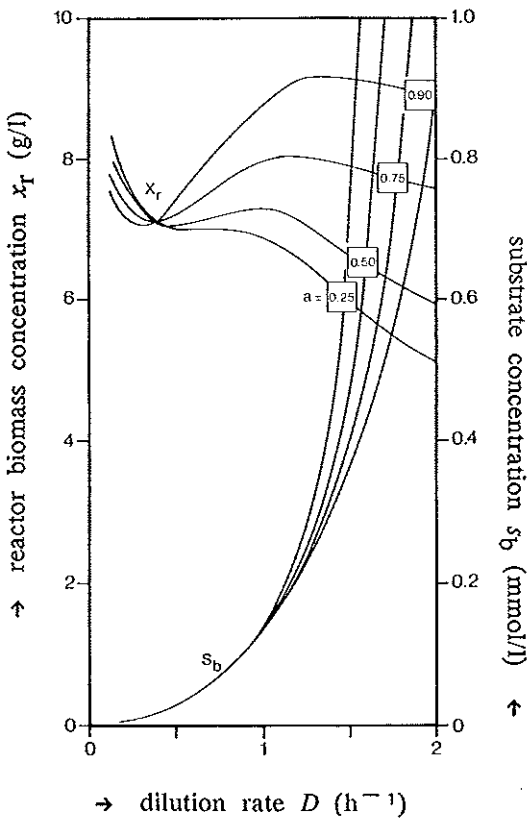

Fig. 9 : Influence of the sloughing/attrition ratio a on steady−state biomass and substrate concentration (x_r and s_b, respectively).

in the fraction of large aggregates produced. Whereas $a = 0.9$ resulted in a positive x_r/D relation (at least for a range of D—values), a decrease in a (*i.e.* a more prominent formation of small aggregates) reduced biomass concentrations at high dilution rates and resulted in a negative x_r/D relation throughout. At the same time, reduced substrate conversions and higher s_b—values were found.

DISCUSSION

The present model describes the dynamic behaviour of bacterial aggregates in a steady—state continuous—flow reactor of the AGLR—type. Dynamics is essentially described as a cyclic process, involving increase in size by growth on the one hand, and decrease in size by fragmentation on the other. Substrate consumption by aggregates is to be regarded as input to this cycle, while wash—out of aggregates constitutes the output. The final distribution of aggregate sizes and, consequently, the overall reactor characteristics result from the complex interaction of these processes. It was appreciated that such complexity would preclude any off—hand discussion of reactor behaviour on a strictly qualitative basis. This notion was the prime motive for developing the present mathematical model, which should provide a quantitative framework for the interpretation of experimental results.

The main result obtained is that it is possible indeed to calculate reactor performance, biomass concentrations, and biomass retention without recourse to such unattractive assumptions as a non—growth existence for rapidly consuming microbes, or the uniformity of aggregates. The present predictions on reactor performance are, to a considerable extent, based on mechanistic concepts.

As an important conclusion with practical relevance it was found that biomass retention R, whether expressed on a biovolume or on a dry—weight basis, is strongly dilution—rate dependent. It has been common practice to assume a D—independent R for the description of reactors with biomass retention (*e.g.* Pirt, 1975; Pirt & Kurowski, 1970; Wang *et al.*, 1979). The present results clearly demonstrate that variation in R should be taken into consideration whenever varying physical properties might be expected for the particles to be retained. Only at fixed dilution rates, R was found constant and was not influenced by variations in the influent concentration s_0 either. Only in its response to s_0 variation, the system may be compared to a CSTR: any such variations do not influence the activity or the chemical environment of an individual aggregate, but rather manifest themselves in changes in numerical concentrations of aggregates.

Continuous—flow reactors retaining biomass have been described on the assumption of a negligible effluent biomass concentration (Heijnen, 1984). As a rationale, substrate consumption was taken to equal

maintenance requirements exactly, which excludes any net growth. Satisfaction of this condition, however, requires a single specific substrate concentration. Therefore, it is incompatible with heterogeneous systems, which characteristically involve substrate gradients. It is felt that the present approach is more realistic in accounting for a spatial separation of growth and non−growth conditions (*i.e.* the outer shell and the inner core of an aggregate, respectively).

Atkinson & Rahman (1979) have modelled a continuous−flow reactor which contained a range of aggregates. They did not, however, consider a dynamic behaviour for individual aggregates on the basis of growth or fragmentation. Using arbitrary distribution functions as input parameters to their model, they concluded that reactor operation could be described just as well with a single characteristic aggregate instead of a complete distribution. Although this may be true (as it seems trivial), these authors do not provide a recipe to predict the properties of such a typical aggregate on the basis of operating conditions.

The calculated distribution functions mainly show negative (dn^i/dd^i)−values, *i.e.* have a negative slope over almost the entire diameter range. Only for high D−values and for low a−values (enhanced production of small aggregates from fragmentation), negative and positive (dn^i/dd^i)−values and bimodal distributions were observed. The sign of the slope of the distribution function is determined by the fragmentation process, as may be appreciated from Eq. 36. The right−hand side of this equation contains one positive term (*i.e.* $\delta \dot{r}_{fr}^i$), whereas the remaining terms are negative. Therefore, the magnitude of $\delta \dot{r}_{fr}^i$ determines whether n^{i-1} is smaller or greater than n^i.

Experimentally observed distributions invariably exhibited a maximum somewhere around $d^i = 0.8$ mm (*this thesis*, Chapter V). At present, it cannot be excluded that these maxima are an artefact. The experimental technique relied on the visualization of aggregates on a digitizer screen, and a lower detection level of *ca.* 0.5 mm is quite conceivable for such a procedure. Using different techniques, however, Wiegant & De Man (1986) and also Hulshoff Pol *et al.* (1986) have observed similar maxima, while Parker *et al.* (1971) reported bimodal distributions. The present model offers the possibility to explain these maxima by adopting a specific fragmentation mechanism (*i.e.* without recourse to experimental artefacts).

As a simplification, the microbial population was considered spatially homogeneous with respect to its kinetics constants. It has been shown by Kissel and co−workers (Kissel, 1985; Kissel *et al.*, 1984), however, that inhomogeneity with respect to bacterial population composition is quite conceivable for reactors with an immobilized mixed culture. Environmental conditions are a function of the position within an immobilized aggregate, and therefore the competitive position of the various bacterial species would also be depth−dependent. It would be of interest to combine the present model and the approach by Kissel and

co−workers to investigate the possibility of a diameter−specific physiology for a range of aggregate sizes. If so, the overall physiological behaviour of a reactor as a function of dilution rate could be predicted, as the latter variable is shown to affect the size distribution of aggregates.

The model shows that, except for the lowest dilution rates, intermediate aggregates hardly contribute to the total substrate conversion. The distribution of activity is strongly bimodal, with a large part of the total consumption being performed by large aggregates. Nevertheless, it is conceivable that the model underestimates the role of the smallest category of aggregates in particular. If Δ_d−values are chosen sufficiently small, the smallest aggregate ($i=1$) may in fact represent an individual bacterial cell. No attention was given, however, to the eco−physiological likelyhood of suspended growth, and bi−division of individual cells as a result of substrate consumption is not allowed for in the present formulations. Increase in size is the only type of growth taken into account, and as fragmentation of large aggregates is the exclusive source of the smallest ones, this latter process constitutes a *conditio sine qua non*. Quite likely, bacterial division would relieve this condition and would increase the fraction of the smallest aggregates ("cells"), and therefore their contribution to the total conversion.

The mathematical description of some of the processes incorporated in the present model admittedly is tentative, and surely would benefit from further research. Nevertheless, the main conclusions are not necessarily affected by modifications in individual processes. A dilution−rate dependency for biomass retention, *e.g.*, was invariably established, notwithstanding drastic adjustments in the fragmentation pattern. Furthermore, it is felt that the present model could aid in directing future research into constituent processes, as it may pronounce upon the general impact of alternative mechanisms for growth, fragmentation, and wash−out.

ACKNOWLEDGEMENTS

Symbols and units, roman

A	: cross−sectional area reactor effluent port (L^2)
a	: fraction specifying fragmentation of aggregates $(-)$
A_a	: fractional area occupied by cells in micrograph $(-)$
C_D	: drag coefficient $(-)$
d, $d^{1,i,m,z}$	: diameter of an aggregate; c.q. in category 1, i, m, z (L)
d_p^i	: diameter of the core of an aggregate in class i which is not fully penetrated with substrate (L)
d_s	: Sauter mean diameter of a size distribution (L)
D	: dilution rate (T^{-1})
D_e	: effective diffusivity of substrate in biomass (L^2/T)
F	: influent flow rate (L^3/T)
g	: acceleration due to gravity (L^2/T)
i	: integer, indicating category of aggregate $(-)$
K_s	: kinetic constant in Monod equation (M/L^3)
l	: length of bacterial aggregate in digitizer procedure (L)
Mo, Mo_b	: Monod number or degree of saturation; with respect to bulk−liquid conditions $(-)$
m	: integer, indicating category of aggregate $(-)$
n	: integer, indicating category of aggregate $(-)$
$n^{1,i,m,z}$	: numerical concentration of aggregates in class 1, i, m, z (L^{-3})
N_v	: numerical concentration of cells (L^{-3})
p	: volumetric reactor biomass productivity $(M/L^3 \cdot T)$

Q : lump parameter for calculation of settling velocity ($L^{2.09}.M^{0.71}.T$)

R, R^i : biomass retention on dry−weight basis; *c.q.* in a category of aggregates (−)

s, s_0, s_b : substrate concentration; *c.q.* influent; bulk liquid (M/L^3)

s_e : substrate concentration above which $\mu_e = 0$ (M/L^3)

t : time (T)

t_d : bacterial doubling time, $(\ln 2)/\mu$ (T)

v_∞, v_∞^i : settling velocity of an aggregate; *c.q.* in class i (L/T)

v_l : liquid velocity reactor effluent (L/T)

V : volume of bulk liquid and aggregates (L^3)

V_a, V_a^i : volume of an aggregate; *c.q.* of type i (L^3)

V_b : volume of bulk liquid (L^3)

V_c : bacterial cell volume (L^3)

V_ν : fractional volume occupied by cells in an aggregate (−)

w : width of an aggregate in digitizer procedure (L)

x : dry−weight biomass concentration (M/L^3)

x_e, x_r : overall dry−weight biomass concentration in the effluent; reactor (M/L^3)

x_0 : standard dry−weight biomass concentration in substrate−−penetrated parts of aggregates (M/L^3)

x^i : overall dry−weight biomass concentration within aggre−gate of type i (M/L^3)

x_c^i : decreased dry−weight biomass concentration in substrate−free core of an aggregate of type i (M/L^3)

Y : stoichiometric yield coefficient (−)

z : integer, indicating largest category of aggregate (−)

z_0 : concentration of carrier material at dilution−rate shift−up (M/L^3)

Symbols and units, greek

β : dimensionless diameter (−)

$\delta_{gr}^{\rightarrow i}$: specific rate of increase in n^i due to growth (T^{-1})

$\delta_{gr}^{i\to}$	: specific rate of decrease in n^i due to growth (T^{-1})
δ_{wo}^{i}	: specific rate of decrease in n^i due to wash−out (T^{-1})
$\delta_{fr}^{i\to}$	: specific rate of decrease in n^i by fragmentation (T^{-1})
$\delta_{fr}^{\to i}$	: specific rate of increase in n^i by fragmentation (T^{-1})
Δ	: dimensionless dilution rate, D/μ_{max} $(-)$
Δ_d	: constant diameter difference between subsequent types of aggregates (L)
Δ_x^i	: difference in biomass between aggregates i and $i+1$ (M)
$\eta,\ \eta^i,\ \bar{\eta}$	: effectiveness factor; for type i; reactor−volume averaged $(-)$
μ	: specific bacterial growth rate (T^{-1})
μ_e	: specific rate of cellular lysis (T^{-1})
μ_{max}	: kinetic constant, maximum specific growth rate (T^{-1})
M	: dimensionless specific growth rate, μ/μ_{max} $(-)$
λ^i	: substrate conversion per unit time and per aggregate in class i (M/T)
Π	: dimensionless volumetric rate of production $(-)$
ρ_0	: specific density of bulk liquid (M/T^3)
$\rho_a,\ \rho_a^i$	: overall specific density of an aggregate; in category i (M/L^3)
ρ_x	: specific density of bacterial dry matter (M/L^3)
Σ	: dimensionless substrate concentration, s/K_s $(-)$
Σ_0	: dimensionless influent substrate concentration, s_0/K_s $(-)$
τ	: dimensionless time, $D \cdot t$ $(-)$
$\tau_{3,a}$	: dimensionless time characterizing onset of the HPr− −producing aggregates as determined on basis of fatty−acid concentrations $(-)$
$\tau_{3,x}$	: idem, with the aid of biomass concentrations $(-)$
$\tau_{4,a}$	: dimensionless time characterizing onset of HBt− −producing aggregates, with fatty−acid concentrations as indicator $(-)$
$\tau_{4,x}$	: idem, using biomass concentrations as an indicator $(-)$

φ, φ^i : modified Thiele−modulus; for aggregate of type i (−)

X, X_e, X_r : dimensionless biomass concentration $x/Y \cdot K_s$; in the effluent; in the reactor (−)

Abbreviations

AGLR	:	anaerobic gas−lift reactor
BSP	:	biological support particles
CF	:	continuous flow
CSTR	:	continuous−flow stirred−tank reactor
DMB	:	density marker beads®
EPS	:	extracellular polymeric material
Glc	:	glucose
HAc	:	acetic acid
HBt	:	butyric acid
HPr	:	propionic acid
HVa	:	valeric acid
Lac	:	lactic acid
LM	:	light microscopy
SEM	:	scanning electron microscopy
TEM	:	transmission electron microscopy
TOC	:	total organic carbon

REFERENCES

Afschar, A. S., H. Biebl, K. Schaller, and K. Schügerl (1985). Pro—
duktion von Aceton und Butanol durch *Clostridium acetobutylicum*
in kontinuierlicher Kultur mit Zellrückführung.
Chem. Ing. Tech. **57**, 352−357.

Akazawa, T., and E. E. Conn (1958). The oxidation of reduced pyridine
nucleotides by peroxidase.
J. Biol. Chem. **232**, 403−415.

Alleman, J. E., J. A. Veil, and J. T. Canaday (1982). Scanning
electron microscope evaluation of rotating biological contactor
biofilm.
Water Res. **16**, 543−550.

Andrews, G. F. (1986). Selecting particles for fluidized−bed bioreactors
with flocculent biomass.
Biotechnol. Proc. **2**, 16−22.

Andrews, G. F., and J. Przezdzlecki (1986). Design of fluidized−bed
fermentors.
Biotechnol. Bioeng. **28**, 802−810.

Anonymus (1980). Percoll® , methodology and applications; density mar—
ker beads for calibration of gradients of Percoll®.
Pharmacia Fine Chemicals, Uppsala.

Anonymus (1985). Percoll® reference list.
Pharmacia Fine Chemicals, Uppsala.

Atkinson, B. (1981). Immobilized biomass − a basis for process devel—
opment in wastewater treatment.
In: Biological fluidised bed treatment of water and wastewater (P.
F. Cooper and B. Atkinson, eds.), pp. 22−34.
Ellis Horwood, Chichester.

Atkinson, B., and I. S. Daoud (1976). Microbial flocs and flocculation.
Adv. Biochem. Eng. **4**, 41−124.

Atkinson, B, and A. J. Knights (1975). Microbial film fermenters : their
present and future applications.
Biotechnol. Bioeng. **17**, 1245− 1267.

Atkinson, B., and F. Mavituna (1983). Biochemical engineering and bio—
    technology handbook.
    Macmillan Publishers Ltd., London.
Atkinson, B., and F.—U. Rahman (1979). Effect of diffusion limitation
    and floc size distributions on fermentor performance and the
    interpretation of experimental data.
    Biotechnol. Bioeng. 21, 221—251.
Atkinson, B., G. M. Black, P. J. S. Lewis, and A. Pinches (1979).
    Biological particles of given size, shape, and density for use in
    biological reactors.
    Biotechnol. Bioeng. 21, 193—200.
Atkinson, B., J. D. Cunningham, and A. Pinches (1984). Biomass
    hold—ups and overall rates of substrate (glucose) uptake of
    support particles containing a mixed microbial culture.
    Chem. Eng. Res. Des. 62, 155—164.
Bailey, J. E. (1980). Biochemical reaction engineering and biochemical
    reactors.
    Chem. Eng. Sci. 35, 1854—1886.
Bazin, M. J. (1981). Theory of continuous culture.
    In: Continuous culture of cells (P. H. Calcott, ed.), pp. 27—62.
    CRC Press, Boca Raton.
Becker, H. A. (1959). Effects of shape and Reynolds number on drag in
    the motion of a freely oriented body in an infinite fluid.
    Can. J. Chem. Eng. 37, 85—91.
Beeftink, H. H., and P. Staugaard (1983). Acidification of glucose:
    architecture of biofilms as developed in an anaerobic gas—lift
    reactor with sand as adhesion support.
    In: Proceedings of the European Symposium on Waste Water
    Treatment (W. J. van den Brink, ed.), pp. 107—116.
    TNO Corp. Comm. Dep., The Hague.
Beeftink, H. H., and P. Staugaard (1986). Structure and dynamics of
    anaerobic bacterial aggregates in a gas—lift reactor.
    Appl. Environm. Microbiol. 52, 1139—1146.
Beeftink, H. H., and J. C. van den Heuvel (1986). A novel anaerobic
    gas—lift reactor (AGLR) with retention of biomass: start—up
    routine and establishment of hold—up.
    Biotechnol. Bioeng., accepted for publication.
Beeftink, H. H., M. van Dillen, and J. C. van den Heuvel (1986).
    Formation of bacterial aggregates in a continuous—flow reactor:
    influence of carrier availability.
    Biotechnol. Lett. submitted for publication.
Bennet, H. S. (1963). Morphological aspects of extracellular polysaccha—
    rides.
    J. Histochem. Cytochem. 11, 14—23.
Berkeley, R. C. W., J. M. Lynch, J. Melling, P. R. Rutter, and B.
    Vincent (1980). Microbial adhesion to surfaces.

Ellis Horwood Ltd., Chichester.

Bischoff, K. B. (1965). Effectiveness factors for general reaction rate forms.
AIChE. J. **11**, 351−355.

Bitton, G., and K. C. Marshall (1980). Adsorption of microorganisms to surfaces.
John Wiley & Sons, New York.

Blenke, H. (1979). Loop reactors.
Adv. Biochem. Eng. **13**, 121−214.

Bochem, H. P., S. M. Schoberth, B. Sprey, and P. Wengler (1982). Thermophilic biomethanation of acetic acid: morphology and ultrastructure of a granular consortium.
Can. J. Microbiol. **28**, 500−510.

Bornstein, B. T., and H. A. Barker (1948). The energy metabolism of *Clostridium kluyveri* and the synthesis of fatty acids.
J. Biol. Chem. **172**, 659−669.

Bowles, J. A., and D. H. Marsh (1982). Glycocalyx, capsule, slime, or sheath − which is it?
ASM News **48**, 295.

Breure, A. M. (1986). Hydrolysis and acidogenïc fermentation of protein and carbohydrates in anaerobic waste treatment.
PhD. thesis, University of Amsterdam, Amsterdam.

Brohan, B., and A. J. McLaughlin (1984). Characterization of the physical properties of yeast flocs.
Appl. Microbiol. Biotechnol. **20**, 16−22.

Buckland, B. C., D. R. Omstead, and V. Santamarina (1985). Novel β−lactam antibiotics.
In: Comprehensive biotechnology, Vol. III (H. W. Blanch, S. W. Drew, and D. I. C. Wang, eds.), pp. 49−68.
Pergamon Press, Oxford.

Bull, M. A., R. M. Sterritt, and J. N. Lester (1983). An evaluation of four start−up regimes for anaerobic fluidized bed reactors.
Biotechnol.Lett. **5**, 333−338.

Bull, M. A., M. R. Sterritt, and J. N. Lester (1984). The distribution of bacterial activity in an anaerobic fluidized bed reactor.
Water Res. **18**, 1017−1020.

Bu'lock, J. D., D. M. Comberbach, and O. Ghommidh (1984). A study of continuous ethanol production using a highly flocculent yeast in the gas lift tower fermenter.
Biochem. Eng. J. **29**, B9−B24.

Button, D. K. (1985). Kinetics of nutrient−limited transport and microbial growth.
Microbiol. Revs. **49**, 270−297.

Characklis, W. G. (1973). Attached microbial growths − II. Frictional resistance due to microbial slimes.
Water Res. **7**, 1249−1258.

Characklis, W. G., and K. E. Cooksey (1983). Biofilms and microbial fouling.
   Adv. Appl. Microbiol. **29**, 93−138.
Cheng, F. S., and G. D. Christian (1977). Amperometric measurement of enzyme reactions with an oxygen electrode using air oxidation of reduced nicotinamide adenine dinucleotide.
   Anal. Chem. **49**, 1785−1788.
Clark, D. S. (1962). Submerged citric acid fermentation of ferrocyanide− −treated beet molasses: morphology of pellets of *Aspergillus niger*.
   Can. J. Microbiol. **8**, 133−136.
Clift, R., J. R. Grace, and M. E. Weber (1978). Bubbles, drops, and particles.
   Academic Press, New York.
Cohen, A. (1983). Optimization of anaerobic digestion of soluble carbohydrate containing wastewaters by phase separation.
   PhD. thesis, University of Amsterdam.
Cohen, A., R. J. Zoetemeyer, A. van Deursen, and J. G. van Andel (1979). Anaerobic digestion of glucose with separated acid production and methane formation.
   Water Res. **13**, 571−580.
Cohen, A., A. M. Breure, J. G. van Andel, and A. van Deursen (1980). Influence of phase separation on the anaerobic digestion of glucose − I. Maximum COD−turnover rate during continuous operation.
   Water Res. **14**, 1439−1448.
Cohen, A., A. M. Breure, J. G. van Andel, and A. van Deursen (1982[a]). Influence of phase separation on the anaerobic digestion of glucose − II. Stability, and kinetic responses to shock loadings.
   Water Res. **16**, 449−455.
Cohen, A., A. van Deursen, J. G. van Andel, and A. M. Breure (1982[b]). Degradation patterns and intermediates in the anaerobic digestion of glucose: experiments with ^{14}C−labeled substrates.
   Antonie van Leeuwenhoek **48**, 337−352.
Cohen, A., J. M. van Gemert, R. J. Zoetemeyer, and A. M. Breure (1984). Main characteristics and stoichiometric aspects of acidogenesis of soluble carbohydrate containing wastewaters.
   Proc. Biochem. **19**, 228−232.
Cooney, C. L. (1983). Strategies for optimizing microbial growth and product formation.
   ACS Symp. Ser. **207**, 179−198.
Cooper, P. F. (1985). Biological fluidized bed reactors for treatment of sewage and industrial effluents.
   In: Comprehensive biotechnology, Vol.4 (C. W. Robinson and J. A. Howell, eds.), pp. 993−1006.

Pergamon Press, Oxford.

Cooper, D. J., and D. E. Clough (1985). Real−time estimation of dynamic particle−size distributions in a fluidized bed: theoretical foundation.
AIChE. J. **31**, 1202−1212.

Costerton, J. W., G. G. Geesey, and K.−J. Cheng (1978). How bacteria stick.
Sci. Am. **238**, 86−95.

Davis, R. H., and T. P. Hunt (1986). Modeling and measurement of yeast flocculation.
Biotechnol. Progr. **2**, 91−97.

Deinema, M. H., and L. P. T. M. Zevenhuizen (1971). Formation of cellulose fibrils by Gram−negative bacteria and their role in bacterial flocculation.
Arch. Mikrobiol. **78**, 42−57.

Dixon, B. (1984). Microbial adhesion slowly stirs.
Chem. Ind. **1984**, 198.

Doelle, H. W. (1975). Bacterial metabolism.
Academic Press, New York.

Dunnill, P. (1981). Biotechnology and industry.
Chem. Ind. **1981**, 204−217.

Dussap, G., and J. B. Gros (1982). Energy consumption and interfacial mass transfer area in an air−lift fermentor.
Chem. Eng. J. **25**, 151−162.

Eckenfelder, W. W., J. Patoczka, and A. T. Watkin (1985). Wastewater treatment.
Chem. Eng. **92**, 60−74.

Eighmy, T. T., D. Maratea, and P. L. Bishop (1983). Electron−microscopic examination of wastewater biofilm formation and structural components.
Appl. Environm. Microbiol. **45**, 1921−1931.

Ellwood, D. C., J. Melling, and P. Rutter (1979). Adhesion of microorganisms to surfaces.
Academic Press, London.

Emery, A. N., and D. A. Mitchell (1986). Operational considerations in the use of immobilised cells.
In: Process engineering aspects of immobilised cell systems (C. Webb, G. M. Black, and B. Atkinson, eds.), pp. 87−99. Institution of Chemical Engineers, Rugby.

Fletcher, M., and G. D. Floodgate (1973). An electron−microscopic demonstration of an acidic polysaccharide involved in the adhesion of a marine bacterium to solid surfaces.
J. Gen. Microbiol. **74**, 325−334.

Geesey, G. G. (1982). Microbial exopolymers: ecological and economic considerations.
ASM News **48**, 9−14.

Goldstein, I. (1985). Single cell protein.
    Springer Verlag, Berlin.
Grady, C. P. L. (1982). Modeling of biological fixed films — a state —
    —of—the—art review.
    In: Proc. 1st. Int. Conf. Fixed—Film Biol. Proc. (Y. C. Wu, E.
    D. Smith, R. D. Miller, and E. J. O. Patken, eds.), pp.
    344—404. University of Pittsburgh.
Grin, P., R. Roersma, G. Lettinga, and J. te Marvelde (1983). Start—up
    of anaerobic reactors for the treatment of raw sewage.
    In: Proc.Eur.Symp. Anaerobic Waste Water Treatm. (W. J. van
    den Brink, ed.), p. 440.
    TNO Corp.Comm.Dept., The Hague.
Gurr, E. (1965). Alcian blue for bacterial polysaccharides and capsules.
    In: The rational use of dyes in biology (E. Gurr, ed.), pp.
    170—171.
    Leonard Hill, London.
Häggström, L. (1981). Immobilized cells of *Clostridium acetobutylicum*
    for butanol production.
    Adv. Biotechnol. **2**, 79—83.
Hamer, G. (1982). Recycle in fermentation processes.
    Biotechnol. Bioeng. **24**, 511—531.
Harremoës, P., J. la Cour Jansen, and G. Holm Kristensen (1980).
    Practical problems related to nitrogen bubble formation in fixed
    film reactors.
    Progr. Water Technol. **12**, 253—269.
Hawkes, H. A. (1957). Film accumulation and grazing activity in the
    sewage filters at Birmingham.
    J. Proc. Inst. Sew. Purif. **1957**, 88—110.
Heijnen, J. J. (1984). Biological industrial waste—water treatment
    minimizing biomass production and maximizing biomass
    concentration.
    PhD. thesis, Delft Technical University, Delft.
Henrici, A. T. (1928). Morphologic variation and the rate of growth of
    bacteria.
    Bailliere, Tindall, & Cox, London.
Herbert, D. (1961). The chemical composition of micro—organisms as a
    function of their environment.
    Symp. Soc. Gen. Microbiol. **11**, 391—416.
Heukelian, H., and E. S. Crosby (1956). Slime formation in polluted
    waters.
    Sewage Ind. Wastes **28**, 78—92.
Hoehn, R. C., and A. D. Ray (1973). Effects of thickness on bacterial
    film.
    J. Water Poll. Contr. Fed. **45**, 2302—2320.
Howell, J. A., and B. Atkinson (1976^{a}). Influence of oxygen and
    substrate concentration on the ideal substrate uptake rate in

microbial film fermenters.
Biotechnol. Bioeng. **18**, 15−35.

Howell, J. A., and B. Atkinson (1976[b]). Sloughing of microbial film in trickling filters.
Water Res. **10**, 307−315.

Hsu, Y. C., and M. P. Dudukovič (1980). Gas holdup and liquid recirculation in gas−lift reactors.
Chem. Eng. Sci. **35**, 135−141.

Hulshoff Pol, L. W., W. J. de Zeeuw, C. T. M. Velzeboer, and G.Lettinga (1983). Granulation in UASB−reactors.
Water Sci. Technol. **15**, 291−304.

Hulshoff Pol, L. W., J. Dolfing, K. van Straten, W. J. de Zeeuw, and G. Lettinga (1984). Pelletization of anaerobic sludge in upflow anaerobic sludge bed reactors on sucrose−containing substrates.
In: Current perspectives in microbial ecology (M. J. Klug and C. A. Reddy, eds.), pp. 636−642.
American Society for Microbiology, Washington.

Hulshoff Pol, L. W., J. J. M. van de Worp, G. Lettinga, and W. A. Beverloo (1986). Physical characterization of anaerobic granular sludge.
In: Anaerobic treatment, a grown−up technology (NVA / EWPCA, eds.), pp. 89−102.
Industrial Presentations Group, Schiedam.

Jagadish, M. N., A. Lorincz, and B. L. A. Carter (1977). Cell size and cell division in yeast cultured at different growth rates.
FEMS Microbiol. Lett. **2,**235−237.

Jermyn, M. A. (1975). Increasing the sensitivity of the anthrone method for carbohydrate.
Anal. Biochem. **68**, 332−335.

Kennedy, K. J., and L. van den Berg (1985). Anaerobic downflow stationary fixed film reactors.
In: Comprehensive biotechnology, Vol.4 (C. W. Robinson and J. A. Howell, eds.), pp. 1027−1049.
Pergamon Press, Oxford.

Kierstan, M., and C. Bucke (1977). The immobilization of microbial cells, subcellular organelles, and enzymes in calcium alginate gels.
Biotechnol. Bioeng. **19**, 387−397.

Kinner, N. E., D. L. Balkwill, and P. L. Bishop (1983). Light and electron microscopic studies of microorganisms growing in rotating biological contactor biofilms.
Appl. Environm. Microbiol. **45**, 1659−1669.

Kissel, J. C. (1985). Numerical simulation of mixed−culture biofilms.
PhD. thesis, Stanford University.

Kissel, J. D., P. L. McCarty, and R. L. Street (1984). Numerical simulation of mixed−culture biofilms.
J. Environm. Eng. **110**, 393−411.

Klapwijk, A., H. Smit, and A. Moore (1981). Denitrification of domestic wastewater in an upflow sludge—blanket reactor without carrier material for the biomass.
In: Biological fluidised bed treatment of water and wastewater (P. F. Cooper and B. Atkinson, eds.), pp. 205—216.
Ellis Horwood Ltd., Chichester.

Kossen, N. W. F. (1986). The characteristics of immobilised cell particles.
In: Process engineering aspects of immobilised cell systems (C. Webb, G. M. Black, and B. Atkinson, eds.), pp. 103—116.
The Institution of Chemical Engineers, Rugby.

Krouwel, P. G., and N. W. F. Kossen (1980). Gas production by immobilized microorganisms: theoretical approach.
Biotechnol. Bioeng. **22**, 681—687.

Krouwel, P. G., and N. W. F. Kossen (1981). Gas production by immobilized microorganisms: calculation of theoretical maximum productivity.
Biotechnol. Bioeng. **23**, 651—655.

Kubota, H., Y. Hosono, and K. Fujie (1978). Characteristic evaluations of ICI air—lift type deep shaft aerator.
J. Chem. Eng. Japan **11**, 319—325.

Lapple, C. E., and C. B. Shepherd (1940). Calculation of particle trajectories.
Ind. Eng. Chem. **32**, 605—617.

Lee, T. H., J. C. Ahn, and D. D. Y. Ryu (1982). Performance of an immobilised yeast reactor system for ethanol production.
Enzyme Microb. Technol. **5**, 41—45.

Lettinga, G., A. F. M. van Velsen, S. W. Hobma, W. de Zeeuw, and A. Klapwijk (1980). Use of the upflow sludge blanket (USB) reactor concept for biological wastewater treatment, especially for anaerobic treatment.
Biotechnol. Bioeng. **22**, 699—734.

Linden, J. C., A. R. Moreira, and T. G. Lentz (1985). Acetone and butanol.
In: Comprehensive biotechnology, Vol. III (H. W. Blanch, S. W. Drew, and D. I. C. Wang, eds.), pp. 915—931.
Pergamon Press, Oxford.

MacDonald, J., P. T. V. Reeve, J. D. Ruddlesden, and F. H. White (1984). Current approaches to brewery fermentations.
Progr. Ind. Microbiol. **19**, 47—198.

Mack, W. N., J. P. Mack, and A. O. Ackerson (1975). Microbial film development in a trickling filter.
Microb. Ecol. **2**, 215—226.

Magara, Y., S. Nambu, and K. Utosawa (1976). Biochemical and physical properties of an activated sludge on settling characteristics.

Water Res. **10**, 71−77.

Marshall, K. C. (1980). Bacterial adhesion in natural environments.
In: Microbial adhesion to surfaces (R. C. W. Berkeley, J. M. Lynch, J. Melling, P. R. Rutter, and B. Vincent, eds.), pp. 187−196.
Ellis Horwood Ltd., Chichester.

Matson, J. V., and W. G. Characklis (1976). Diffusion into microbial aggregates.
Water Res. **10**, 877−885.

Matsuura, A., and L.−S. Fan (1984). Distribution of bubble properties in a gas−liquid−solid fluidized bed.
AIChE. J. **30**, 894−903.

Meadows, P. S., and J. G. Anderson (1966). Microorganisms attached to marine and freshwater sand grains.
Nature **198**, 610−611.

Merchuk, J. C., Y. Stein, and R. I. Mateles (1980). Distributed parameter model of an airlift fermentor.
Biotechnol. Bioeng. **22**, 1189−1211.

Molin, G., and I. Nilsson (1985). Sand administration as an instrument for biofilm control of *Pseudomonas putida* ATCC 11172.
Biotechnol. Bioeng. **27**, 117−120.

Monod, J. (1950). La technique de culture continue.
Ann. Inst. Pasteur **79**, 390−410.

Moo−Young, M., and H. W. Blanch (1983). Kinetics and transport phenomena in biological reactor design.
ACS Symp. Ser. **207**, 335−354.

Moo−Young, M., and T. Kobayashi (1972). Effectiveness factors for immobilized−enzyme reactions.
Can. J. Chem. Eng. **50**, 162−167.

Moresi, M. (1981). Optimal design of airlift fermenters.
Biotechnol. Bioeng. **23**, 2537−2560.

Muroyama, K., and L.−S. Fan (1985). Fundamentals of gas−liquid−solid fluidization.
AIChE. J. **31**, 1−34.

Nanninga, N., and C. L. Woldringh (1985). Cell growth, genome duplication and cell division.
In: Molecular cytology of *Escherichia coli* (N. Nanninga, ed.), pp. 259−318.
Academic Press, London.

Neijssel, O. M., and D. W. Tempest (1976). The role of energy−spilling reactions in the growth of *Klebsiella aerogenes* NCTC 418 in aerobic chemostat culture.
Arch. Microbiol. **110**, 305−311.

Nilsson, I., S. Ohlson, L. Häggström, N. Molin, and K. Mosbach (1980). Denitrification of water using immobilized *Pseudomonas denitrificans* cells.

Eur. J. Appl. Microbiol. Biotechnol. **10**, 261−274.

Novick, A., and L. Szillard (1950). Description of the chemostat.
Science **112**, 715−716.

Novitsky, J. A. (1986). Degradation of dead microbial biomass in a marine sediment.
Appl. Environm. Microbiol. **52**, 504−509.

Onken, U., and P. Weiland (1983). Airlift fermenters: construction, behavior, and uses.
Adv. Biotechnol. Proc. **1**, 67−95.

Ottenstein, D. M., and D. A. Bartley (1971). Separation of free acids C_2-C_5 in dilute aqueous solution column technology.
J. Chromatogr. Sci. **9**, 673−681.

Parker, D. S., W. J. Kaufman, and D. Jenkins (1971). Physical conditioning of activated sludge.
J. Water Poll. Contr. Fed. **43**, 1817−1833.

Patwardhan, V. S., and C. Tien (1985). Sedimentation and fluidization in solid−liquid systems: a simple approach.
AIChE J. **31**, 146−149.

Pirt, S. J. (1972). Prospects and problems in continuous flow culture of microorganisms.
J. Appl. Chem. Biotechnol. **22**, 55−64.

Pirt, S. J. (1975). Principles of microbe and cell cultivation.
Blackwell Scientific Publications, Oxford.

Pirt, S. J., and W. M. Kurowski (1970). An extension of the theory of the chemostat with feedback of organisms. Its experimental realization with a yeast culture.
J. Gen. Microbiol. **63**, 357−366.

Pohland, F. G., and S. Ghosh (1971). Anaerobic stabilization of organic wastes: two−phase concept.
Environm. Lett. **1**, 255.

Powell, M. S., and N. K. H. Slater (1982). Removal rates of bacterial cells from glass surfaces by fluid shear.
Biotechnol. Bioeng. **24**, 2527−2537.

Richardson, J. F., and W. N. Zaki (1954). Sedimentation and fluidization, I.
Trans. Inst. Chem. Engrs. **32**, 35−53.

Robinson, R. W., D. E. Akin, R. A. Nordstedt, M. V. Thomas, and H. C. Aldrich (1984). Light and electron microscopic examinations of methane−producing biofilms from anaerobic fixed−bed reactors.
Appl. Environm. Microbiol. **48**, 127−136.

Roels, J. A. (1983). Energetics and kinetics in biotechnology.
Elsevier Biomedical Press, Amsterdam.

Rousseau, I., and J. D. Bu'lock (1980). Mixing characteristics of a simple air−lift.
Biotechnol. Lett. **2**, 475−480.

Ryter, A., E. Kellenberger, A. Birch−Andersen, and O. Maaløe (1958).

Etude au microscope électronique de plasmas contenant de l'
acide désoxyribonucléique. I. Les nucléoides des bactéries en
croissance active.
Z. Naturforschung **13B**, 597−605.

Salkinoja−Salonen, M. S., E.−J. Nyns, P. M. Sutton, L. van den Berg,
and A. D. Wheatley (1983). Starting−up of an anaerobic
fixed−film reactor.
Water Sci. Technol. **15**, 305−308.

Sanders, W. M. (1966). Oxygen utilization by slime organisms in a
continuous culture.
Int. J. Air Water Poll. **10**, 253−276.

Savage, D. C. (1980). Colonization by and survival of pathogenic
bacteria on intestinal mucosal surfaces.
In: Adsorption of microorganisms to surfaces (G. Bitton and K.
C. Marshall, eds.), pp. 175−206.
John Wiley & Sons, New York.

Savage, D. C., and M. Fletcher (1985). Bacterial adhesion −
mechanisms and physiological significance.
Plenum Press, New York.

Sevilla, M.−J., and F. C. Odds (1986). Development of *Candida albica*
hyphae in different growth media − variations in growth rates,
cell dimensions and timing of morphogenetic events.
J. Gen. Microbiol. **132**, 3083−3088.

Shieh, W. K., and C.−Y. Chen (1984). Biomass hold−up correlations
for a fluidized bed biofilm reactor.
Chem. Eng. Res. Des. **62**, 133−136.

Shieh, W. K., P. M. Sutton, and P. Kos (1981). Predicting reactor
biomass concentration in a fluidized−bed system.
J. Water Poll. Contr. Fed. **53**, 1574−1584.

Shiotani, T., and T. Yamane (1981). A horizontal packed bed reactor to
reduce carbon dioxide gas hold−up in the continuous production
of ethanol by immobilised yeast cells.
Eur. J. Appl. Microbiol. Biotechnol. **13**, 96−101.

Stephenson, T., and J. N. Lester (1986). Evaluation and startup of four
anaerobic processes treating a synthetic meat waste.
Biotechnol. Bioeng. **28**, 372−380.

Stewart, G. G., and I. Russell (1985). Modern brewing technology.
In: Comprehensive biotechnology, Vol. III (H. W. Blanch, S.
Drew, and D. I. C. Wang, eds.), pp. 335−381.
Pergamon Press, Oxford.

Strand, S. E., A. J. McDonnell, and R. F. Unz (1985). Concurrent
denitrification and oxygen uptake in microbial films.
Water Res. **19**, 335−344.

Switzenbaum, M. S., and W. J. Jewell (1980). Anaerobic attached−film
expanded−bed reactor treatment.
J. Water Poll. Contr. Fed. **52**, 1953−1965.

Switzenbaum, M. S., K. C. Scheuer, and K. E. Kallmeyer (1985). Influence of materials and precoating on initial anaerobic biofilm development.
Biotechnol. Lett. **7**, 585–588.

Tago, Y., and K. Aida (1977). Exocellular mucopolysaccharide closely related to bacterial floc formation.
Appl. Environm. Microbiol. **34**, 308–314.

Tambo, N., and H. Hozumi (1979). Physical characteristics of flocs — II. Strength of floc.
Water Res. **13**, 421–427.

Tambo, N., and Y. Watanabe (1979). Physical characteristics of flocs — I. The floc density function and aluminium floc.
Water Res. **13**, 409–419.

Tempest, D. W., and O. M. Neijssel (1984). The status of Y_{ATP} and maintenance energy as biologically interpretable phenomena.
Ann. Rev. Microbiol. **38**, 459–486.

Tempest, D. W., O. M. Neijssel, and W. Zevenboom (1983). Properties and performance of microorganisms in laboratory culture; their relevance to growth in natural ecosystems.
Symp. Soc. Gen. Microbiol. **34**, 119–152.

Timmermans, P., and A. van Haute (1984). Influence of the type of organisms on the biomass hold–up in a fluidized–bed reactor.
Appl. Microbiol. Biotechnol. **19**, 36–43.

Toldrá, F., A. Flors, J. L. Lequerica, and S. Vallés (1986). Fluidized bed biomethanation of acetic acid.
Appl. Microbiol. Biotechnol. **23**, 336–341.

Trulear, M. G., and W. G. Characklis (1982). Dynamics of biofilm processes.
J. Water Poll. Contr. Fed. **54**, 1288–1301.

Van den Heuvel, J. C. (1985). The acidogenic dissimilation of glucose: a kinetic study of substrate and product inhibition.
PhD. thesis, University of Amsterdam.

Van den Heuvel, J. C., and H. H. Beeftink (1986). Kinetic effects of the simultaneous inhibition by substrate and product.
Biotechnol. Bioeng., submitted for publication.

Van den Heuvel, J. C., and R. J. Zoetemeyer (1982). Stability of the methane reactor: a simple model including substrate inhibition and cell recycle.
Proc. Biochem. **17**, 14–19.

Vanderborght, J. P., and Ch. Gilliard (1981). BOD removal in fluidised beds: high biomass concentration or high oxygen transfer?
In: Biological fluidised bed treatment of water and wastewater (P. F. Cooper and B. Atkinson, eds.), pp. 383–389.
Ellis Horwood Ltd., Chichester.

Van Gemerden, H. (1968). Growth measurements of *Chromatium* cultures.

Arch. Mikrobiol. **64**, 103−110.

Verlaan, P. (1985). Airlift−loop bioreactor.
PT Procestechniek **40**, 60−63.

Wang, D. I. C., C. L. Cooney, A. L. Demain, P. Dunnill, A. E. Humphrey, and M. D. Lilly (1979). Fermentation and enzyme technology.
John Wiley & Sons, New York.

Weibel, E. R. (1979). Stereological methods. Vol. 1. Practical methods for biological morphometry.
Academic Press, London.

Weise, W., and G. Rheinheimer (1978). Scanning electron microscopy and epifluorescence investigation of bacterial colonization of marine sand sediments.
Microb. Ecol. **4**, 175−188.

Wheatley, A. D. (1981). Investigations into the ecology of biofilms in waste treatment using scanning electron microscopy.
Environm. Technol. Lett. **2**, 419−424.

White, F. H., and A. D. Portno (1978). Continuous fermentation by immobilized brewers yeast.
J. Inst. Brew. **84**, 228−230.

Wiegant, W. M., and W. A. de Man (1986). Granulation of biomass in thermophilic upflow anaerobic sludge blanket reactors treating acidified wastewaters.
Biotechnol. Bioeng. **28**, 718−727.

Williams, A. G., and J. W. T. Wimpenny (1978). Exopolysaccharide production by *Pseudomonas* NCIB 11264 grown in continuous culture.
J. Gen. Microbiol. **104**, 47−57.

Wimpenny, J. W. T., R. W. Lovitt, and J. P. Coombs (1983). Laboratory model systems for the investigation of spatially and temporally organised ecosystems.
Symp. Soc. Gen. Microbiol. **34**, 67−117.

Woldringh, C. L., J. S. Binnerts, and A. Mans (1981). Variations in *Escherichia coli* buoyant density measured in percoll gradients.
J. Bacteriol. **148**, 58−63.

Zevenhuizen, L. P. T. M. (1981). Cellular glycogen, β−1,2−glucan, poly−β−hydroxybutyrate and extracellular polysaccharides in fast growing species of *Rhizobium*.
Antonie van Leeuwenhoek **47**, 481−497.

Zoetemeyer, R. J. (1982). Acidogenesis of soluble carbohydrate−−containing wastewaters.
PhD. thesis, University of Amsterdam.

Zoetemeyer, R. J., J. C. van den Heuvel, and A. Cohen (1982). pH influence on acidogenic dissimilation of glucose in an anaerobic digestor.
Water Res. **16**, 303−311.

nSUMMARY

SUMMARY

Chemical conversions that are mediated by micro—organisms exhibit, necessarily, an autocatalytic nature. In Chapter I, this point is elaborated, and it is shown that in continuous—flow systems, the maximum specific growth rate of micro—organisms sets an undesirably low limit to the rate at which a bioreactor may be operated. When bacteria can be grown in the form of clumps (called aggregates in this thesis), it becomes possible to operate a continuous—flow reactor at far higher loadings, as such aggregates are less subjected to wash—out from the reactor, and may be retained with some efficiency. This hold—up or retention of biomass finds its physical basis in the settling characteristics of aggregates. Unfortunately, however, mathematical descriptions for such systems are rather simplistic and unsatisfactory, as knowledge on physical characteristics of aggregates is lacking. The research in this thesis therefore aimed at a description and understanding of the development of bacterial aggregates, with particular emphasis on physical characteristics. As a model process, anaerobic acidification by a mixed bacterial population was studied in a mineral medium with glucose as the growth—limiting carbon and energy source.

Chapter II gives a description and justification of the anaerobic gas—lift reactor (AGLR) used in this research. A start—up routine employing a dilution—rate shift—up ensured the rapid formation of aggregates from freely suspended cells, provided carrier material (sand) was available. A characteristic change in overall metabolism of the mixed population was observed to coincide with aggregate formation. Under the latter conditions, the main products were propionate, acetate, and valerate. Preliminary observations indicated transport limitations of the substrate (glucose) into aggregates. Due to these limitations, cells in the centre of aggregates were starved and, consequently, subject to cellular lysis. The absence of sand in the ultimate steady—state aggregates is explained with sloughing of biofilm fragments on the basis of lysis.

Chapter III presents more detailed data on the complicated role of carrier material during the first stages of aggregate formation. Also, it was found that one of two types of aggregate was formed: a (most frequently encountered) propionate—producing type, and a butyrate— —producing type. In the absence of carrier material, neither type was formed. But, although sand was essential in the rapid formation of aggregates, elevated concentrations had a detrimental effect. Depending on the type of aggregate formed, an increase in sand concentration resulted in either a delay or in a lower rate of aggregate formation. An optimum initial concentration of sand was found to be 5 g/l.

Chapter IV illustrates the development of aggregates with data from

scanning and transmission electronmicroscopy, and from light microscopy. The initial colonization of the carrier material preferently occurred in surface irregularities on the sand grains, reflecting liquid turbulence. From such primary colonies, a confluent biofilm developed. During biofilm growth, however, fragments were seen to break away from the carrier surface. Such fragments were large enough to be retained, and ultimately constituted the only remaining type of aggregate. Carrier material had virtually disappeared by wash−out and sampling. The final type of steady−state aggregate was found to have high cellular densities at its periphery of 10^{12} cells per milliliter, which occupied 25 % of the local volume. In the centre of large aggregates, however, a pronounced void with a low biomass concentration was observed. The results were summarized in a working hypothesis on aggregate dynamics, involving cellular lysis due to substrate insufficiency.

In Chapter V, data are presented on prolonged AGLR operation. Although aggregate formation in itself was accomplished rapidly, the stabilization of reactor operation was delayed to some extent. Rather large aggregates were found initially, but were seen to disappear from the AGLR once substrate became depleted. This loss in retention could be attributed to the loss in specific weight, and the concomitant decrease in settling velocity. After this shift in biomass hold−up, the reactor was operated for a considerable time span under stable conditions. The events during this rearrangement of aggregate characteristics could be explained in terms of the previously developed working hypothesis.

In Chapter VI, the previous findings on the development of aggregates are summarized in a mathematical form. A model is presented describing overall reactor characteristics in terms of the dynamic behaviour of individual aggregates. As a result of substrate consumption, aggregates are growing, and thus increase in size. On the other hand, substrate depletion in the centre of large aggregates causes an internal deterioration by cellular lysis. As a result, large aggregates desintegrate into smaller ones. Overall biomass retention was formulated in terms of the settling velocity of individual aggregates. On the basis of these highly mechanistic formulations, retention was found to depend on the dilution rate, but not on the influent substrate concentration. Reactor biomass concentrations exhibited a complex pattern, depending on the choise of the fragmentation pattern. The importance of the result resides in the possiblity to predict reactor biomass concentration and retention without taking recourse to commonly used, but unattractive, assumptions on the absence of bacterial growth and the uniformity of aggregates.

SAMENVATTING

Voor allerlei praktijkdoeleinden wordt dankbaar gebruik gemaakt van het vermogen van microörganismen een veelheid van chemische omzettingen te bewerkstelligen. Dergelijke transformaties kunnen uitgevoerd worden in reactoren die ladingsgewijs bedreven worden, óf in continu—doorstroomde reactoren. Het laatste type reactor kent, naast een aantal gewichtige voordelen, een ernstige belemmering. De continue verversing van de reactorinhoud veroorzaakt een voortdurend verlies (uitspoeling) van de voor het verloop van de reactie zo essentiële microörganismen. Omdat tegelijkertijd de microörganismen groeien door tweedeling, komt het niet tot een volledig verlies van celmateriaal, maar stelt zich een evenwicht in tussen aanwas en verlies. Een dergelijk evenwicht wordt echter alleen bereikt, indien de snelheid waarmee microörganismen verloren gaan (verdunningssnelheid, D) de snelheid waarmee ze onstaan (specifieke groeisnelheid, μ) niet te boven gaat. Groeisnelheden van microörganismen zijn weliswaar variabel, maar slechts binnen zekere grenzen (maximale waarde: μ_{max}). Derhalve kan een reguliere continu reactor slechts een beperkte belasting verwerken ($D < \mu_{max}$), en deze beperking is vanuit economisch oogpunt onwenselijk.

De bovengenoemde beperking kan echter verruimd worden. Micro—örganismen, welke normaliter voorkomen als losse, microscopisch kleine cellen, kunnen ertoe gebracht worden zich te verenigen tot (en te groeien als) meercellige "aggregaten". Het belang hiervan is gelegen in de bezinksnelheid van zulke aggregaten, welke vele malen hoger is dan die van losse cellen. Deze bezinking maakt het mogelijk de reactor hoog te belasten bij een hoge verdunningssnelheid ($D > \mu_{max}$), terwijl toch celmateriaal in de vorm van aggregaten in de reactor gehouden kan worden ("terughoud" of "retentie"). Hiertoe wordt veelal een bezinker op de reactoruitgang geplaats, waarin eventueel uitspoelende aggregaten kunnen sedimenteren en teruggevoerd kunnen worden naar de eigenlijke reactor.

Uit het bovenstaande volgt direct, dat de eigenschappen van een continu—doorstroomde reactor met biomassa—retentie in sterke mate worden bepaald door de eigenschappen van bacteriële aggregaten. Terwijl echter bijna alle bioreactoren voor praktijkdoeleinden gebruik maken van terughoud van biologisch materiaal, bestaat er toch een belangrijk gebrek aan kennis omtrent de eigenschappen en het gedrag van bacteriële aggregaten. Het in dit proefschrift beschreven onderzoek richt zich dan ook op deze eigenschappen, teneinde door een verbeterd begrip te komen tot een meer rationeel ontwerp en bedrijf van terughoud—reactoren.

In Hoofdstuk II wordt een beschrijving gegeven van de bij het

onderzoek gebruikte "anaerobe gas—lift reactor" (AGLR). Middels een plotselinge verhoging van de verdunningssnelheid werdt bewerkstelligd dat individuele cellen zich hechten op een in de reactor aanwezig (zwaar) dragermateriaal (zandkorrels). Deze aggregaatvorming in de gedaante van een "biofilm" rond een zandkorrel had een verschuiving van bacteriestofwisseling tot gevolg: de oorspronkelijke vergisting van glucose tot boterzuur en azijnzuur werd vervangen door de productie van propionzuur, valeriaanzuur, en azijnzuur. Er werden aanwijzingen gevonden, dat cellen binnen in zulke aggregaten onvoldoende werden voorzien van substraat (glucose) vanuit de bulk—vloeistof. Als gevolg hiervan trad desintegratie (lysis) van deze cellen op, waardoor de aanhechting van de biofilm op de zandkorrel verzwakte. Fragmenten biofilm braken los van de zandkorrel, maar konden toch teruggehouden worden in de reactor. Uiteidelijk werden alleen nog maar dergelijke zand—vrije aggregaten aangetroffen.

Hoofdstuk III verschaft gegevens omtrent de invloed van zand tijdens de opstartprocedure. Hierbij bleek, dat meestal de bovengenoemde propionzuurproducerende aggregaten gevormd werden; in een aantal gevallen werden echter boterzuurproducerende aggregaten gevonden. In afwezigheid van zand werden geen van beide typen aggregaten gevormd. Hoewel dragermateriaal dus essentieel was gaf variatie in de beschikbare hoeveelheid zand een gecompliceerd beeld te zien: hogere zandconcentraties bleken de snelheid, waarmee propionzuurproducerende aggregaten gevormd werden, te vertragen, terwijl anderzijds het tijdstip, waarop de vorming van boterzuuraggregaten een aanvang nam, werd uitgesteld. Voor beide gevallen werd geconcludeerd, dat zand beschikbaar diende te zijn, maar in een lage concentratie (ca. 5 g/l).

In Hoofdstuk IV wordt, met behulp van licht— en electronen— microscopische technieken, een visueel beeld gegeven van de ontwikkeling van aggregaten. Hierbij bleek dat zandkorrels in eerste instantie begroeid raken met een beginnende biofilm in oneffenheden en groefjes in hun oppervlak. Dergelijke plaatsen bieden beschutting tegen de schurende werking van langsstromende vloeistof. In een later stadium kon inderdaad worden waargenomen, dat dikkere fragmenten biofilm van het zand— oppervlak braken. Deze brokstukken vormden de basis voor de uit— eindelijke aggregaten, welke geen zand meer bevatten. In de buitenste schil van deze aggregaten bleek 25 % van het plaatselijke volume ingenomen te worden door bacteriecellen, corresponderend met 10^{12} cellen per milliliter. In het centrum van aggregaten echter waren de gevolgen van lysis zichtbaar in de vorm van grotendeels afwezig bacteriemateriaal.

Hoofdstuk V geeft gegevens over het gedrag van de AGLR bij langdurige bedrijfsvoering, volgend op een opstartprocedure. Het bleek,

dat het realiseren van een stationaire toestand meer tijd vergde, dan het vormen van bacterieaggregaten op zich. Een verklaring hiervoor werd gevonden door de fysische eigenschappen van de gevormde aggregaten te bestuderen. Ten alle tijde bleek een heel scala aan aggregaatdiameters voor te komen. Maar terwijl direct na de eerste vorming van aggregaten nog vrij grote exemplaren werden gevonden (tot 4 mm), bleken deze vervolgens weer te verdwijnen. Dit verwijnen viel samen met het uitputten van de energiebron glucose in de reactor. Op grond hiervan werd verondersteld, dat juist grote aggregaten onderhevig zouden raken aan lysis in hun centrum ten gevolge van belemmeringen in het glucosetransport. Met behulp van dichtheidsgradiëntcentrifugatie kon inderdaad worden aangetoond, dat deze grote aggregaten een relatief lage soortelijke massa hadden. Klaarblijkelijk bracht dit een verzwakking van deze aggregaten met zich mede. Krachten vanuit de omringende vloeistof, en gasvorming door het bacteriemetabolisme zouden het uiteenvallen van dergelijke aggregaten kunnen bewerkstelligen.

Hoofdstuk VI geeft een samenvatting in mathematische vorm van de voorgaande waarnemingen. Een model werd opgesteld, waarmee het dynamische gedrag van aggregaten in de AGLR wordt beschreven. Enerzijds neemt een individueel aggregaat voortdurend in omvang toe door substraatconsumptie en de daaraan gekoppelde groei. Anderzijds werd het uiteenvallen van aggregaten tot kleine fragmenten beschreven als uiteindelijke functie van lysis in het centrum van (vooral grote) aggregaten. De uitspoeleing, of, omgekeerd, het terughouden, werd geformuleerd op grond van hun bezinksnelheid. Op grond van een dergelijk mechanistisch model werd gevonden dat de gemiddelde terughoud een functie is van de verdunningssnelheid, maar niet van de substraatconcewntratie in het reactorinfluent. De biomassaconcentratie in de reactor vertoonde een complex beeld als functie van D, dat bovendien sterk beinvloed werd door de precieze formulering van de fragmentatie. Het belang van deze resultaten is in de eerste plaats gelegen in de mogelijkheid met het gepresenteerde model gedetailleerde voorspellingen te doen omtrent het reactorgedrag, zonder toevlucht te moeten nemen tot onaantrekkelijke en vaak uitermate onrealistische simplificaties.

DANKWOORD